

An-Najah National University

Faculty of Graduate Studies

**Reduction of Nitrate Ion from Water
using Nano-Copper Based
Electrocatalyst**

By

Heba Nassar Izzat Nassar

Supervisor

Prof. Hikmat S. Hilal

Co-Supervisor

Dr. Ahed Zyoud

**This Thesis is Submitted in Partial Fulfillment of the Requirements for
the Degree of Ph.D. of Chemistry, Faculty of Graduate Studies, An-
Najah National University, Nablus, Palestine.**

2021

**Reduction of Nitrate Ion from Water using
Nano-Copper Based Electrocatalyst**

By

Heba Nassar Izzat Nassar

This thesis was defended successfully on 21 / 4 / 2021 and approved by:

Defense Committee Members

Signature

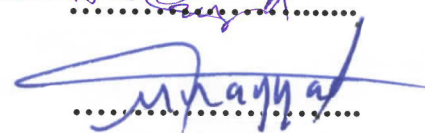
- Prof. Hikmat S. Hilal/ Supervisor



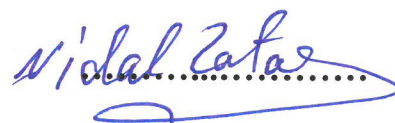
- Dr. Ahed Zyoud/ Co-Supervisor



- Dr. Muayad Abu Saa/ External Examiner



- Dr. Nidal Zatar/ Internal Examiner



III

Dedication

To my dear parents.....

To my wonderful daughters

To you, dear reader.....

Acknowledgments

After thanking Allah, who gave me the ability to finish this work. My greatest appreciation goes to my main supervisor, Prof. Hikmat Hilal for his scientific support, advice, and valuable knowledge he provided me with throughout this process. Many thanks to my research co-supervisor Dr. Ahed Zyoud for his never-ending encouragement, guidance, and constructive advice.

I would like to extend my gratitude to everyone at the Chemistry Department at An-Najah National University, especially Dr. Nidal Zatar. Especial thanks to Mr. Omair Al-Nabulsi and Mr. Nafith Dweikat from the Laboratory staff. I also would like to thank Dr. Dae Hoon Park (Dansuk Co., Seoul, S. Korea) for performing SEM, EDS, XRD and XPS measurements.

My acknowledgement also goes to the Middle East Desalination Research Centre (MEDRC) for offering me a fellowship to complete my Ph.D. study. Also, not to forget the solid support of the Palestinian Water Authority.

My warm thanks to my dear friends and fellows for all their support. Last but not least, my sincere appreciation and deepest gratitude to my parents, brothers and sisters for their trust and unconditional support throughout my study. My sweet daughters **Salma and Yasmine** thanks for your love which always carried me through the way. Dear **Afnan Nassar** thanks a lot for everything.

Heba Nassar

الإقرار

أنا الموقعة أدناه مقدمة الرسالة التي تحمل العنوان:

Reduction of Nitrate Ion from Water using Nano-Copper Based Electrocatalyst

أقرُّ بأن ما اشتملت عليه الرسالة إنما هو نتاج جهدي الخاص، باستثناء ما تمت الإشارة إليه حيثما ورد، و أنّ هذه الرسالة ككل، أو أي جزء منها لم يقدم من قبل لنيل أية درجة علمية أو بحث لدى أية مؤسسة تعليمية أو بحثية أخرى.

Declaration

This work provided in this thesis, unless otherwise referenced, is the researcher's own work, and has not been submitted elsewhere for any other degree or qualification.

Student's name:

اسم الطالبة: هبة نصّار عزت نصّار

Signature:

التوقيع: هبة نصّار عزت نصّار

Date:

التاريخ: 2021/4/21

List of Contents

No.	Content	Page
	Dedication	III
	Acknowledgments	IV
	Declaration	V
	List of Contents	VI
	List of Tables	X
	List of Figures	XI
	List of Abbreviations	XVI
	Abstract	XVII
	Chapter One: Introduction	1
1.1	The Imbalance of Nitrogen Cycle	2
1.2	Environmental and Health Risks	4
1.3	Regulations and Recommendations	4
1.4	Nitrate Removal Methods	4
1.4.1	Biological Methods	5
1.4.2	Physical Methods	5
1.4.3	Chemical Reduction	5
1.4.4	Electrochemical Reduction	6
1.4.4.1	Electroreduction Processes	6
1.4.4.2	Electrochemical Cell Designs for Denitrification	7
1.4.4.3	Electrolysis Modes	8
1.4.4.4	Performance of Electrochemical Reduction of Nitrate	9
1.4.4.5	Inorganic Basics of Nitrate Electroreduction	10
1.4.4.6	Copper Catalyst	11
1.4.4.7	Nitrate Electroreduction Products and Intermediates	11
1.5	Thesis Outline	12
	Chapter Two: Literature Review	14
2.1	Classification of Electrode Materials for Nitrate Electroreduction	15
2.1.1	Copper and Related Electrocatalysts	15
2.1.1.1	Pristine Cu Electrode	15
2.1.1.2	Cu/X Bimetallic Electrode	16
2.1.1.2.1	Cu/Zn Bimetallic Electrode	16
2.1.1.2.2	Cu/Pd Bimetallic Electrode	17
2.1.1.2.3	Cu/Ni Bimetallic Electrode	17
2.1.1.2.4	Cu/Pt Bimetallic Electrode	17
2.1.1.3	Graphene Modified Cu Electrode	18

2.1.1.4	Polypyrrole Film Modified with Copper Oxide Particles	18
2.1.1.5	Copper Phthalocyanine	19
2.1.1.6	Deposited Cu on Boron Doped Diamond (BDD) Electrode	19
2.1.1.7	Pd–Cu/ γ Al ₂ O ₃	19
2.1.2	Other Electrocatalysts	20
2.2	Thesis Scope	20
2.3	Questions of the Study	22
2.4	Objectives	23
2.4.1	Strategic Objectives	23
2.4.2	Technical Objectives	23
2.5	Assumptions	24
2.6	Significance and Novelty	24
	Chapter Three: Methodology	26
3.1	Chemicals and Materials	27
3.2	Equipment	27
3.3	Preparation of the Electrodes	28
3.3.1	Copper Electrodes	28
3.3.2	FTO Electrodes	28
3.3.3	Modified FTO Electrodes	29
3.3.3.1	FTO Electrodes Modified with Cu	29
3.3.3.2	FTO Electrodes Modified with Graphite	30
3.3.3.3	FTO/Graphite Electrodes Modified by Cu Nanoparticles	30
3.3.3.4	FTO Electrodes Modified with Functionalized MWCNTs	31
3.3.3.5	FTO/MWCNTs Electrodes Modified with Cu	32
3.4	Characterization of the Electrodes	33
3.4.1	Scanning Electron Microscopy (SEM)	33
3.4.2	Energy-Dispersive X-ray Analysis (EDS)	33
3.4.3	X-Ray Diffraction (XRD)	33
3.4.4	X-Ray Photoelectron Spectroscopy (XPS)	34
3.4.5	Voltammetric Investigation of Nitrate Reduction	34
3.5	Electroreduction Experiments and Electrochemical Measurements	35
3.5.1	Set up of Nitrate Electroreduction Experiments	35
3.5.1.1	Glassware and Solutions	35
3.5.1.2	Cell and Electrodes	35
3.5.1.3	Analysis Methods	36

VIII

3.5.2	Effect of Different Factors on Nitrate Electroreduction	37
3.5.2.1	Effect of Electrode Type	37
3.5.2.2	Effect of Applied Potential	37
3.5.2.3	Effect of Electrolyte Type	38
3.5.2.4	Effect of Electrolyte Concentration	38
3.5.2.5	Effect of Stirring	38
3.5.2.6	Effect of Distance between Electrodes	39
3.5.2.7	Effect of Temperature	39
3.5.2.8	Effect of Initial NO ₃ ⁻ Concentration	40
3.5.2.9	Effect of Initial pH	40
3.5.2.10	Effect of Electroreduction Time	40
3.5.3	Alkalinity Measurements	41
3.5.4	Performance and Reproducibility of the Modified FTO/MWCNT-Cu Electrode in Nitrate Electroreduction	41
	Chapter Four: Result and Discussion	42
4.1	FTO/Cu Electrode	43
4.1.1	Characterization	43
4.1.1.1	SEM Analysis	43
4.1.1.2	EDS Analysis	44
4.1.1.3	XRD Analysis	45
4.1.1.4	XPS Analysis	47
4.1.1.5	Cyclic Voltammetry Investigation	49
4.1.2	Electroreduction of Nitrate	52
4.1.2.1	Electroreduction Experiments	52
4.1.2.1.1	Effect of Electrode Type	52
4.2	FTO/Gr Electrodes	57
4.2.1	Characterization	57
4.2.1.1	SEM analysis	57
4.2.1.2	EDS Analysis	58
4.2.1.3	XRD Analysis	58
4.2.1.4	XPS Analysis	60
4.2.1.5	Cyclic Voltammetry Investigations	61
4.2.2	Electroreduction of Nitrate	62
4.2.2.1	Electroreduction Experiments	62
4.2.2.1.1	Effect of Electrode Type	62
4.3	FTO/ MWCNT Electrodes	65
4.3.1	Characterization	65
4.3.1.1	SEM Analysis	65
4.3.1.2	EDS Analysis	66

4.3.1.3	XRD Analysis	66
4.3.1.4	XPS Analysis	68
4.3.1.5	Cyclic Voltammetry Investigations	71
4.3.2	Electroreduction of Nitrate	73
4.3.2.1	Electroreduction Experiments	73
4.3.2.1.1	Effect of Electrode Type	73
4.3.2.2	Parameter Effects on FTO/MWCNT-Cu Efficiency	76
4.3.2.2.1	Effect of Applied Voltage	76
4.3.2.2.2	Effect of Electrolyte Type	77
4.3.2.2.3	Effect of Electrolyte Concentration	80
4.3.2.2.4	Effect of Solution Stirring	81
4.3.2.2.5	Effect of Distance between Electrodes	81
4.3.2.2.6	Effect of Temperature	82
4.3.2.2.7	Effect of Initial Nitrate Concentration	83
4.3.2.2.8	Effect of Initial pH	84
4.3.2.3	Kinetics of Nitrate Electroreduction	85
4.3.2.4	Prolonged Electroreduction Time	90
4.3.2.5	Alkalinity Change during Process	93
4.3.2.6	Stability and Reuse of the Electrode	94
	Chapter Five: Conclusion	99
5.1	Conclusion	100
5.2	Future Work Suggestions	101
	References	103
	المخلص	ب

List of Tables

No.	Table	Page
Table 1.1	Main cathodic reactions in electrochemical reduction of aqueous nitrates and their standard E° values.	12
Table 4.1	Analysis of XRD pattern of FTO/Cu-a and FTO/Cu-b electrodes.	47
Table 4.2	Selectivity for ammonium, nitrite and nitrogen on FTO, Cu, and FTO/Cu-b electrodes. Experiments were conducted using (70 mL; 0.05 M Na_2SO_4 + 200 mg/L NO_3^-) at: $25 \pm 1^\circ\text{C}$, intrinsic pH, $D = 0.75$ cm, 2 h, and -1.80 V vs. SCE.	56
Table 4.3	Analysis of XRD pattern of FTO/Gr and FTO/Gr-Cu electrodes.	59
Table 4.4	Selectivity for ammonium, nitrite and nitrogen on FTO/ Gr, and FTO/Gr-Cu. Experiments were conducted using (70 mL; 0.05 M Na_2SO_4 + 200 mg/L NO_3^-) at: $25 \pm 1^\circ\text{C}$, intrinsic pH, $D = 0.75$ cm, 2 h, and -1.80 V vs. SCE.	64
Table 4.5	Elemental analysis of FTO/MWCNT-Cu (a) before and after use (b).	66
Table 4.6	XRD analysis for Cu and related compounds in fresh and used FTO/MWCNT-Cu electrode.	68
Table 4.7	Selectivity for ammonium, nitrite and nitrogen on FTO/WCNT and FTO/MWCNT-Cu. Experiments were conducted using (70 mL; 0.05 M Na_2SO_4 + 200 mg/L NO_3^-) at: $25 \pm 1^\circ\text{C}$, intrinsic pH, $D = 0.75$ cm, 2 h, and -1.80 V vs. SCE.	75
Table 4.8	Selectivity for ammonium, nitrite and nitrogen on FTO/MWCNT-Cu, in the presence of 0.075 M NaCl and 0.05 M Na_2SO_4 . Experiments were conducted using (70 mL; 200 mg/L NO_3^-) at: $25 \pm 1^\circ\text{C}$, intrinsic pH, $D = 0.75$ cm, 2 h, and -1.80 V vs. SCE.	78
Table 4.9	Comparison of order and rate constant of nitrate electroreduction values for FTO/MWCNT-Cu electrode with literature.	90
Table 4.10	Selectivity for ammonium, nitrite and nitrogen on FTO/MWCNT-Cu. Experiments were conducted using (70 mL; 0.05 M Na_2SO_4 + 200 mg/L NO_3^-) at: $25 \pm 1^\circ\text{C}$, intrinsic pH, $D = 0.75$ cm, -1.80 V vs. SCE, and different time of electrolysis (2 h, 3 h, and 7 h).	92
Table 4.11	Comparison between the present electrodes with reported ones in nitrate electroreduction.	97

List of Figures

No.	Figure	Page
Figure 1.1	Simplified scheme for nitrogen cycle.	2
Figure 1.2	Molecular orbitals during electroreduction of nitrate ((reproduced based on [98]).	10
Figure 2.1	Structures of various graphitic materials.	21
Figure 3.1	Schematic design of the electroreduction system.	36
Figure 4.1	SEM micrographs measured for (a) FTO/Cu-a and (b) FTO/Cu-b	44
Figure 4.2	EDS spectra measured for (a) FTO/Cu-a, and (b) FTO/Cu-b	45
Figure 4.3	Measured XRD patterns for (a) FTO/Cu-a and (b) FTO/Cu-b.	46
Figure 4.4	Measured XPS spectra for FTO/Cu-a, (a) complete spectrum, (b) copper peak and (c) oxygen peak.	48
Figure 4.5	Measured XPS spectra for FTO/Cu-b, (a) complete spectrum, (b) copper peak and (c) oxygen peak.	49
Figure 4.6	Cyclic voltammograms on (a) FTO, (b) Cu and (c) FTO/Cu-b in ——— 0.05M Na ₂ SO ₄ and in (0.05 M Na ₂ SO ₄ + 200 mg/L NO ₃ ⁻), scan rate 20 mVs ⁻¹ .	51
Figure 4.7	Percentage of nitrate conversion on ● FTO, ■ Cu and ▲ FTO/Cu-b vs. electrolysis time. Experiments were conducting using (70 mL; 0.05 M Na ₂ SO ₄ + 200 mg/L NO ₃ ⁻), at: 25 ± 1°C, intrinsic pH, D = 0.75 cm, 2 h, and -1.80 V vs. SCE.	53
Figure 4.8	Variation of ● nitrate, ■ nitrite and ▲ ammonia concentration vs. electrolysis time on (a) FTO, (b) Cu and (c) FTO/Cu-b electrodes. Experiments were conducted using (70 mL; 0.05 M Na ₂ SO ₄ + 200 mg/L NO ₃ ⁻), at: 25 ± 1°C, intrinsic pH, D = 0.75 cm, 2 h, and -1.80 V vs. SCE.	54
Figure 4.9	SEM micrographs measured for (a) FTO/Gr and (b) FTO/Gr-Cu.	57
Figure 4.10	EDS spectra measured for FTO/Gr-Cu electrode.	58
Figure 4.11	Measured XRD patterns for (a) FTO/Gr and (b) FTO/Gr-Cu.	59
Figure 4.12	Measured XPS spectra for FTO/Gr-Cu, (a) complete spectrum, (b) copper peak and (c) oxygen peak.	60

Figure 4.13	Cyclic voltammograms on (a) FTO/Gr and (b) FTO/Gr-Cu in ——— 0.05 M Na ₂ SO ₄ and in - - - - 0.05 M Na ₂ SO ₄ + 200 mg/L NO ₃ ⁻ . Scan rate 20 mVs ⁻¹ .	62
Figure 4.14	Percentage of nitrate conversion on ● FTO/Gr and ▲ FTO/Gr-Cu vs. electrolysis time. Experiments were conducted using (70 mL; 0.05 M Na ₂ SO ₄ + 200 mg/L NO ₃ ⁻), at: 25 ± 1°C, intrinsic pH, D = 0.75 cm, 2 h, and -1.80 V vs. SCE.	63
Figure 4.15	Variation of ● nitrate, ■ nitrite and ▲ ammonium concentration vs. electrolysis time on (a) FTO/Gr, and (b) FTO/Gr-Cu electrodes. Experiments were conducted using (70 mL; 0.05 M Na ₂ SO ₄ + 200 mg/L NO ₃ ⁻), at: 25 ± 1°C, intrinsic pH, D = 0.75 cm, 2 h, and -1.80 V vs. SCE.	64
Figure 4.16	SEM images for (a) FTO/MWCNT, (b) fresh FTO/MWCNT-Cu and (c) used FTO/MWCNT-Cu.	65
Figure 4.17	Measured XRD patterns for (a) FTO/MWCNT, (b) fresh FTO/MWCNT-Cu and (c) used FTO/MWCNT-Cu.	67
Figure 4.18	Measured XPS spectra for fresh FTO/MWCNT-Cu electrode, (a) complete spectrum, (b) copper peak and (c) oxygen peak.	69
Figure 4.19	Measured XPS spectra for used FTO/MWCNT-Cu electrode, (a) complete spectrum, (b) copper peak and (c) oxygen peak.	70
Figure 4.20	Cyclic voltammograms for (a) FTO/MWCNT and (b) FTO/MWCNT-Cu in ——— 0.05 M Na ₂ SO ₄ and in - - - - 0.05 M Na ₂ SO ₄ + 200 mg/L NO ₃ ⁻ . Scan rate 20 mVs ⁻¹ .	71
Figure 4.21	Cyclic voltammograms for (a) FTO, (b) FTO/Cu-b, (c) FTO/Gr, (d) FTO/Gr-Cu, (e) FTO/MWCNT and (f) FTO/MWCNT-Cu in 0.05 M Na ₂ SO ₄ + 200 mg/L NO ₃ ⁻ . Scan rate 20 mVs ⁻¹ .	72
Figure 4.22	Percentage of nitrate conversion on ● FTO/MWCNT and ▲ FTO/MWCNT-Cu vs. electrolysis time. Experiments were conducted using (70 mL; 0.05 M Na ₂ SO ₄ + 200 mg/L NO ₃ ⁻), at: 25 ± 1 °C, intrinsic pH, D = 0.75 cm, 2 h and -1.80 V vs. SCE.	73

Figure 4.23	Variation in concentration of ● nitrate, ▲ ammonium and ■ nitrite on (a) FTO/MWCNT and (b) FTO/MWCNT-Cu. Experiments were conducted using (70 mL; 0.05 M Na ₂ SO ₄ + 200 mg/L NO ₃ ⁻) at: 25 ± 1°C, intrinsic pH, D = 0.75 cm, 2 h, and -1.80 V vs. SCE.	75
Figure 4.24	Percentage of nitrate conversion at (■ -1.50 V, ● -1.80 V, and ▲ -2.10 V) vs. SCE against electrolysis time, on FTO/MWCNT-Cu electrode. Experiments were conducted using (70 mL; 0.05 M Na ₂ SO ₄ + 200 mg/L NO ₃ ⁻), at: 25 ± 1 °C, intrinsic pH, D = 0.75 cm, and 2 h.	76
Figure 4.25	Percentage of nitrate conversion using (● 0.05 M Na ₂ SO ₄ and ▲ 0.075 M NaCl) as electrolyte, vs. electrolysis time, on FTO/MWCNT-Cu electrode. Experiments were conducted using (70 mL; 200 mg/L NO ₃ ⁻), at: 25 ± 1°C, intrinsic pH, D = 0.75 cm, 2 h and -1.80 V) vs. SCE.	77
Figure 4.26	Variation in concentration of ● nitrate, ■ nitrite and ▲ ammonium on FTO/MWCNT-Cu, in (a) the presence of 0.075 M NaCl and (b) 0.05 M Na ₂ SO ₄ . Experiments were conducted using (70 mL; 200 mg/L NO ₃ ⁻) at: 25 ± 1 °C, intrinsic pH, D = 0.75 cm, 2 h, and -1.80 V vs. SCE.	79
Figure 4.27	Percentage of nitrate conversion at (●0.025 M Na ₂ SO ₄ , ▲ 0.05 M Na ₂ SO ₄ and ■ 0.10 M Na ₂ SO ₄) vs. electrolysis time, on FTO/MWCNT-Cu electrode. Experiments were conducted using (70 mL; 200 mg/L NO ₃ ⁻), at: 25 ± 1°C, intrinsic pH, D = 0.75 cm, 2 h, and -1.80 V vs. SCE	80
Figure 4.28	Effect of stirring the working solution on nitrate conversion percent using FTO/MWCNT-Cu electrode. Experiments were conducted using (70 mL; 0.05 M Na ₂ SO ₄), at: 25 ± 1°C, intrinsic pH, D = 0.75 cm, 2 h, and -1.80 V vs. SCE.	81
Figure 4.29	Percentage of nitrate conversion on FTO/MWCNT-Cu electrode at (● D = 3.5 cm, and ▲ D = 0.75 cm) vs. electrolysis time on FTO/MWCNT-Cu electrode. Experiments were conducted using (70 mL; 0.05 M Na ₂ SO ₄ + 200 mg/L NO ₃ ⁻), at: 25 °C ± 1, intrinsic pH, 2 h, and -1.80 V vs. SCE.	82

Figure 4.30	Nitrate conversion percent at (● 10 °C, ▲ 25 °C and ■ 35 °C) vs. the electrolysis time on FTO/MWCNT-Cu electrode. Experiments were conducted using (70 mL; 0.05 M Na ₂ SO ₄ + 200 mg/L NO ₃ ⁻), at: intrinsic pH, D = 0.75 cm, 2 h, and -1.80 V vs. SCE.	83
Figure 4.31	Percentage of nitrate conversion vs. the electrolysis time on FTO/MWCNT-Cu electrode, using different initial concentrations of NO ₃ ⁻ (● 200 mg/L, ▲ 600 mg/L and ■ 1000 mg/L). Experiments were conducted using (70 mL; 0.05 M Na ₂ SO ₄), at: 25 ± 1°C, intrinsic pH, D = 0.75 cm, 2 h, and -1.80 V vs. SCE.	84
Figure 4.32	Variation of percentage of nitrate conversion against the intrinsic pH on FTO/MWCNT-Cu, for (70 mL; 0.05 M Na ₂ SO ₄ + 200 mg/L NO ₃ ⁻). Experiments were conducted at : 25 ± 1°C, D = 0.75 cm, 2 h, and -1.80 V vs. SCE.	85
Figure 3.33	Kinetics of nitrate electroreduction according to (a) the zero-order law, (b) the first-order law and (c) to the second-order law by FTO/MWCNT-Cu electrode. Experiments were conducted using (70 mL; 0.05 M Na ₂ SO ₄ + 200 mg/L NO ₃ ⁻), at: 25 ± 1 °C, intrinsic pH, D = 0.75 cm, 2 h and -1.80 V vs. SCE.	87
Figure 4.34	Effect of initial concentration of nitrate on initial rate of electroreduction.. Experiments were conducted using FTO/MWCNT-Cu electrode, (70 mL; 0.05 M Na ₂ SO ₄), at: 25 ± 1 °C, intrinsic pH, D = 0.75 cm, 2 h, and -1.80 V vs. SCE.	89
Figure 4.35	Plot of ln Rate _{initial} vs. ln [C] _o on FTO/MWCNT-Cu electrode. Experiments were conducted using (70 mL; 0.05 M Na ₂ SO ₄), at: 25 ± 1 °C, intrinsic pH, D = 0.75 cm, 2 h, and -1.80 V vs. SCE.	89
Figure 4.36	Variation of the concentration of nitrate, nitrite and ammonium against the electrolysis time on FTO/MWCNT-Cu. Experiments were conducted using (70 mL; 0.05 M Na ₂ SO ₄ + 200 mg/L NO ₃ ⁻) at: 25 ± 1 °C, intrinsic pH, D = 0.75 cm, and -1.80 V vs. SCE.	91
Figure 4.37	Simplified scheme for nitrate electroreduction pathways on FTO/MWCNT-Cu electrode.	92

Figure 4.38	pH changes during five hours of electrolysis. Experiment was conducted using (70 mL; 0.05 M Na ₂ SO ₄ + 200 mg/L NO ₃ ⁻) at: 25 ± 1 °C, intrinsic pH, D = 0.75 cm, -1.80 V vs. SCE.	94
Figure 4.39	Percentage of nitrate conversion for three consecutive times (2 h each), using the same electrode (FTO/MWCNT-Cu). Experiments were conducted using (70 mL; 0.05 M Na ₂ SO ₄ + 200 mg/L NO ₃ ⁻), at: 25 ± 1 °C, intrinsic pH, D = 0.75 cm, and -1.80 V vs. SCE.	95

List of Abbreviations

Symbol	Abbreviation
CNT	Carbon nanotubes
CV	Cyclic voltammetry
D	Distance between electrodes
E	Electric potential
E°	Standard reduction potentials
EDS	Energy-dispersive X-ray spectroscopy
eV	Electron-Volt
FTO	Fluorine doped tin oxide
Gr	Graphite
HOMO	Highest occupied molecular orbital
LUMO	Lowest unoccupied molecular orbital
MWCNT	Multi-walled carbon nanotubes
R²	Correlation coefficient
S	Selectivity
SCE	Saturated calomel electrode
SEM	Scanning electron microscopy
SWCNT	Single-walled carbon nanotubes
UV-Vis	Ultraviolet visible
WHO	World Health Organization
XPS	X-Ray photoelectron spectroscopy
XRD	X-ray diffraction

**Reduction of Nitrate Ion from Water using Nano-Copper Based
Electrocatalyst****By****Heba Nassar Izzat Nassar****Supervisor****Prof. Hikmat S. Hilal****Co-Supervisor****Dr. Ahed Zyoud****Abstract**

Modification of nitrate removal methods from aqueous solutions has drawn deeper attention from researchers all over the world. This is due to nitrate contamination in ground and surface water. The primary cause for this contamination is known to be the improper use of nitrate-based chemical fertilizers.

The major objective of this research is to modify new safe electrodes for nitrate electroreduction from aqueous solutions, with high efficiency and cheap production cost. In this study, nitrate electroreduction was studied using the potentiostatic mode, since it lowers power consumption, although the galvanostatic mode is widely used in literature. Concentrations of remaining NO_3^- together with resulting NO_2^- and NH_4^+ were measured during the experiments.

Potentiostatic electroreduction of nitrate from aqueous solutions was conducted using a bench-scale undivided electrochemical cell. The electrochemical cell was equipped with three electrodes. Electrodes in the cell were saturated calomel electrode (SCE) as the reference electrode, Pt

sheet as the counter electrode, and one of the new modified electrodes has been used as the working electrode.

In this work, three different categories of electrodes have been modified using fluorine doped tin oxide on glass sheets (FTO/Glass) as substrate. Cu sheet and FTO sheets were used for comparison purposes. Characterization of the modified electrodes have been done by scanning electron microscopy (SEM), X-Ray diffraction (XRD), elemental energy dispersive spectroscopy (EDS) and X-ray photoelectron spectroscopy (XPS). Electrochemical behavior of the prepared electrodes for nitrate electroreduction was investigated by cyclic voltammetry (CV).

Different types of electrodes have been prepared. The first category includes FTO/Cu electrodes which have been prepared by Cu electrodeposition on FTO surface. Electrodeposition was made at -0.80 V from two different solutions; (0.85 M CuSO₄ + 0.55 M H₂SO₄) and using (0.01 M CuSO₄ + 0.10 M KCl). Electrode prepared by Cu electrodeposition from (0.85 M CuSO₄ + 0.55 M H₂SO₄), which was named FTO/Cu-b, shows more stability than other electrodes from same category.

Percentage of nitrate conversion by FTO/Cu-b after 2 h of electrolysis at -1.80 V was found to be 39.90% and nitrogen (N₂) selectivity% was 29.58%. FTO/Cu-b shows better efficiency in nitrate electroreduction compared to Cu sheet which shows 35.13% conversion percentage and 1.10% N₂ selectivity under the same conditions.

The second category involved FTO/Gr electrodes which were prepared by applying graphite thin film on FTO substrate to get FTO/Gr electrode. FTO/Gr electrode was modified by Cu electrodeposition on its surface from (0.85 M CuSO₄ + 0.55 M H₂SO₄) at -0.80 V, this modified electrode was named FTO/Gr-Cu electrode. Modification of FTO/Gr electrode by Cu slightly increases the percentage of nitrate conversion, with 24.00% and 25.69% for FTO/Gr and FTO/Gr-Cu, respectively, after 2 h of electrolysis at -1.80 V. This may be due to a low amount of Cu particles loaded on the electrode surface, with 12.92 atomic% according to EDS analysis. On the other hand, this modification increases the stability of the electrode, as XRD analysis only shows the presence of Cu nanoparticles at the electrode surface without any copper oxides even long time after preparation.

The third category involved FTO/MWCNT systems which were prepared by spray coating of modified multi-walled carbon nanotubes (MWCNTs) suspension on FTO surface. Preparation of the new modified electrode FTO/MWCNT-Cu electrode was made by spray coating of MWCNT-Cu composite on FTO/Glass surface. MWCNT-Cu nanocomposite was prepared by a new modified cheap and simple method. The average size of copper particles was determined from XRD analysis to be 35.28 nm.

FTO/MWCNT-Cu electrode shows the best percentage of nitrate conversion 65.27% in 2 h of electrolysis at -1.80 V. Therefore, it was used throughout this work. The kinetic analysis of the experimental results was studied by the

initial rate method, and the reaction order with respect to nitrate was (0.76) with a rate constant $4.53 \times 10^{-2} \text{ min}^{-1}$.

Nitrate electroreduction on FTO/MWCNT-Cu electrode was investigated when varying parameters including the applied voltage, electrolyte type and concentration, distance between electrodes, solution stirring, pH, temperature, time of electrolysis and nitrate concentration. Results indicates that increasing the applied potential, temperature (while stirring the solution and 0.75 cm distance between electrodes) increases the efficiency of nitrate electroreduction.

When the experiment was conducted for 7 h almost all nitrate ions in the solution have been converted with 65.31% selectivity for N_2 . This shows how advantageous the new modified electrode FTO/MWCNT-Cu is. Moreover, results of XRD and EDS for fresh and used FTO/MWCNT-Cu electrode showed higher stability of this electrode upon recovery and reuse. Nitrate reduction efficiency for the same electrode remained unchanged for three different consecutive electrolysis experiments at -1.80 V for 2 h each.

In comparison with other electrodes in literature, the FTO/MWCNT-Cu electrode is highly promising, due to its stability, nitrogen selectivity and efficiency. It is recommended to use this electrode for water purification from nitrate, as a simple and efficient catalyst for nitrate electroreduction system at low voltage.

Chapter One

Introduction

Chapter One

Introduction

1.1 The Imbalance of the Nitrogen Cycle

The bio geochemical nitrogen cycle involves both abiotic and biological processes where various oxidative and reductive processes occur. Nitrogen can be found mainly in several oxidation states such as in ammonia (3-) and nitrate (5+) [1]. A simplified scheme of the nitrogen cycle is shown in Figure 1.1. One of the important nitrogen compounds in the cycle is nitrate, which is fixed from the environment by nitrogen fixing microorganisms, plants and industrial processes [2].

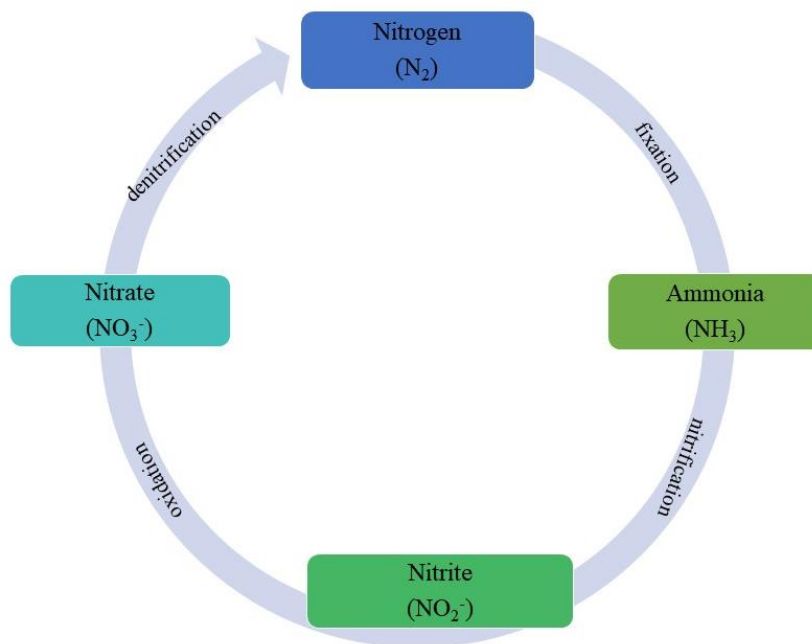


Figure 1.1: Simplified scheme for nitrogen cycle.

A nitrogen fixation process transforms the atmospheric nitrogen into ammonia, after that a nitrification process converts it to nitrite which is

further oxidized to nitrate. When absorbed by plants, nitrates ions undergo some plant reactions and are then taken by animals. When humans and animals die and decompose, nitrates will go back to nature by microbial degradation, which will be further reduced to nitrogen through the denitrification process [3].

The increase in human activities affect the equilibrium of the nitrogen cycle [4]. The imbalance of the natural nitrogen cycle and the effective administration of it in water is one of the 21st century challenges [5]. Contamination of surface and ground water with nitrate (NO_3^-) is one of the most serious global challenges [6]. Many areas in Palestine suffer from this problem [7, 8]. Consequently, people may consume water with nitrate concentrations above the regulated limits.

Nitrate contamination of ground water all over the world, has been recorded in the range ($50 - 100 \text{ mg L}^{-1} \text{ NO}_3^-$), and may reach 500 mg L^{-1} in some region of South Africa [9]. In Palestine nitrate contamination reaches $200 \text{ mg L}^{-1} \text{ NO}_3^-$ in more than one region in West Bank [8]. The average value of nitrate contamination in Gaza Strip was recorded to be $\sim 200 \text{ mg L}^{-1} \text{ NO}_3^-$ [7]. Nitrate concentrations in aquatic water have increased due to human activities. Although the massive use of fertilizers in agriculture, industrial wastewater and domestic water are the main sources [10-14], nitrate also comes from nuclear industries in some countries [15, 16].

1.2 Environmental and Health Risks

Because of their metabolic reduction to nitrites, high concentrations of nitrates in drinking water can cause severe health issues to humans. Nitrate reduction takes place in the saliva of people of all age groups, but particularly in infant gastrointestinal tract. Nitrites in the red blood cells react with hemoglobin to form methaemoglobin, which is unable to bind to oxygen, leading to cyanosis and methaemoglobinaemia “blue baby syndrome” in infants [17-24], liver disease and cancer [25-27].

High concentration of nitrate ions may also cause eutrophication of seas, rivers and lakes that appear through uncontrolled growth of algae [28, 29]. Therefore, developing an efficient technology for nitrate removal from water at large and small scales is needed.

1.3 Regulations and Recommendations

The main source of human exposure to nitrate is drinking water. In order to minimize the health risk of nitrate contamination, World Health Organization (WHO) has set a maximum limit for nitrate concentrations in surface and groundwater to 50 mg L^{-1} expressed as NO_3^- [30].

1.4 Nitrate Removal Methods

Various methods have been proposed for nitrate removal from contaminated water such as:

1.4.1 Biological Methods

The biological method is considered as a good method of choice [31, 32]. However, this method is slow, difficult to control, produces organic residues [33-35] and cannot be used for concentrations larger than 1000 mg L⁻¹ of NO₃⁻, since higher ones can be poisonous to the bacteria [32-34]. High investments costs and technical limitations in monitoring the process parameters are considered to be the major shortcomings for a large-scale application [29].

1.4.2 Physical Methods

Physical methods include ionic exchange by resins [36], reverse osmosis [34, 37, 38], electrodialysis [39], coagulation and flocculation [40]. These methods require regular regeneration and are considered expensive and lead to concentrated nitrate effluents since nitrates are only separated, not destroyed [34, 37, 41, 42].

1.4.3 Chemical Reduction

Chemical reduction, generally with hydrogen, which is a difficult gas to handle [43-45], in the presence of metal catalysts such as aluminium, amalgam, or zero-valence iron powder [34]. This method requires large amounts of metals and may produce undesirable by-products, such as nitrite and ammonium [18, 45-47].

1.4.4 Electrochemical Reduction

Electrochemical reduction technology was developed by Olin for the treatment of aqueous solutions containing hazardous chemicals such as oxynitrogen, like nitrates (NO_3^-), nitrites (NO_2^-) and/or oxyhalides such as chlorite (ClO_2^-) and chlorine dioxide (ClO_2) [48-50]. Electrocatalytic processes have been extensively studied recently [16, 51-54]. In the 1980s, nitrate electroreduction was considered as a promising method for recycling caustic solutions of radioactive wastes with high nitrate concentrations [53, 55, 56]. More recently, this method has been used to treat groundwater, ion-exchange brines, municipal wastewater and urine [57-60].

Electrochemical methods could be applied to large nitrate concentrations with simple reactor configuration, producing no sludge and requiring no start-up period, which lowers the costs [57, 61]. Therefore, electrochemical methods may help in nitrate de-contamination [62].

1.4.4.1 Electroreduction Processes

In electrocatalysis, reactions occur at the electrode/reactant interface. The reaction can be improved by a higher charge transfer between the electrodes and the electrolyte [63].

Nitrate electrocatalytic reduction occurs via three processes [64]:

- (i) Addition of electrocatalytically active ions to the solution being treated [65].
- (ii) Catalyst immobilization on the cathode surface [66].

(iii) Electroreduction catalysed directly on solid electrodes [16, 54, 67, 68].

1.4.4.2 Electrochemical Cell Designs for Denitrification

Nitrate electroreduction is normally carried out in different designs of electrolytic cells, each with two electrodes at least:

Undivided Electrochemical Cells:

These involve one-chamber cells without separators between the anode and the cathode reaction products. In these reactors, the overall faradaic efficiency may decrease as some of the reduced species may be re-oxidized at the anode [69, 70].

Divided Electrolytic Cells:

These cells have more than one chamber, with ion exchange membrane (or salt bridges) between the anodic and the cathodic half-cells (catholyte compartment and anolyte compartment). In the catholyte compartment the aqueous solution is added, while in the anolyte compartment a conductive electrolyte is added [71].

In divided cells ions flow from one half-cell to other half-cell with no mixing between solutions [72]. Thus, cationic exchange membrane keeps the nitrite (reduced product of nitrate) away from the anode. The reduced ions cannot be re-oxidized and the faradaic efficiency increases [72]. For these reasons, divided electrochemical cells save energy [73].

1.4.4.3 Electrolysis Modes

Two distinct operational modes occur in electrolysis, namely galvanostatic and potentiostatic [74].

Galvanostatic Mode:

Galvanostatic electrolysis is performed by the conduction of a constant current density (j in mAcm^{-2}) through electrochemical cell with only two electrodes. Galvanostatic system is favoured in industrial applications due to its ease of operation. However, the faradaic efficiency is lowered here by competitive reactions in the absence of potential reference control [75-77].

Potentiostatic Mode:

In potentiostatic electrolysis a constant electric potential (E in V) is used through the electrochemical cell with three electrodes: a reference electrode, a counter electrode and a working electrode (the cathode) at which electroreduction occurs. In this type, only needed reactions can be selectively conducted based on potential suitability [78].

However, the nitrate reduction needs potentials slightly higher than theoretically needed (over-potentials), due to thermodynamic reasons [79]. The over potential is needed to overcome high activation energy [80-82]. In this type, the nitrate reduction rate is slower than in galvanostatic system, due to the high activation energy.

1.4.4.4 Performance of Electrochemical Reduction of Nitrate

Nitrate electroreduction efficiency and selectivity depend on several parameters such as electrode material [33, 83], applied current or potential [33, 83], electrolyte pH [83, 84], temperature [84], time [83, 84], and electrode separation distance (D) [28, 85]. Mass transfer and nitrate concentration also affect efficiency and selectivity, by affecting the diffusion rate in solution to cathode, as explained by Fick's law [81, 86, 87]. Type and concentration of electrolyte in nitrate solution also affect the process [84, 88]. Therefore, different electrolytes have been investigated such as NaCl [89, 90], Na₂SO₄ [73, 91, 92], HClO₄ [93, 94] and NaOH [95, 96].

As can be noted, there are no unified approaches to the nitrate electroreduction parameters. Literature shows different philosophies with irreproducibility and inconsistency in results and discussions. Literature reviewing leads to no unified practices by researchers. Therefore, in order to design a practical nitrate electroreduction system, it is important to study the effect of different variables listed above on the experiment.

Our major goal here is to prepare an electrode with a high surface area. The relative amount of free surface catalytic sites on the electrodes determines the achievable reaction rate when treating nitrate solutions of high concentrations [97]. Enhancing the electrode surface for nitrate selectively over co-occurring anions, and optimizing the surface area of the electrodes, are necessary. Electrolysis with no catalysts will also be assessed here. All

these issues will be investigated in this work, in order to reach a system with optimal efficiency in nitrate electroreduction.

1.4.4.5 Inorganic Basics of Nitrate Electroreduction

The lowest unoccupied molecular orbital (LUMO, π^*) of nitrate has a high energy level. Therefore, it is difficult to add electronic charges to the LUMO in the nitrate ion. This increases the activation energy and slows down the reduction reaction [80-82]. Therefore, the cathode potential must be sufficiently high to add electrons to the (LUMO) of nitrate, (Figure 1.2) [98].

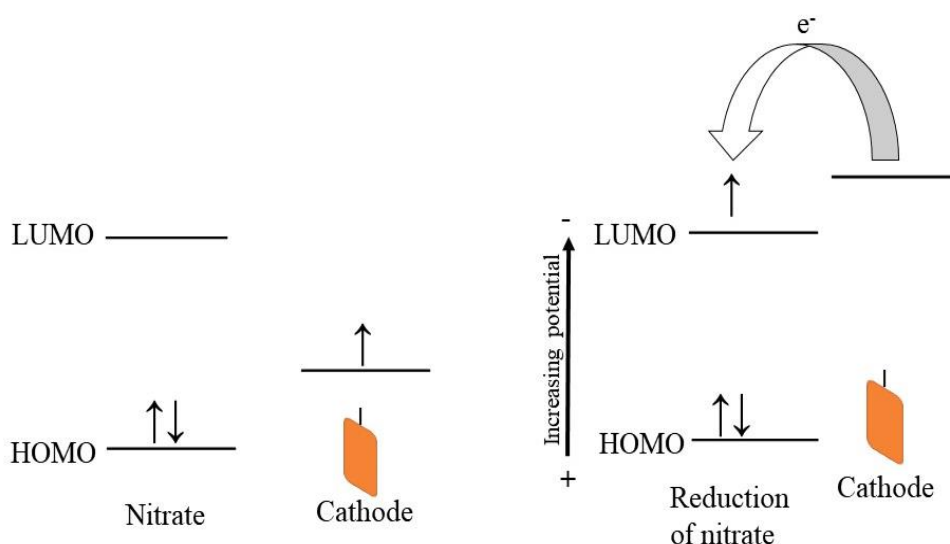


Figure 1.2: Molecular orbitals during electroreduction of nitrate (reproduced based on [98]).

Metals with heavily occupied or partially filled d-orbital shells (Cu, Ag, Pt, etc.) can promote electrochemical NO_3^- reduction, depending on the difference in d-orbital energy levels of those metals and LUMO for the nitrate [99].

1.4.4.6 Copper Catalyst

In addition to its low cost, copper is known as the most active metal in nitrate electroreduction [100]. However, using copper cathodes in water treatment is restricted due to lack of stability (corrosion and leaching) and because they generate ammonia as main by-product [101]. To date, numerous attempts have been done to design Cu-based electrocatalysts for nitrate reduction [6]. Different recent attempts on electrodes modification for nitrate electroreduction, especially Cu-based electrocatalysts will be discussed in the next Chapter.

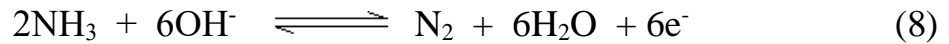
1.4.4.7 Nitrate Electroreduction Products and Intermediates

The main reactions with standard reduction potentials (E°) values in nitrate electrochemical reduction, are given in Table 1.1 [102-104]. Nitrate electroreduction is a complex process [100], but nitrate electrochemical reduction is normally described by reactions No. (2) and (3) [105] in Table 1.1. Nitrate reduction to harmless nitrogen gas is the ultimate objective of electrochemical research [6]. Ammonia and nitrite commonly occur as two main products. This lowers electrochemical denitrification efficiency [6, 86]. Other products may also occur such as NH_2OH , NO_2 , NO , N_2O and NH_2NH_2 [6].

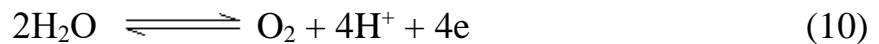
Table 1.1: Main cathodic reactions in electrochemical reduction of aqueous nitrates and their standard E° values [102-104].

No.	Cathodic Reaction	E°
(1)	$\text{NO}_3^- + \text{H}_2\text{O} + 2 e^- \rightleftharpoons \text{NO}_2^- + 2\text{OH}^-$	0.01 V
(2)	$\text{NO}_3^- + 3\text{H}_2\text{O} + 5 e^- \rightleftharpoons 1/2 \text{N}_2 + 6\text{OH}^-$	0.26 V
(3)	$\text{NO}_3^- + 6\text{H}_2\text{O} + 8 e^- \rightleftharpoons \text{NH}_3 + 9\text{OH}^-$	-0.12 V
(4)	$\text{NO}_2^- + 5\text{H}_2\text{O} + 6 e^- \rightleftharpoons \text{NH}_3 + 7\text{OH}^-$	-0.16 V
(5)	$\text{NO}_2^- + 4\text{H}_2\text{O} + 4 e^- \rightleftharpoons \text{NH}_2\text{OH} + 5\text{OH}^-$	-0.45 V
(6)	$2\text{NO}_2^- + 4\text{H}_2\text{O} + 6 e^- \rightleftharpoons \text{N}_2 + 8\text{OH}^-$	0.41 V
(7)	$\text{NO}_2^- + \text{H}_2\text{O} + 2 e^- \rightleftharpoons \text{NO} + 2\text{OH}^-$	0.46 V

Nitrate removal by electroreduction is achieved by direct reaction of electrons from cathode surface with the nitrate to form nitrogen gas and hydroxyl ions (reaction No. 2) [106]. On the other hand indirect reduction processes may take place, especially the oxidation of ammonia on the anode (reaction No. 8) and reduction of nitrite to nitrogen on the cathodic side (reaction No. 6) [28, 107].



Additional electrochemical reactions (No. 9 and 10) may also take place



1.5 Thesis outline

Contents of thesis Chapters are described below:

*Chapter one provides a brief introduction about the source of nitrate in water, health effects, fundamental theory and rationale for using electroreduction.

*Chapter two presents a literature review on recent electrocatalysts for the electrochemical reduction of nitrate, focusing mainly on Cu cathode. The objectives of this research are also included in this chapter.

*Chapter three, describes the experimental set-up and methods used for the work done in this thesis.

* Chapter four, summarizes the results and discussions of this work.

*Chapter five, introduces thesis conclusion and suggestions for future works.

Chapter Two
Literature Review

Chapter Two

Literature Review

In 1998 Kaczur wrote a review of the electrochemical reduction of nitrate [108]. A more recent review of the electrochemical reduction of nitrate was made by Haque and Tariq in 2010 [109]. However, this Chapter critically reviews recent works on the modification of electrodes for nitrate electroreduction especially the Cu cathode.

2.1 Classification of Electrode Materials for Nitrate Electroreduction

Many studies have been carried out on the modification of the cathode material and its surface structure in order to improve the performance of the electroreduction systems. Among these materials, copper is known to be the most efficient electrocatalyst for nitrate electroreduction that yield ammonium as a final product [100].

2.1.1 Copper and Related Electrocatalysts

2.1.1.1 Pristine Cu Electrode

Many studies were conducted in nitrate electroreduction by Cu metal electrode [110-113], where ammonia was the main product of nitrate electroreduction [64, 67, 114]. Reyter *et al.* [100], investigated the electrocatalytic behaviour of a pristine Cu electrode for nitrate (0.1 M NO_3^-) in alkaline media (1 M NaOH) by linear sweep voltammetry, at stationary and rotating disc electrodes. The study showed that electroreduction of the

adsorbed nitrate ion on the Cu electrode to nitrite, was the rate determine step for the reduction process. Hydroxylamine appeared as a short-life intermediate product and was immediately reduced to ammonia.

The reaction mechanism of nitrate reduction with a pure copper electrode was studied in (0.1 M NaOH) [33]. The results showed that electrochemical reduction involved intermediate ($\text{N}_2\text{O}_2^{2-}$), which was further reduced to NH_4OH (at potential values lower than -1.4 V) and to N_2 (at ~ -1.3 V), vs. SCE. Galvanostatic nitrate electrolysis on copper electrode, showed that the efficiency increased when using Na_2SO_4 as supporting electrolyte [115]. Electrochemical nitrate reduction, on Cu with selected surface orientations (111) and (100), occurred by different mechanisms in acidic and alkaline media [116]. Cylindrical Cu cathode and anode electrodes, were also described to prevent the electrode deactivation during nitrate electroreduction [113].

2.1.1.2 Cu/X Bimetallic Electrode

To further improve the performance of the Cu electrode, it was modified with different metals, such as:

2.1.1.2.1 Cu/Zn Bimetallic Electrode

Yang *et al.* [117] studied nitrate electroreduction in alkaline solution using various Cu/Zn oxide composite cathodes, deposited on Ti surface by thermal decomposition.

2.1.1.2.2 Cu/Pd Bimetallic Electrode

Compact and porous Cu-Pd alloy films were prepared and examined for nitrate reduction in basic solutions. The porous electrodes showed higher catalytic activity, but higher NO_2^- and NH_3 and lower N_2 amounts were observed [118]. To improve N_2 selectivity of Cu/Pd alloy, Zhang *et al.* [119] electrophoretically deposited carbon nanotube onto Ti sheets. The Cu/Pd alloys were then electrodeposited on the Ti/CNT substrates using various Cu/Pd atomic ratios.

Pronkin *et al.* [15] deposited the active nitrate electroreduction bimetallic Pd/Cu catalysts. Copper was electrochemically deposited onto cylindrical glassy carbon-supported Pd particles. The Cu adlayer onto Pd increased nitrate electroreduction activity.

2.1.1.2.3 Cu/Ni Bimetallic Electrode

Porous Cu/Ni alloy was prepared by Mattarozzi *et al.* [120]. The microporous and spongy Cu/Ni alloys were used in nitrate reduction in basic solutions. Electrodeposition of porous copper onto nickel modified graphite was described. The system was employed in a one-cycle continuous-flow, ammonium was the main product of nitrate reduction process [6].

2.1.1.2.4 Cu/Pt Bimetallic Electrode

Ehrenburg *et al.* [121] used two types of platinum nanoparticles (Pt NPs): cubic NPs with preferential (100) faces and unshaped (polyoriented) NPs. The NPs were supported on glassy carbon and then coated with Cu adatoms,

it was found that Cu adlayer on Pt NPs (100) yielding the more stable, with faster nitrate reduction.

Kinetics and mechanism of nitrate reduction using Pt (1 1 1) and Cu-modified Pt (1 1 1) electrodes were investigated by cyclic voltammetry [122]. Molodikana *et al.* [123] studied the kinetics and mechanism of reduction of nitrite and nitrate using Cu-modified Pt (100) electrode.

Addition of sodium inositol phytate increased Pt-Cu efficiency in nitrate electroreduction in basic media [124]. Stability of copper to oxidation also increased by this addition.

2.1.1.3 Graphene Modified Cu Electrode

Graphene-modified Cu electrodes were prepared by chemical vapor deposition (CVD) of graphene onto copper sheet surfaces [125]. Cyclic voltammetry indicated higher activity than bare copper electrode, in nitrate electroreduction.

2.1.1.4 Polypyrrole Film Modified with Copper Oxide Particles

Hamam *et al.* [126] conducted nitrate electroreduction in a synthesized electrode by chemical polymerization of polypyrrole onto cellulosic substrate. Then they modified the surface of the polypyrrole film by copper oxide particles. Also, reduction of nitrate ion was investigated on a polypyrrole coated copper electrode (PPy/Cu) in acidic aqueous medium [127].

2.1.1.5 Copper Phthalocyanine

Rajmohan *et al.* [128] deposited copper phthalocyanine by impregnation method on two different support materials: multi-walled carbon nanotubes (CuPc/CNT) and carbon black (CuPc/C). Results of cyclic voltammetry showed higher catalytic activity of CuPc/CNT towards nitrate reduction than CuPc.

2.1.1.6 Deposited Cu on Boron Doped Diamond (BDD) Electrode

Copper nanoparticle electrodeposition on Boron doped diamond (BDD) films (supported on silicon) were strongly affected by the film surface treatments with hydrogen and oxygen plasma. Cyclic voltammetry showed that BDD treated with oxygen plasma presented the best response and reproducibility in nitrate reduction [129]. Another attempt for BDD electrode modification has been carried by Ribeiro *et al.* [130], who modified the surface of the electrode by copper photo-electrodeposition process on BDD electrode that was grown on Ti substrate by hot filament chemical vapour deposition. This method gives high density and uniformity of the deposited copper all over crystal faces.

2.1.1.7 Pd–Cu/ γ Al₂O₃

Pd–Cu/ γ Al₂O₃ catalyst were prepared by impregnation method and 1.0 g/L of it was added to denitrification cell with two graphite plates as the cathode and anode [131]. This catalyst enhanced the nitrate removal efficiency and N₂ selectivity.

2.1.2 Other Electrocatalysts

Attempts were made to prepare nitrate electroreduction electrodes, with no Cu. The target was to increase N_2 selectively, and reaction rate with minimal energy spending [56]. Various materials have been examined, such as Pt [122], Pd [132], Rh [92, 133, 134], Ni [53, 114, 135], Ag [136], Ti [89, 90, 137], Pb [64, 138], Zn [138], Ru [139], Ir [68], Sn [96], Al [73, 85] and Fe [73, 84, 85]. Alloys of different materials have been modified for nitrate electroreduction such as Sn/Pd [15], Cu/Sn [64]. Also, modification of metal surface with different materials such as Sn/Pd, Sn/Pt [137] have been done.

2.2 Thesis Scope

A lot of work and scientific research has been done on nitrate electroreduction, but there are still challenges to achieve highly active, stable and low cost electrocatalysts for nitrate reduction that can be applied in different aqueous media.

In this work, attention is paid to increasing the electrode surface area by preparing nanocomposite electrodes. Composite electrodes are designed to lower the cost of materials while improving the kinetics of nitrate reduction. Nanoparticles provide higher catalytic surface areas, which are critical for speeding up electrochemical nitrate reduction. For these purposes, Cu nanoparticles will be immobilized on stable conductive materials (fluorine-doped tin oxide (FTO), graphite and multi-walled carbon nanotubes (MWCNTs)).

Different supporting materials have been used in the electrode preparations for nitrate electroreduction such as pyrolytic graphite [93], glassy carbon [92, 95] and boron doped diamond [96]. In the present work, MWCNTs films were deposited onto conductive fluorine-doped tin oxide (FTO/glass) plates. To our knowledge, FTO/glass has not been described as a substrate for electrodes in electroreduction experiments. It was chosen here due to its high stability, low resistance, safety and availability.

Carbon nanotubes (CNTs) have recently been used due to their special structural, electrical, mechanical, optical and magnetic properties in various fields of research and applications [140, 141], such as composite matrices with improved properties and performance [142, 143]. CNTs diameters range between 1-100 nm and can be up to millimetres long [144]. CNTs with single layers are called single-walled CNTs (SWCNTs), and those with multi-layers, are called multi-walled CNTs (MWCNTs) [145, 146]. An effective and economic way to prepare well dispersed Cu-MWCNTs composite is reported here.

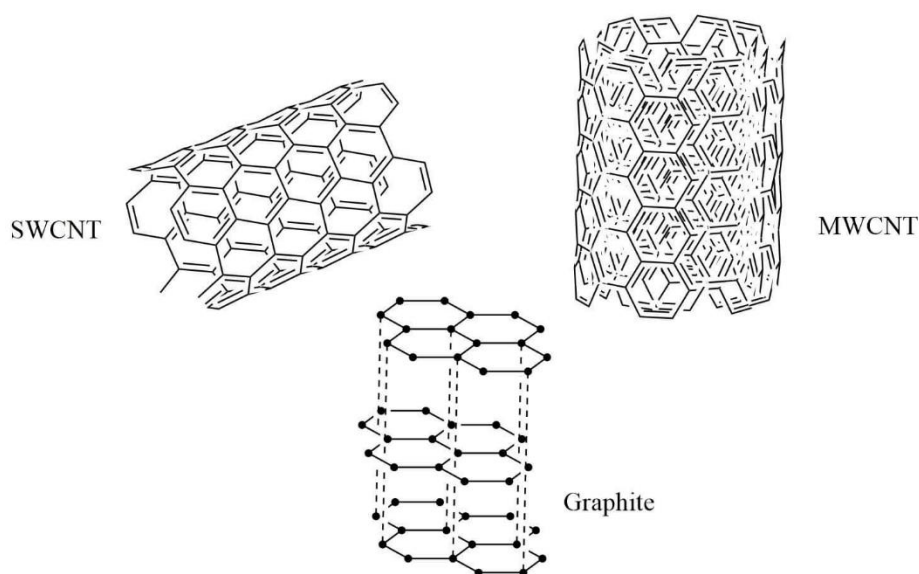


Figure 2.1: Structures of various graphitic materials.

Graphite is also examined here for electrode preparation, because it is an abundant carbon material with high conductivity and specific surface area. Furthermore, graphite may provide the devices with long-term stability and improve charge transfer in the system [146, 147]. Figure 2.1 shows the structures of SWCNT, MWCNT and graphite.

In this study FTO/Glass has been used as a substrate for copper nanoparticles in three different ways: direct electrodeposition, electrodeposition on graphite thin film onto FTO/Glass and MWCNT/Cu nanocomposite onto FTO/Glass. The porosity of the carbon substrate materials allows copper nanoparticle formation with limited agglomeration. The supported copper catalysts on the graphite or MWCNTs that have been deposited on FTO/Glass, are anticipated to have soundly good conductivity with high adherence into the pores. In this work, the new modified electrodes were characterized and used for nitrate electroreduction from pre-contaminated solutions.

2.3 Questions of the Study

This study will answer the following questions:

- How to develop low cost electrocatalysts with high activity and stability for nitrate electroreduction?
- How to increase the efficiency with lower electrical power consumption in nitrate electroreduction?

2.4 Objectives

2.4.1 Strategic Objectives

Nitrate contamination of ground water sources is becoming a major problem. This research attempts to find practical and economical way to remove nitrate from water.

2.4.2 Technical Objectives

1. Copper nanoparticles will be electrodeposited on FTO/Glass.
2. Copper nanoparticles will be deposited on graphite thin films supported on FTO/Glass.
3. Nanocomposite of MWCNT_s and Cu nanoparticles will be prepared and supported on FTO/Glass.
4. Characterization of the prepared electrodes by different techniques such as: X-ray Photoelectron Spectroscopy (XPS), Energy-Dispersive Spectroscopy (EDS), X-ray Diffraction (XRD), Scanning Electron Microscopy (SEM), and Cyclic Voltammetry (CV).
5. Catalytic efficiency of the prepared electrodes in aqueous nitrate electroreduction from pre-contaminated aqueous solutions will be studied and critically compared.
6. Effects of different parameters (pH, temperature, contaminant concentration, composition of electrolytic medium, electrolysis potential, hydrodynamics (stirring) of solution, distance between electrodes and time of contact) on electroreduction will be studied.

7. Reproducibility and efficiency of the prepared catalyst electrodes on nitrate electroreduction, will be investigated.
8. Long term stability of the prepared electrodes will be studied.

2.5 Assumptions

Higher real electrode surface area is assumed to give greater contact of electrolyte with the electrode surface. The use of nanoparticles and MWCNTs provide high catalytic surface. This should improve the electrode performance. This work suggests that preparation of the modified electrode by electrodeposition of copper nanoparticles on graphite substrate and applying MWCNT-Cu nanocomposite on FTO substrate will provide a new way for electroreduction of nitrates in acidic or basic media, as well as in neutral media. The good contact between the copper nanoparticles with graphite and MWCNTs should yield a highly stable catalyst system.

2.6 Significance and Novelty

Nitrate contamination of ground and surface water is a serious global problem. In this work, removal of nitrate ions from water will be conducted by practical and economic processes. Electroreduction on a newly modified highly porous cathode material, prepared by electrodeposition of copper nanoparticles on FTO/Glass is relevant to the de-nitration field. Copper electrodeposition on Graphite/FTO/Glass, and MWCNT-Cu nanocomposite deposition onto FTO/Glass are also relevant to the field. The present study aims to find an efficient catalyst for water purification from nitrate ion in

a safe economic way with minimal energy consumption. The main target is to reduce the nitrate into a non-hazardous material such as nitrogen gas (N_2). The work, which aims to find practical solutions to remove nitrate from water, is highly valuable to Palestine and other countries, which suffer from water contamination.

Chapter Three

Methodology

Chapter Three

Methodology

3.1 Chemicals and Materials

All chemicals were purchased with analytical grade and used without further purification. Sodium hydroxide and ammonium chloride were purchased from Frutarom. Hydrochloric acid (37%), sulphuric acid (98%), copper nanoparticles were provided by Riedel-de-Haen.

Fluorine doped tin oxide coated glass slide, acetyl acetone, Triton-X-100, ethanol (99%), acetone, isopropyl alcohol, graphite, copper sheets ($\geq 99.5\%$), were purchased from Sigma-Aldrich. Copper sulphate, sodium nitrate, sodium nitrite, sodium sulphate was purchased from Alfa. MWCNTs (HONANO-CNTs-010-0, purity $> 95\%$ (w/w), synthesized by a thermal chemical vapour deposition process, with inner diameter 3-5 nm, and outer diameter 8-15 nm and a length $\sim 12 \mu\text{m}$), were provided from (bjxdkj-technology Company-China).

3.2 Equipment

Potentiostat (Corrtest, China), UV-vis spectrometer (UV-3101PC, Shimadzu), pH meter (Jenway-3510), electrical furnace (Boekel, 107905), four degenerate electrical balance (Radwag-200/2000C/2), atomic absorption spectrometer (Thermo scientific-iCE 3000), ultracentrifuge (Thermo-sorvall lynx 6000), freeze-dryer (Miiirock-85C) and sonicator (Power sonic 405) were used.

Electrode characterizations by scanning electron microscopy (SEM) images, and the X-ray spectroscopy (EDS) measurements, were investigated on a Field Emission SEM (FE-SEM, JEOL JSM-6700F). X-ray diffraction (XRD) measurements were done by PANalytical X'Pert PRO X-ray diffractometer, with Cu K α rays. X-Ray photoelectron spectroscopy (XPS) analysis were made using a Multi Lab 2000 spectrometer with a micro-focusing monochromated Al K α X-ray (1486.6 eV) source. SEM, EDS, XRD and XPS, were conducted at Korean Institute of Energy Research, Daejeon, South Korea.

3.3 Preparation of the Electrodes

3.3.1 Copper Electrodes

Copper sheets were cut into (1 cm \times 5 cm) slides. Before use in experiments, they were immersed in 10% (w/w) of HNO₃ for 10 seconds (s), then they were washed several times with distilled water. These electrodes were named Cu electrodes and used for comparison purposes.

3.3.2 FTO Electrodes

Fluorine doped tin oxide (FTO) sheets were cut into (2 cm \times 5 cm) slides. Prior to use, the slides were sonicated in isopropyl alcohol and in acetone for 5 min each time. They were then washed several times with deionized water. These electrodes were called FTO electrodes, and have been used for further modification and for comparison purposes.

3.3.3 Modified FTO Electrodes

3.3.3.1 FTO Electrodes Modified with Cu

FTO substrate modified directly with Cu were obtained by electrodeposition at room temperature (25 ± 1 °C). Electrodeposition preparations were conducted on electrochemical workstation (Corrtest, Cs350), in a 100 mL electrochemical cell. The electrochemical cell contained three electrodes; standard saturated calomel electrode (SCE) as the reference electrode, Pt plate as a counter electrode and the FTO as working electrode. Different attempts have been made to increase the stability of the deposited electrode:

- a) One method was to deposit Cu from (0.85 M CuSO_4 + 0.55 M H_2SO_4) using cyclic voltammetry. The voltage scan rate was fixed 100 mV/s from 0.25 V to -0.80 V as reported in literature [148]. Deposition by this method was performed for different times (10 cycle, 20 cycle and 30 cycle). Those electrodes were named FTO/Cu-10, FTO/Cu-20, and FTO/Cu-30.
- b) In another method potentiostatic deposition was used by applying -0.80 V for 600 s. Deposition was done firstly using (0.01 M CuSO_4 + 0.10 M KCl) as reported in literature [149], and this gave us an electrode that has been named FTO/Cu-a. Another electrode was prepared by applying -0.80 V for 200 sec, using (0.85 M CuSO_4 + 0.55 M H_2SO_4) and the prepared electrode from this bath was named FTO/Cu-b. The two solutions were pre-purged with high purity N_2 for 5 min to remove O_2 before deposition experiments, and they were

stirred continuously with magnetic stirrer during the depositions. The prepared electrodes were then rinsed with deionized water and ethanol, dried, and stored in a desiccator for further use.

3.3.3.2 FTO Electrodes Modified with Graphite

Graphite nanopowder was well mixed with acetyl acetone, triton X-100 and H₂O at a ratio of 10: 20: 30: 40 to form a slurry. This method was applied in literature for the preparation of FTO electrodes with MWCNT thin film [150]. FTO plates were coated with aluminium foil (2 cm × 1 cm) for protection. Then thin graphite film was applied on hot FTO surface by drop-casting process.

Graphite film with thickness greater than ~111.90 μm, was found to peel off during the electroreduction experiments. Finally, the aluminium foils were removed and those electrodes were sintered for 1 hour (h) at 300 °C, to improve the compactness of the thin film. FTO/Gr name was given for this electrode.

Other attempts to modify electrodes by graphite thin film were done according to different procedures described in literature [151, 152], they didn't give the stable electrodes.

3.3.3.3 FTO/Graphite Electrodes Modified by Cu Nanoparticles

Copper nanoparticles were deposited on graphite by electrochemical deposition at (25 ± 1 °C). Deposition of Cu on the FTO/Gr electrode was done from (0.85 M CuSO₄ + 0.55 M H₂SO₄) at -0.80 V for 600 sec. After the

potentiostatic deposition, the prepared electrode was rinsed with deionized water and ethanol respectively to remove traces of surface impurities. Those electrodes were stored in a desiccator for further use. The modified electrode was named as

FTO/Gr-Cu.

3.3.3.4 FTO Electrodes Modified with Functionalized MWCNTs

Chemical modification of MWCNTs was done by sonicating (1.00 g) of MWCNTs in 80 mL 3:1 (v/v) mixture of H₂SO₄ 95%, HNO₃ 70% at 60 °C for 6 h, analogous to another work [148]. After that, 200 mL cooled deionized water was added dropwise to the prepared suspension. This suspension was centrifuged for 20 min at 8000 rounds per minute. Washing of the modified MWCNTs with deionized water, and centrifuging them with the same above procedure was repeated many times for neutral pH solution. The neutral suspension was then transferred to a -20 °C freezer for 24 h, followed by freeze-drying for 24 h and stored in a glass container in desiccator, for subsequent experiments.

MWCNTs functionalization by oxygen-containing groups, enhances its exfoliation and dispersion in polar media [153, 154]. This modification was done in order to make MWCNTs useful in further surface modification.

Fabrication of the surface of FTO electrode with MWCNTs was done by spray coating process. For the preparation of the spraying suspension, 1.00 mg of modified MWCNTs were mixed with 20 mL anhydrous ethanol. The mixture was sonicated for 15 min in a bath-type sonicator. The

suspension was poured in a glass hand sprayer, and then sprayed on hot FTO substrates, after (2 cm × 1 cm) section of each FTO plate was covered using an aluminium foil (spraying 20 time for each FTO plate from the same distance). The modified electrode was named as FTO/MWCNT. Fabrication by this method using unmodified MWCNTs described in earlier work [155] didn't give stable thin films on FTO surfaces.

Other attempts to apply MWCNTs on FTO substrate, according to different literatures [150, 156-158], didn't give stable electrodes.

3.3.3.5 FTO/MWCNTs Electrodes Modified with Cu

The electrode was prepared by spray coating of MWCNTs-Cu suspension on hot FTO substrate. MWCNT-Cu nanocomposite suspension was prepared by a new modified, simple and cheap method as follows:

- a) Commercial Cu nanoparticles (1.00 g) were placed on filter paper in Buchner funnel and washed with 10% (w/w) HNO₃, deionized water and ethanol.
- b) Certain amounts of Cu nanoparticles and 2.00 mg of functionalized MWCNTs were placed in 150 mL conical flask containing 40 mL pure ethanol 97%.
- c) The prepared suspension was sonicated for 15 min and allowed to stand 24 h at room temperature.
- d) The above mixed slurry was transferred to a fragrance spray glass bottle. Then hot FTO substrates with (2 cm × 1 cm) section of each plate covered using an aluminium foil, was coated with this

suspension by spray coating method (spraying 20 time for each FTO plate). This electrode was named FTO/MWCNT-Cu.

3.4 Characterization of the Electrodes

3.4.1 Scanning Electron Microscopy (SEM)

Scanning electron microscopy analysis was conducted for our prepared electrodes (FTO/Cu-a, FTO/Cu-b, FTO/Gr, FTO/Gr-Cu, FTO/MWCNT, fresh and used FTO/MWCNT-Cu). This was to study the morphologies (surface textures) of different electrodes.

3.4.2 Energy-Dispersive X-ray Analysis (EDS)

EDS for elemental analysis of the prepared electrodes (FTO/Cu-a, FTO/Cu-b, FTO/Gr, FTO/Gr-Cu, FTO/MWCNT, fresh and used FTO/MWCNT-Cu), was conducted.

3.4.3 X-Ray Diffraction (XRD)

The microstructure for the prepared electrodes (FTO/Cu-a, FTO/Cu-b, FTO/Gr, FTO/Gr-Cu, FTO/MWCNT, fresh and used FTO/MWCNT-Cu) was examined by XRD measurements.

The particles sizes were calculated by using Debye-Scherrer's equation (3.1):

$$S = 0.9 \lambda / \beta \cos \theta \dots\dots\dots (3.1)$$

in which (S) is the average particle size (Å), (λ) is the X-ray wavelength of Cu K α radiation ($\lambda = 1.5406 \text{ \AA}$), (β) is the full-width at half-maxima (FWHM) in

radians, and (θ) is the diffraction angle (degree) [159-161]. The structure and the orientations of crystal were measured by using Brag's law (3.2):

$$2d \sin \theta = n \lambda \dots\dots\dots (3.2)$$

in which (d) is the spacing of the crystal layers, (n) is an integer, (θ) is the incident angle [161], and by Miller indices equation (3.3):

$$d_{hkl} = a/(h^2 + k^2 + \ell^2)^{-1/2} \dots\dots\dots(3.3)$$

to specify directions and planes of crystal, where (a) is the lattice constant and (h. k. ℓ) is the lattice planes [161].

3.4.4 X-Ray Photoelectron Spectroscopy (XPS)

The chemical composition and surface oxidation states was investigated for our modified electrodes (FTO/Cu-a, FTO/Cu-b, FTO/Gr, FTO/Gr-Cu, FTO/MWCNT, fresh and used FTO/MWCNT-Cu) using XPS.

3.4.5 Voltammetric Investigation of Nitrate Reduction

Cyclic voltammetry (CV) studies were done in a three-electrode cell. The prepared electrodes were used as working electrodes, saturated calomel electrode (SCE) as reference electrode and the counter electrode was a platinum plate. The experiments were carried out at 25 ± 1 °C. Solutions were deoxygenated by bubbling with nitrogen prior to the electrochemical experiments. In each experiment, the working electrode was one of (FTO, Cu, FTO/Cu-b, FTO/Gr, FTO/Gr-Cu, FTO/MWCNT and FTO/MWCNT-Cu). Each working electrode was cycled from -1.80 V to -0.80 V at a scan rate of 20 mVs⁻¹.

The response of the prepared electrodes was studied in the electrolyte solution 0.05 M Na₂SO₄, and the working solution (0.05 M Na₂SO₄ + 200 mg/L NO₃⁻). Cyclic voltammograms were taken after steady graphs were obtained.

3.5 Electroreduction Experiments and Electrochemical Measurements

3.5.1 Set up of Nitrate Electroreduction Experiments

3.5.1.1 Glassware and Solutions

The glassware was cleaned by a dishwashing liquid and thoroughly washed with deionized water before the experiments. Solutions were prepared with deionized water (resistivity 0.215 MΩ.cm). Fresh (weekly prepared) stock solutions of nitrate, nitrite, and ammonium were made with deionized water and stored at ambient temperature.

Nitrate stock solution (1000 mg/L) was diluted to the desired concentration by supporting electrolyte solution (0.05 M Na₂SO₄) just before use. Working solutions were pre-purged with N₂ gas before each experiment, unless otherwise mentioned.

3.5.1.2 Cell and Electrodes

Nitrate electroreduction experiments were done in a 100 mL glass cell with three electrodes connected to a potentiostat (Corrtest, Cs 350). The reference electrode was SCE, the counter electrode was a platinum sheet,

and in each experiment the working electrode was one of prepared electrodes, see Figure 3.1.

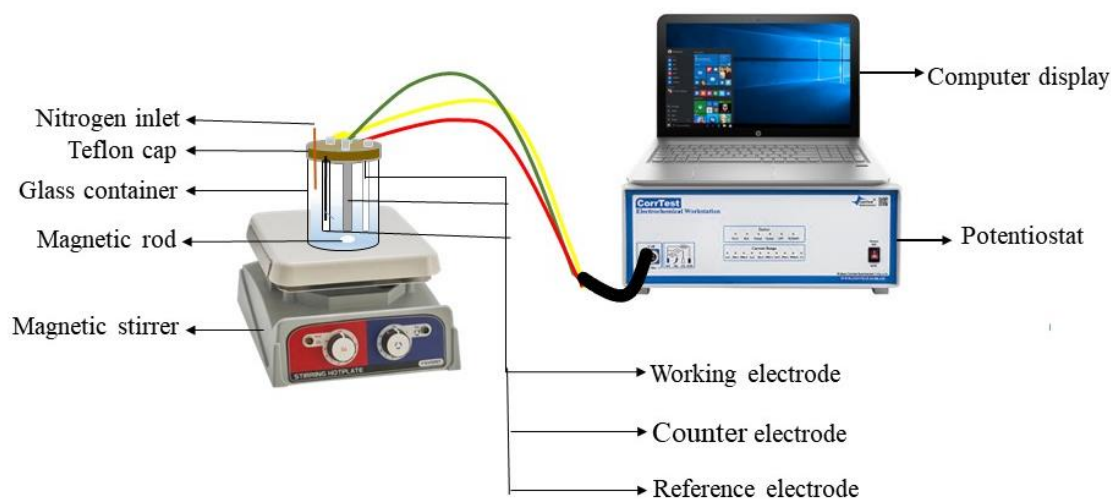


Figure 3.1: Schematic design of the electroreduction system.

A magnetic stirrer was used to stir the solution in the electroreduction experiments. All potentials were measured vs. SCE. Distance between the working and counter electrode was set to 0.75 cm. The geometrical working area of each cathode was 7.60 cm^2 , unless otherwise stated.

3.5.1.3 Analysis Methods

At specific time intervals, certain volumes of samples from the reaction mixture were withdrawn from the electrolytic cell by dropper. Suitable dilutions were done for the samples. The nitrate concentration was then determined by its spectral absorbance at 220 nm. The ammonia and nitrite concentrations were determined by the phenate method (640 nm) and naphthyl ethylenediamine method (543 nm), respectively, using UV-vis spectrophotometry. These methods are standard and described elsewhere

[162]. A calibration curve using standard solutions was used for quantitative determination of each compound.

3.5.2 Effect of Different Factors on Nitrate Electroreduction

3.5.2.1 Effect of Electrode Type

Nitrate electroreduction experiments with different prepared electrodes (Cu, FTO, FTO/Cu-b, FTO/Gr, FTO/Gr-Cu, FTO/MWCNT and FTO/MWCNT-Cu), were conducted in the above described electrochemical cell. In each experiment 70 mL of the working solution (0.05 M Na₂SO₄ + 200 mg/L NO₃) was used with -1.80 V vs. SCE as working potential for 2 h at intrinsic pH (5.40) and 25 ± 1 °C. At selected time intervals, 1.00 mL of the working solution was taken and diluted to appropriate percent in order to measure nitrate, nitrite and ammonium concentrations in the solutions. FTO/MWCNT-Cu showed the highest electroreduction efficiency. Therefore, this new modified electrode was used for further study throughout this work unless otherwise stated.

3.5.2.2 Effect of Applied Potential

Effect of different applied voltage (-1.50 V, -1.80 V and -2.10 V) on nitrate electroreduction was studied. In each experiment, the working solution was 70 mL (0.05 M Na₂SO₄ + 200 mg/L NO₃⁻). Each experiment was conducted for 2 h, at 25 ± 1 °C. At selected time intervals, 0.50 mL of the working solution was taken from the electrochemical cell, in order to measure nitrate concentration after appropriate dilution.

3.5.2.3 Effect of Electrolyte Type

The effect of the electrolyte type on nitrate electroreduction was investigated by carrying electrochemical nitrate reduction experiments in two different working solutions: (70 mL; .0075 M NaCl + 200 mg/L NO_3^-) and (70 mL; 0.05 M Na_2SO_4 + 200 mg/L NO_3^-). Each experiment was conducted at -1.80 V, for 2 h at intrinsic pH (5.40), and 25 ± 1 °C. At selected time intervals, 1.00 mL of the working solution was taken from the electrochemical cell, in order to measure nitrate, nitrite and ammonium concentration after appropriate dilution. Solution of Na_2SO_4 was chosen as electrolyte in the next experiments.

3.5.2.4 Effect of Electrolyte Concentration

Effect of different concentrations of Na_2SO_4 on nitrate electroreduction was studied. Each experiment was conducted in the electrochemical cell with 70 mL of (0.025 M Na_2SO_4 + 200 mg/L NO_3^- , 0.05 M Na_2SO_4 + 200 mg/L NO_3^- , and 0.10 M Na_2SO_4 + 200 mg/L NO_3^-), at intrinsic pH (5.40), under -1.80 V and 25 ± 1 °C. At selected time intervals, 0.50 mL of the working solution was taken from the electrochemical cell, in order to measure nitrate concentration after appropriate dilution. Na_2SO_4 (0.05 M) was chosen as electrolyte in the next experiments.

3.5.2.5 Effect of Stirring

In all the above experiments, the electrochemical cell was provided with a magnetic stirrer. To study the effect of solution stirring, two experiments

were conducted under intrinsic pH (5.40), -1.80 V, and 25 ± 1 °C for 2 h. The working solution was (70 mL; 0.05 M Na₂SO₄ + 200 mg/L NO₃⁻). One experiment was done while stirring the working solution, the other one was conducted without stirring. After each experiment nitrate concentration was measured.

3.5.2.6 Effect of Distance between Electrodes

The effect of the distance between electrodes on nitrate electroreduction was studied, by conducting two electroreduction experiments of (70 mL; 0.05 M Na₂SO₄ + 200 mg/L NO₃⁻) at intrinsic pH (5.04) and 25 ± 1 °C for 2 h, at -1.80 V. The distance between the working and counter electrode was 0.75 cm in the first experiment, and 3.5 cm in the other. Every 30 min, 0.50 mL of the working solution was taken, and nitrate concentration was measured after the appropriate dilution.

3.5.2.7 Effect of Temperature

The effect of temperature on nitrate electroreduction was studied at 10 °C, 25 °C and 30 °C. Working solutions (70 mL; 200 mg/L NO₃⁻ + 0.05 M Na₂SO₄) were used at intrinsic pH (5.40) and -1.80 V working potential. Nitrate concentration was measured at selected time intervals, by taking 0.50 mL of the working solution and making the needed dilution for it, before measuring.

3.5.2.8 Effect of Initial NO_3^- Concentration

Effect of initial nitrate concentration on the electroreduction process was studied at three different initial concentrations of nitrate (200 mg/L, 600 mg/L and 1000 mg/L) with 0.05 M Na_2SO_4 in each. Each experiment, was conducted for 70 mL of the working solution, using -1.80 V on the working electrode, at intrinsic pH (5.40), and 25 ± 1 °C, for 2 h. Nitrate concentration was measured at selected time intervals, by taking 0.50 mL of the working solution and making the needed dilution for it, before measuring.

3.5.2.9 Effect of Initial pH

The effect of initial pH on nitrate electroreduction was studied, using the working solution (70 mL; 0.05 M Na_2SO_4 + 200 mg/L NO_3^-), by adjusting the initial pH of the working solution with NaOH or H_2SO_4 solutions, to basic (11.10 pH), acidic (2.04 pH) and original (5.40 pH) values. The electroreduction experiments were then conducted for 2 h for each, at -1.80 V and 25 ± 1 °C. Aliquots were taken from the working solution every 15 or 30 min, to find nitrate concentration after the appropriate dilutions.

3.5.2.10 Effect of Electroreduction Time

Potentiostatic electroreduction of 70 mL of nitrate working solution (0.05 M Na_2SO_4 + 200 mg/L NO_3^-), at intrinsic pH (5.40) and 25 ± 1 °C, was conducted at -1.80 V. Aliquots (1.00 mL each) of the working solution were pipetted out at different time intervals until 7 h. Nitrate, nitrite and

ammonium concentrations were measured for the samples after appropriate dilution.

3.5.3 Alkalinity Measurements

The pH of the working solution was periodically measured during the electroreduction of the working solution (70 mL; 0.05 M Na₂SO₄ + 200 mg/L NO₃⁻) at -1.80 V and 25 ± 1 °C, using pH meter (Jenway-3510) at 25 °C.

3.5.4 Performance and Reproducibility of the Modified FTO/MWCNT-Cu Electrode in Nitrate Electroreduction

To study the reproducibility of the modified FTO/MWCNT-Cu electrode, the same electrode was used in three separate experiments of nitrate electroreduction. Each experiment was conducted for 2 h at 25 ± 1 °C. The applied potential was -1.80 V, and the working solution was 70 mL of (0.05 M Na₂SO₄ + 200 mg/L NO₃⁻). Nitrate concentration was measured at the end of each experiment.

Chapter Four

Results and Discussion

Chapter Four

Results and Discussion

4.1 FTO/Cu electrode

FTO/Cu electrodes prepared by Cu deposition from (0.85 M CuSO₄ + 0.55 M H₂SO₄) using cyclic voltammetry, named as FTO/Cu-10, FTO/Cu-20 and FTO/Cu-30, were not used in nitrate electroreduction experiments. That was due to poor adhesion between the Cu thin film and FTO surface.

4.1.1 Characterization

4.1.1.1 SEM Analysis

Figure 4.1 (a), (a[^]), (b) and (b[^]) shows SEM images of the electrode surface and cross sectional area of the electrodes FTO/Cu-a and FTO/Cu-b respectively. These two electrodes were obtained by Cu deposition using different solutions.

Potentiostatic deposition of Cu on FTO surface from (0.01 M CuSO₄ + 0.10 M KCl) at -0.80 V, yielded Cu dendritic form. The Cu dendrites have main trunk with short side branches decorated by small particle accumulates on it. As shown in Figure 4.1 (a).

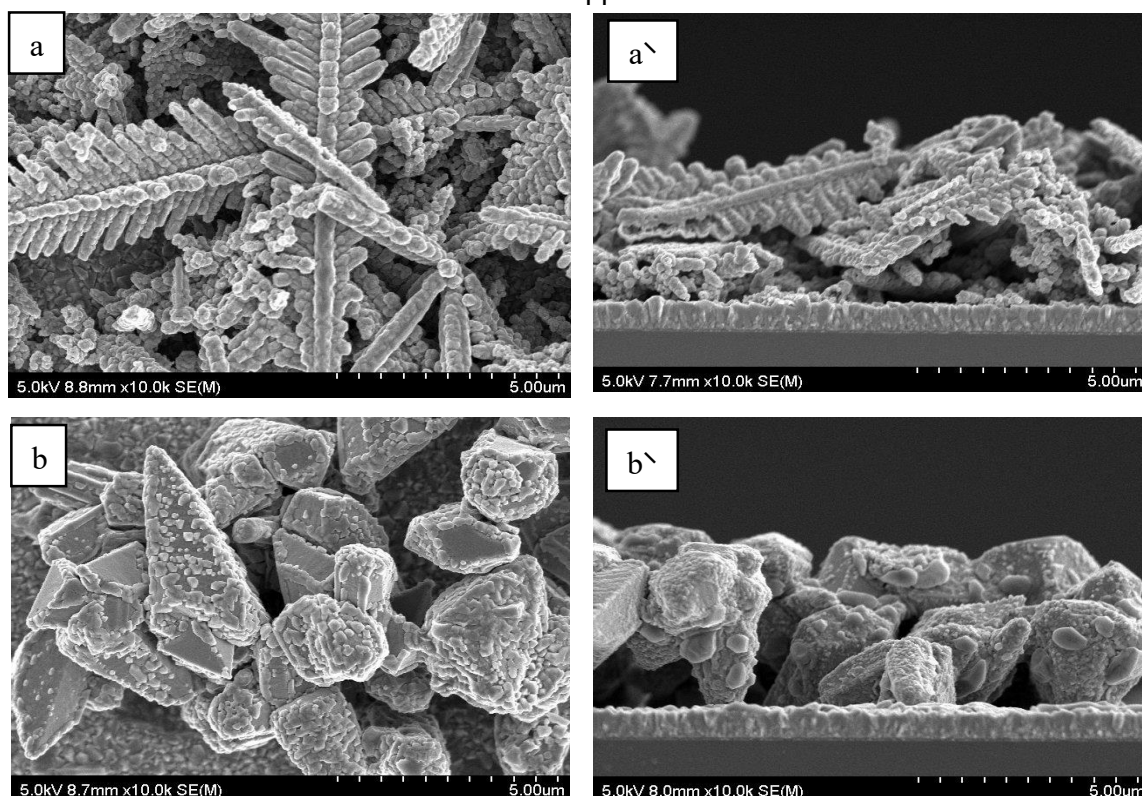


Figure 4.1: SEM micrographs measured for (a) FTO/Cu-a and (b) FTO/Cu-b.

Electrodeposition of Cu on FTO surface from (0.85 M CuSO_4 + 0.55 M H_2SO_4) at -0.80 V, gave Cu film with irregular granular shapes and varying particle sizes of Cu nanoparticles. The average thicknesses of the deposited layer on FTO/Cu-a and FTO/Cu-b, were calculated from cross sectional SEM images to be 4.05 μm and 3.84 μm , respectively.

4.1.1.2 EDS Analysis

The elemental composition of the FTO/Cu-a and FTO/Cu-b films was studied by EDS as shown in Figure 4.2. From the EDS it's clear that the two electrodes contain almost the same weight of Cu, but FTO/Cu-a electrode contains higher percent of oxygen. Other labelled peaks of Sn and O arrive from FTO glass and atmosphere.

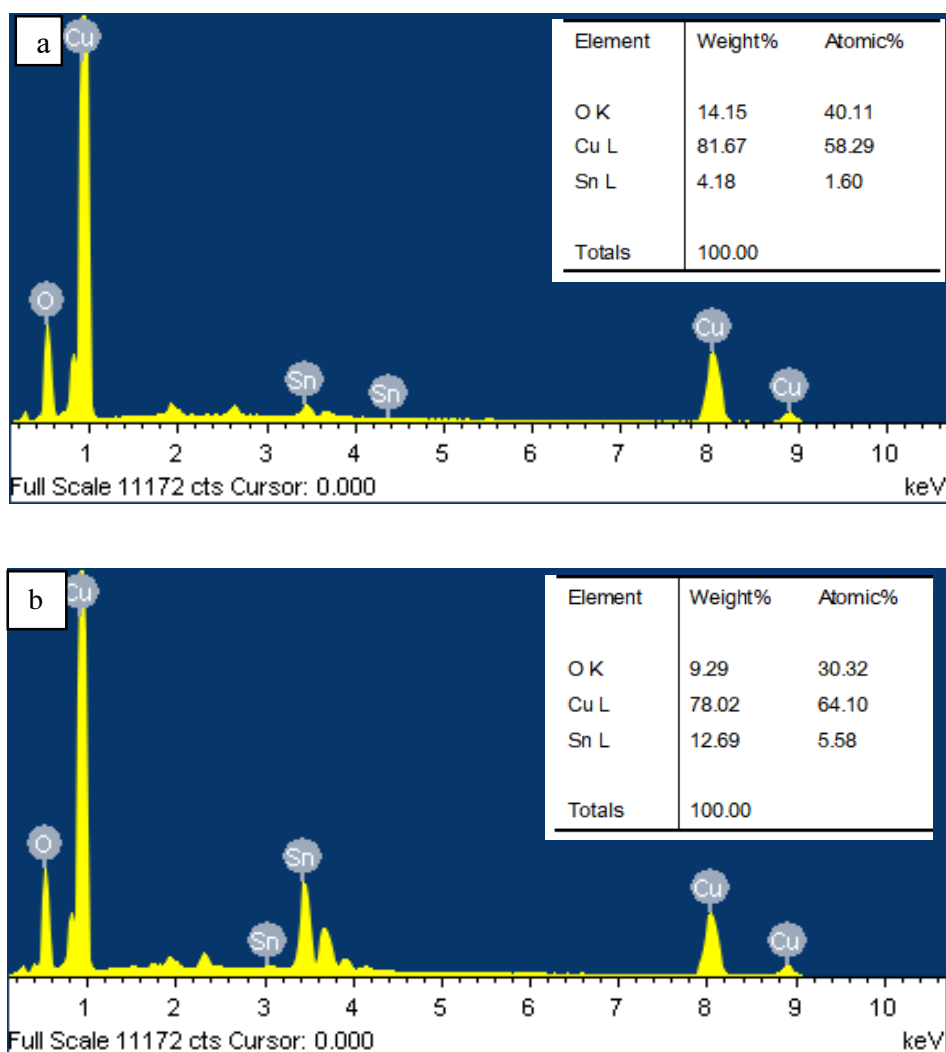


Figure 4.2: EDS spectra measured for (a) FTO/Cu-a, and (b) FTO/Cu-b.

4.1.1.3 XRD Analysis

The crystal structures of FTO/Cu-a and FTO/Cu-b electrodes were studied by XRD analysis, Figure 4.3. In FTO/Cu-a, the signals observed at $2\theta = 36.38^\circ$ (111) and 42.56° (200) are due Cu_2O (JCPDS, 03-0879) [163, 164].

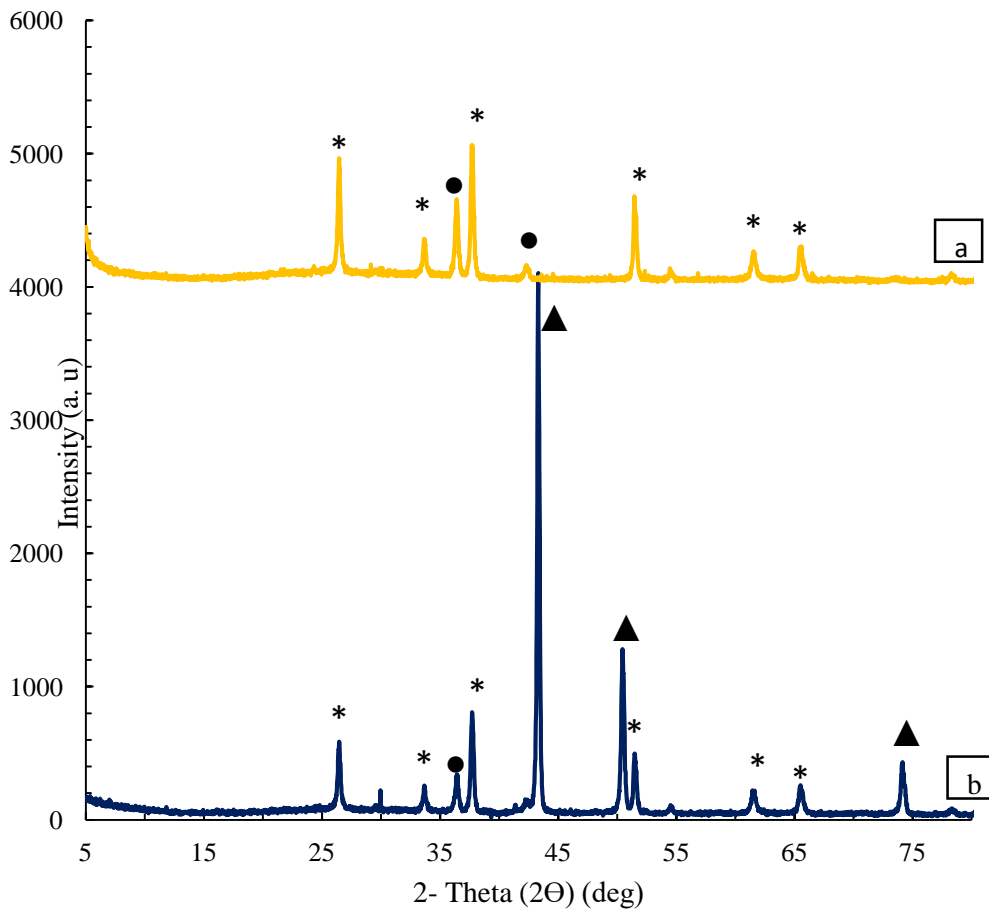
*FTO ▲Cu ●Cu₂O

Figure 4.3: Measured XRD patterns for (a) FTO/Cu-a and (b) FTO/Cu-b.

In the XRD pattern of the electrode FTO/Cu-b, the signal observed at 36.48° (111) is attributed to Cu₂O (JCPDS, 03-0879) [163, 164]. Other signals observed at 43.38° (111), 50.52° (200) and 74.20° (220) are related to Cu (JCPDS, 65-9743) [165, 166]. The average particle size of deposited Cu nanoparticles was found to be 34.20 nm. In Figure 4.3, signals at $2\theta = 26.56^\circ$, 33.76° , 37.68° , 51.56° , 61.68° and 65.68° are related to FTO substrate (JCPDS, 41-1445) [167]. Table 4.1 summarizes results of XRD patterns together with particle sizes for FTO/Cu-a and FTO/Cu-b electrodes.

Table 4.1: Analysis of XRD pattern of FTO/Cu-a and FTO/Cu-b electrodes.

Electrode	$2\theta^\circ$	FWHM	Species	Particle size (nm)	d (Å)	(hkl)
FTO/Cu-a	36.38	0.32	Cu ₂ O	27.30	2.46	(111)
	42.56	0.40	Cu ₂ O	22.25	2.13	(200)
FTO/Cu-b	36.48	0.28	Cu ₂ O	31.21	2.46	(111)
	43.38	0.20	Cu	44.67	2.08	(111)
	50.52	0.28	Cu	32.78	1.80	(200)
	74.20	0.36	Cu	25.16	1.28	(220)

XRD patterns indicate that the deposited film on FTO/Cu-a mostly involves Cu₂O, while FTO/Cu-b mainly involves metallic Cu. Therefore, the prepared electrode FTO/Cu-b was used to study the electrochemical reduction of nitrate. For technical difficulties and transportation limitations, XRD analysis of the prepared electrodes was done after one month of preparation.

4.1.1.4 XPS Analysis

XPS was conducted for further analysis of the deposited film compositions. Figure 4.4, shows XPS spectra of FTO/Cu-a, including high resolutions spectra of the Cu 2p and O 1s peaks. Figure 4.5 also shows XPS spectra for FTO/Cu-b electrode with high resolution spectra of Cu 2p and O 1s spectra included.

The Cu 2p peak in FTO/Cu-a was located at 932.42 eV. In FTO/Cu-b, it is found that the Cu 2p is at 932.08 eV. Cu 2p binding energy fit to Cu 2p^{3/2} and indicates the possibility of the presence of Cu(0), Cu(I) and Cu(II) [168]. It is difficult to differentiate between the binding energies of Cu(0) and Cu(I) by XPS [169-171].

The O 1s peak in the XPS of FTO/Cu-a occurs at 530.77 eV related with the O 1s of Cu_2O [171]. While the O 1s peak of FTO/Cu-b occurs at 532.00 eV may result from other copper oxides or other compounds containing oxygen such as H_2O [171]. The C element detected by XPS is due to the adventitious hydrocarbon from instrument itself.

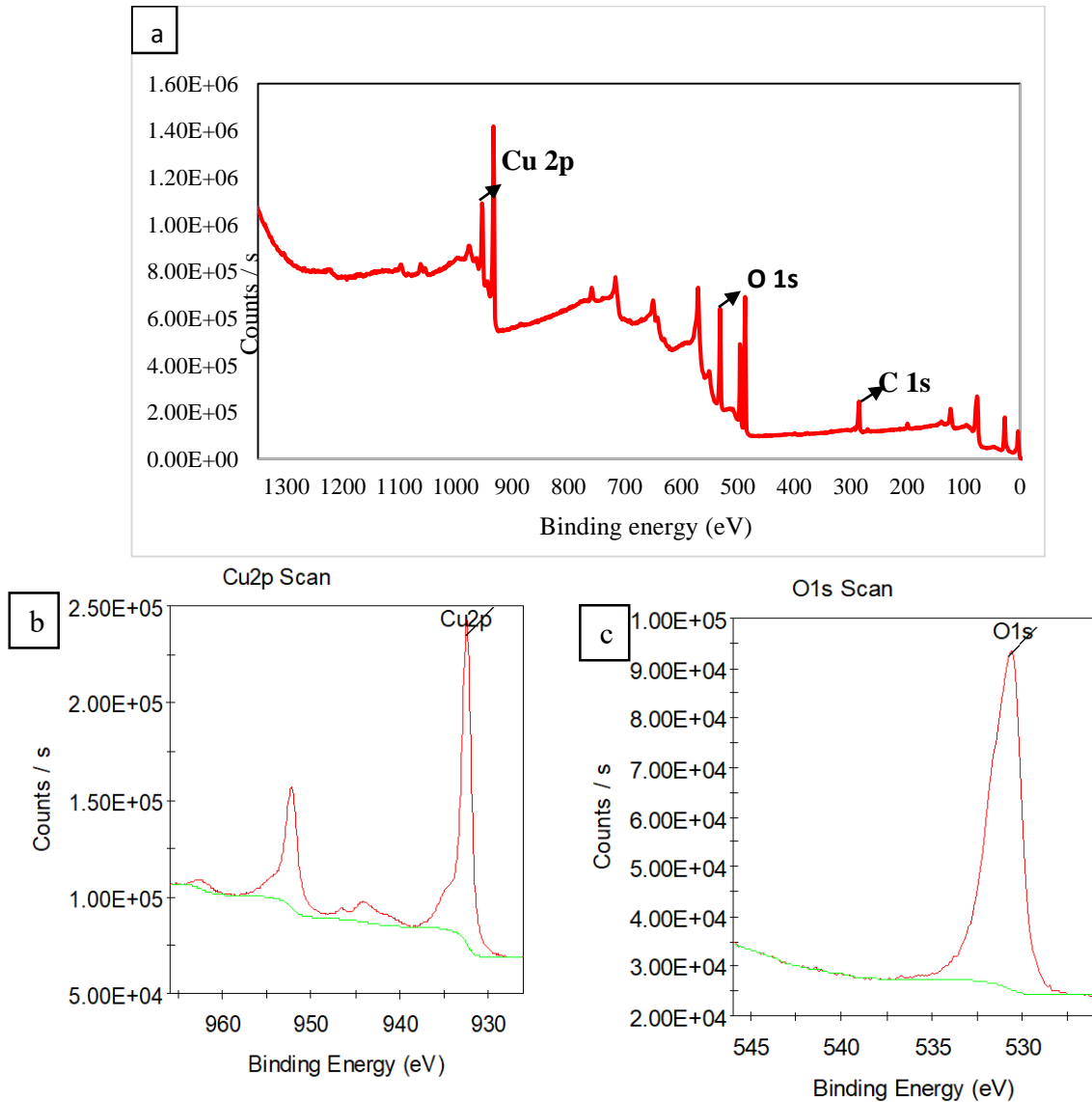


Figure 4.4: Measured XPS spectra for FTO/Cu-a, (a) complete spectrum, (b) copper peak and (c) oxygen peak.

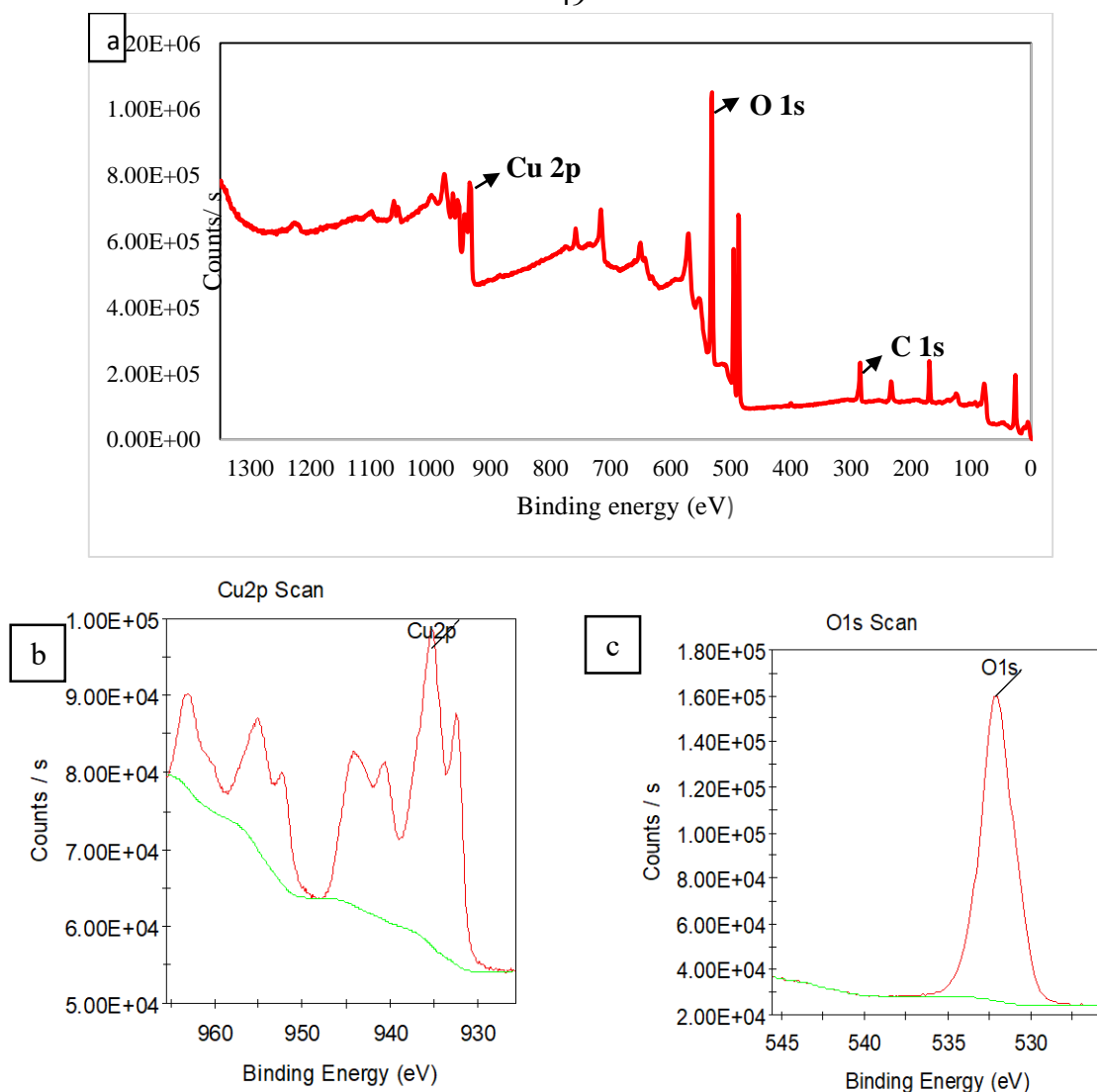
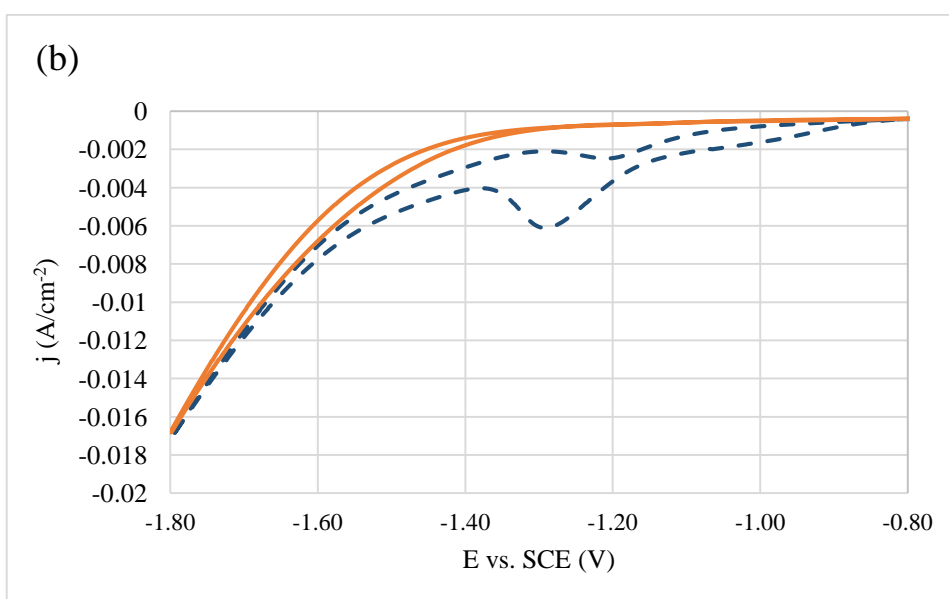
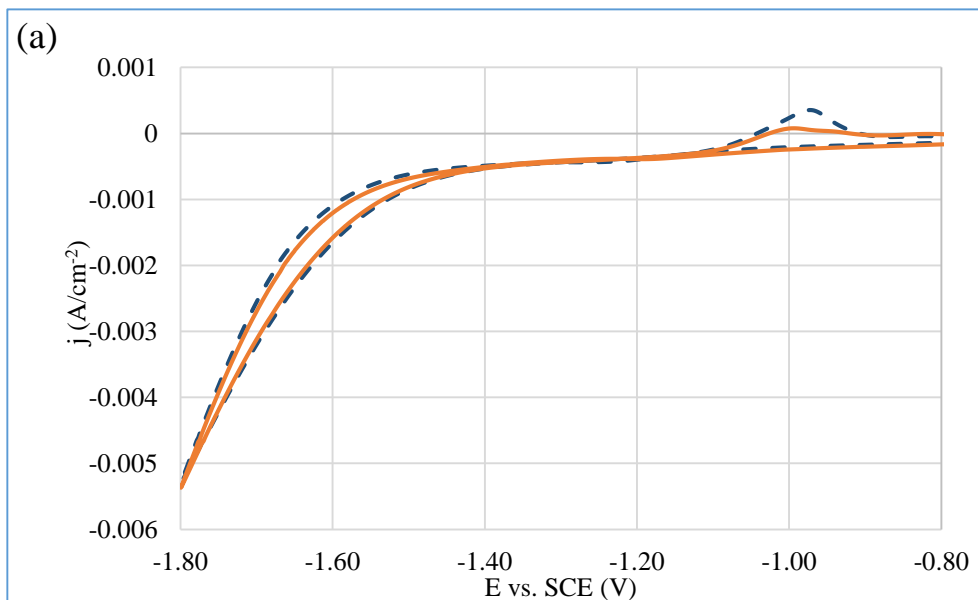


Figure 4.5: Measured XPS spectra for FTO/Cu-b, (a) complete spectrum, (b) copper peak and (c) oxygen peak.

4.1.1.5 Cyclic Voltammetry Investigation

Figure 4.6 (a) shows cyclic voltammograms obtained for FTO in the blank (0.05M Na₂SO₄) compared with the (0.05 M Na₂SO₄ +200 mg/L NO₃⁻). The figure shows slight increase in the reduction current between (-1.50 V and -1.80 V). This indicates the ability of FTO for nitrate reduction, with a very low efficiency. Cyclic voltammograms for Cu in Figure 4.6 (b), show higher

reduction current at all the scan voltages in the working solution compared with the blank solution. At -1.30 V there is also a clear irreversible reduction.



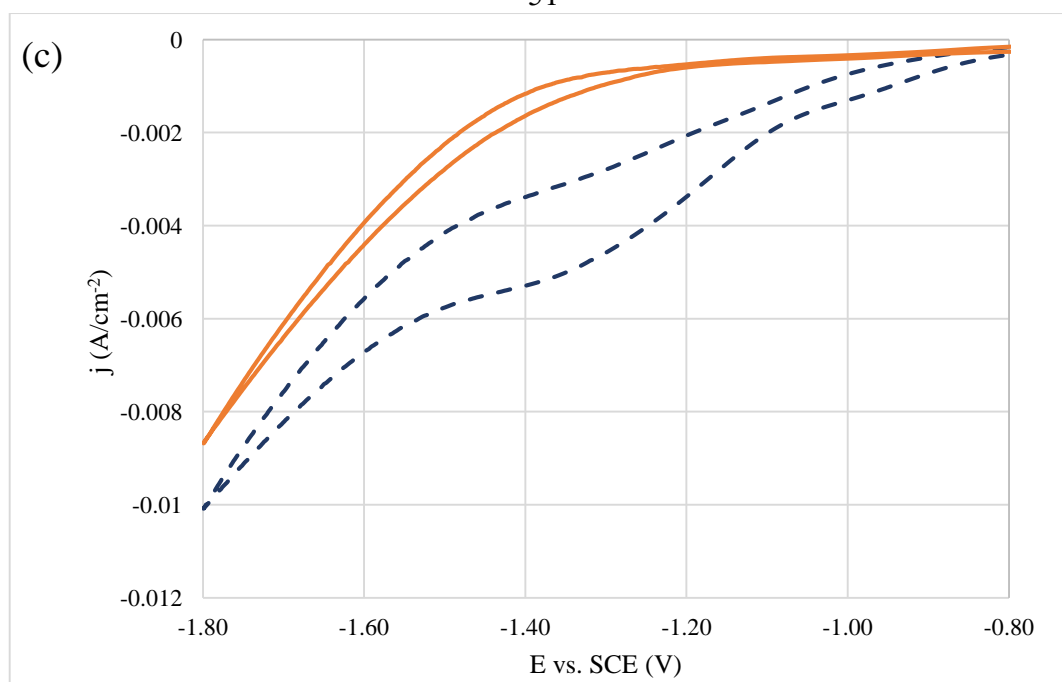


Figure 4.6: Cyclic voltammograms on (a) FTO, (b) Cu and (c) FTO/Cu-b in ——— 0.05 M Na₂SO₄ and in - - - - (0.05 M Na₂SO₄ + 200 mg/L NO₃⁻), scan rate 20 mVs⁻¹.

Cyclic voltammograms for the modified electrode FTO/Cu-b electrode in Figure 4.6(c), shows that this modification has increased the reduction current all over the scan voltage in the presence of nitrate compared with the blank solution. This confirms the ability of this electrode for nitrate reduction.

The current density values at -1.40 V was -1.40 mA/cm², -4.00 mA/cm² and -5.30 mA/cm² for FTO, Cu and FTO/Cu-b electrodes, respectively. This implies that, the modification of FTO surface by Cu nanoparticles increased its efficiency in nitrate reduction. The lack of symmetry in voltammograms for nitrate reduction, indicate irreversible nature of the reaction.

4.1.2 Electroreduction of Nitrate

FTO/Cu-a electrode which has been prepared by potentiostatic deposition at -0.80 V from (0.01 M CuSO₄ + 0.10 M KCl), easily oxidized when exposed to atmospheric oxygen. FTO/Cu-b electrode which has been prepared by potentiostatic deposition at -0.80 V from (0.85 M CuSO₄ + 0.55 M H₂SO₄) have been used to study nitrate electroreduction.

4.1.2.1 Electroreduction Experiments

Nitrate electroreduction experiments were conducted for two hours of electrolysis at -1.80 V using FTO, Cu and FTO/Cu-b as working electrodes. FTO and Cu were used for comparison purposes.

4.1.2.1.1 Effect of Electrode Type

Nitrate conversion percent was calculated according to equation 4.1, where C_i is the initial nitrate concentration and C_t is nitrate concentration at any time t .

$$\text{Nitrate conversion percent} = \frac{C_i - C_t}{C_i} \times 100\% \dots \dots \dots (4.1)$$

Figure 4.7, shows nitrate conversion% by FTO, Cu and FTO/Cu-b electrodes during 2 h of potentiostatic electroreduction at -1.80 V. FTO and Cu electrodes show 5.50% and 35.13%, respectively. While the percentage for FTO/Cu-b was 37.90%, under the same conditions. FTO/Cu-a electrode has not been used in those experiments because its surface easily oxidized by atmospheric oxygen, as mentioned above in its characterization.

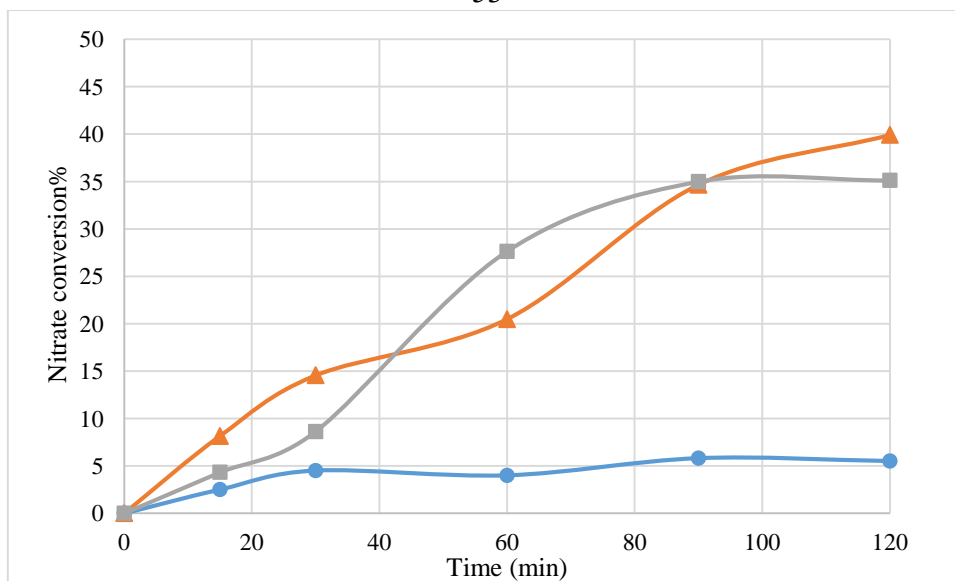


Figure 4.7: Percentage of nitrate conversion on ● FTO, ■ Cu, and ▲ FTO/Cu-b vs. electrolysis time. Experiments were conducting using (70 mL; 0.05 M Na₂SO₄ + 200 mg/L NO₃⁻), at: 25 ± 1 °C, intrinsic pH, D = 0.75 cm, 2 h, and -1.80 V vs. SCE.

Figures 4.8 (a), (b), and (c) show variation in nitrate, nitrite and ammonium ions in the working solutions for FTO, Cu, and FTO/Cu-b respectively, during two hours of electrolysis. As we can see from Figure 4.8 the main product of nitrate electroreduction is NH₄⁺, during 2 h of electrolysis.

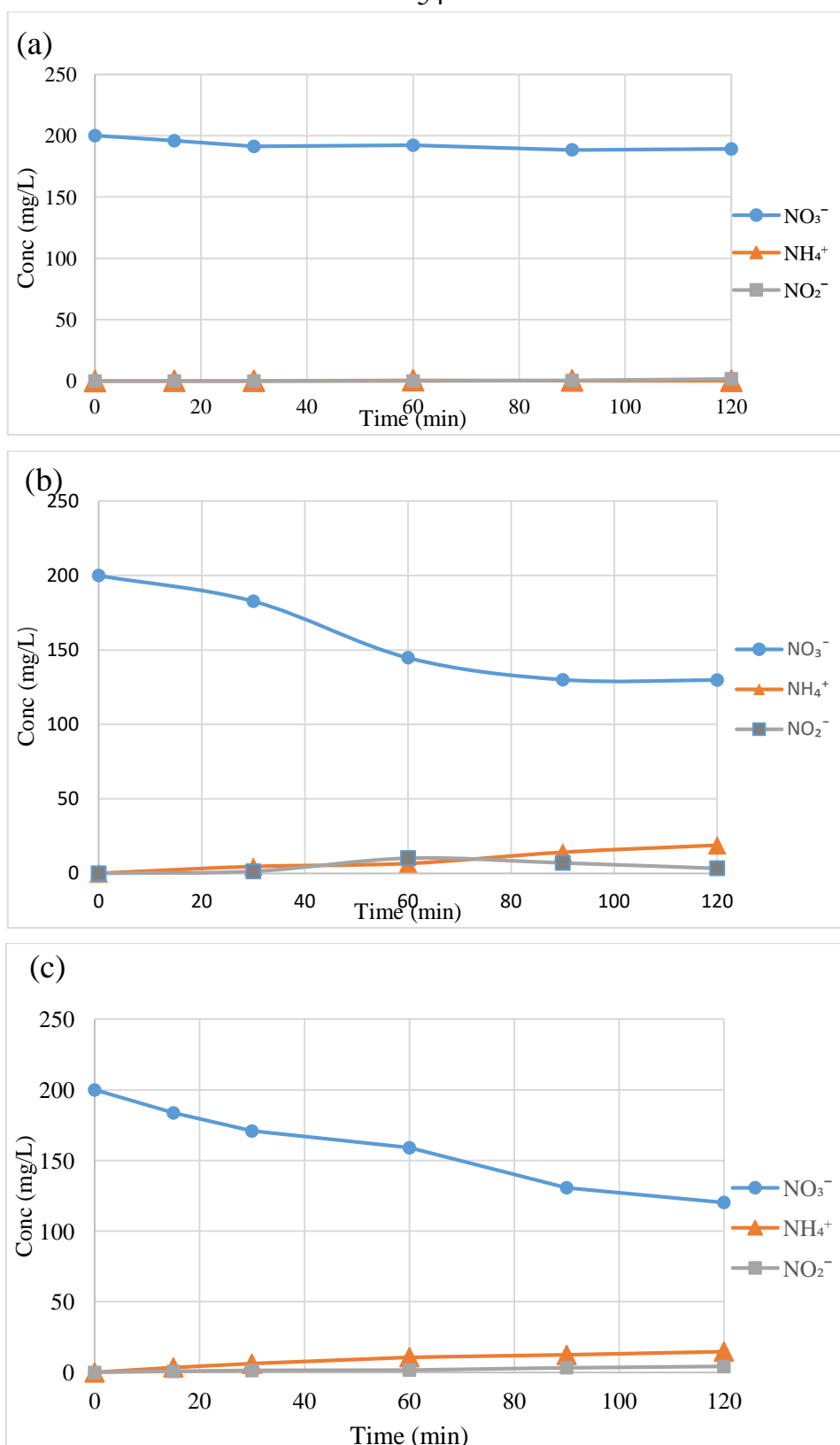


Figure 4.8: Variation of \bullet nitrate, \blacksquare nitrite, and \blacktriangle ammonia concentration vs. electrolysis time on (a) FTO, (b) Cu and (c) FTO/Cu-b electrodes. Experiments were conducted using (70 mL; 0.05 M Na_2SO_4 + 200 mg/L NO_3^-), at: 25 ± 1 °C, intrinsic pH, $D = 0.75$ cm, 2 h, and -1.80 V vs. SCE.

Selectivity values for nitrite ($S_{NO_2^-}$ %) and ammonium ($S_{NH_4^+}$ %) were calculated according to the following equations 4.2, and 4.3, respectively. The %selectivity (S%) was calculated as the fraction of the produced moles of each product to the removed moles of nitrates multiplied by 100 [64, 95, 119, 172]. Selectivity of nitrogen (S_{N_2} %), was found according to equation 4.4 [64, 95, 119, 172], assuming that the amount of by-products such as hydrazine (H_2N-NH_2), nitrous oxide (NO_x), and hydroxylamine (H_2N-OH) were negligible [6, 173, 174].

$$S_{NH_4^+}(\%) = \frac{[NH_4^+]_t}{[NO_3^-]_{initial} - [NO_3^-]_{final}} \times 100 \dots\dots\dots (4.2)$$

$$S_{NO_2^-}(\%) = \frac{[NO_2^-]_t}{[NO_3^-]_{initial} - [NO_3^-]_{final}} \times 100 \dots\dots\dots (4.3)$$

$$S_{N_2}(\%) = 100\% - [S_{NH_4^+}(\%) + S_{NO_2^-}(\%)] \dots\dots\dots (4.4)$$

Where $[NO_3^-]$, $[NH_4^+]$ and $[NO_2^-]$, denotes the molar concentrations of nitrate, ammonium and nitrite ions, respectively in the reaction solution. Table 4.2, shows different selectivity's for the product from nitrate electroreduction using FTO, Cu and FTO/Cu-b as working electrodes.

Table 4.2: Selectivity for ammonium, nitrite and nitrogen on FTO, Cu, and FTO/Cu-b electrodes. Experiments were conducted using (70 mL; 0.05 M Na₂SO₄ + 200 mg/L NO₃⁻) at: 25 ± 1 °C, intrinsic pH, D = 0.75 cm, 2 h, and -1.80 V vs. SCE.

Electrode	NO ₃ ⁻ conversion% (Based on mg L ⁻¹ Conc.)	S% (Based on molar Conc.)		
		NH ₄ ⁺	NO ₂ ⁻	N ₂
FTO	5.50	5.95	21.50	72.55
Cu	35.13	92.50	6.40	1.10
FTO/Cu-b	39.90	63.28	7.14	29.58

The percentage of nitrate conversion by FTO was very low, but its selectivity for nitrogen was the best compared to the other two electrodes, in two hours of electrolysis at -1.80 V. Modification of FTO surface by Cu nanoparticles thin film, in the electrode FTO/Cu-b, improve the nitrate conversion percentage to 39.90%.

Percentage of nitrate conversion by Cu electrode was found to be 35.13% under the same conditions. Although difference in nitrate conversion by FTO/Cu-b and Cu was small, nitrogen selectivity was affected and increases by this electrode FTO/Cu-b. This is a special characteristic for this electrode, since almost all nitrate were converted to NH₄⁺ on Cu electrode, in this work and in literature [100].

4.2 FTO/Gr Electrodes

4.2.1 Characterization

4.2.1.1 SEM Analysis

SEM image for FTO/Gr surface, cross section image of the electrode and surface of FTO/Gr-Cu are shown in Figures 4.9 (a), (a`) and (b) respectively.

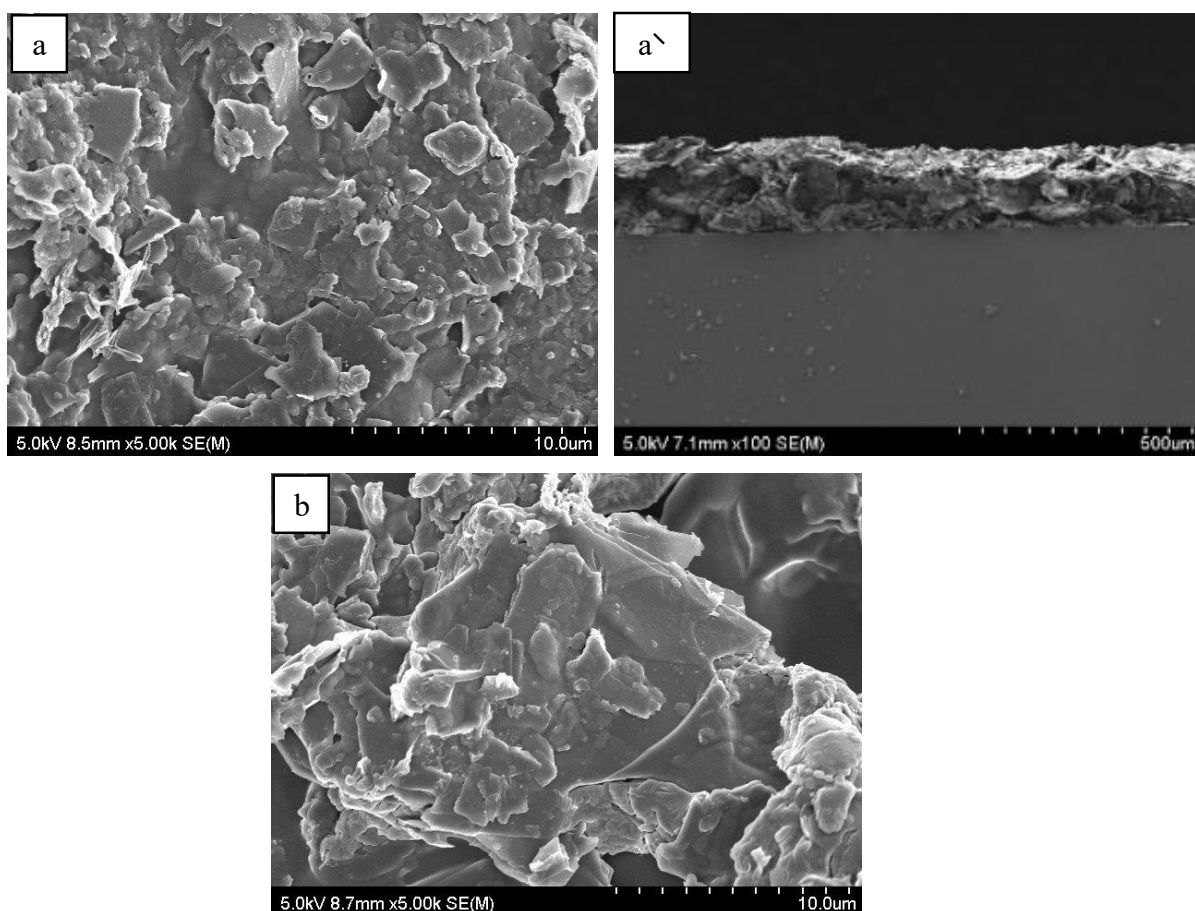


Figure 4.9: SEM micrographs measured for (a) FTO/Gr and (b) FTO/Gr-Cu.

Both images show irregular and uncompact surface structures. While SEM image of FTO/Gr-Cu show small amount of dispersed Cu nanoparticles at the surface of the electrode. Thickness of graphite layer on the surface of

FTO, calculated from the cross-sectional image of the electrode, was $\sim 111.90 \mu\text{m}$.

4.2.1.2 EDS Analysis

The composition of the electrode FTO/Gr-Cu was determined using energy dispersive spectroscopy (EDS), as shown in Figure 4.10, it can be seen that electrode contains 87.08 weight% C and 12.92 weight% Cu.

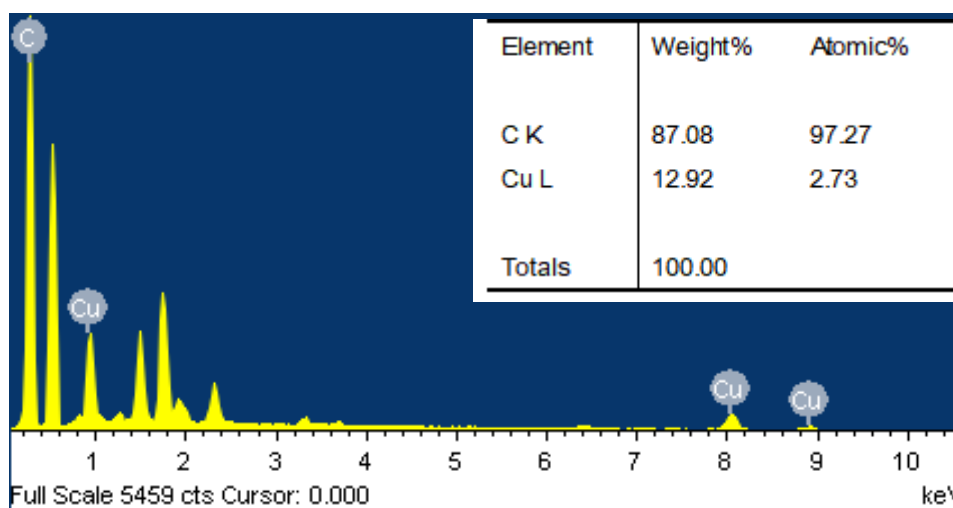


Figure 4.10: EDS spectra measured for FTO/Gr-Cu electrode.

4.2.1.3 XRD Analysis

Analysing the XRD pattern of FTO/Gr and FTO/Gr-Cu in Figure 4.11, shows that signals at $2\theta = 26.56^\circ, 33.76^\circ, 37.68^\circ, 51.56^\circ, 61.68^\circ$ and 65.68° are related to FTO substrate (JCPDS, 41-1445). Sharp signals at $2\theta = 26.58^\circ$ and 54.72° correspond to graphite [175]. XRD pattern of FTO/Gr-Cu shows small signal for Cu (111) at $2\theta = 43.38^\circ$ (JCPDS, 65-9743) [165, 166]. Cu particle size was found to be 37.22 nm. XRD analysis for signals related to graphite and Cu are given in Table 4.3.

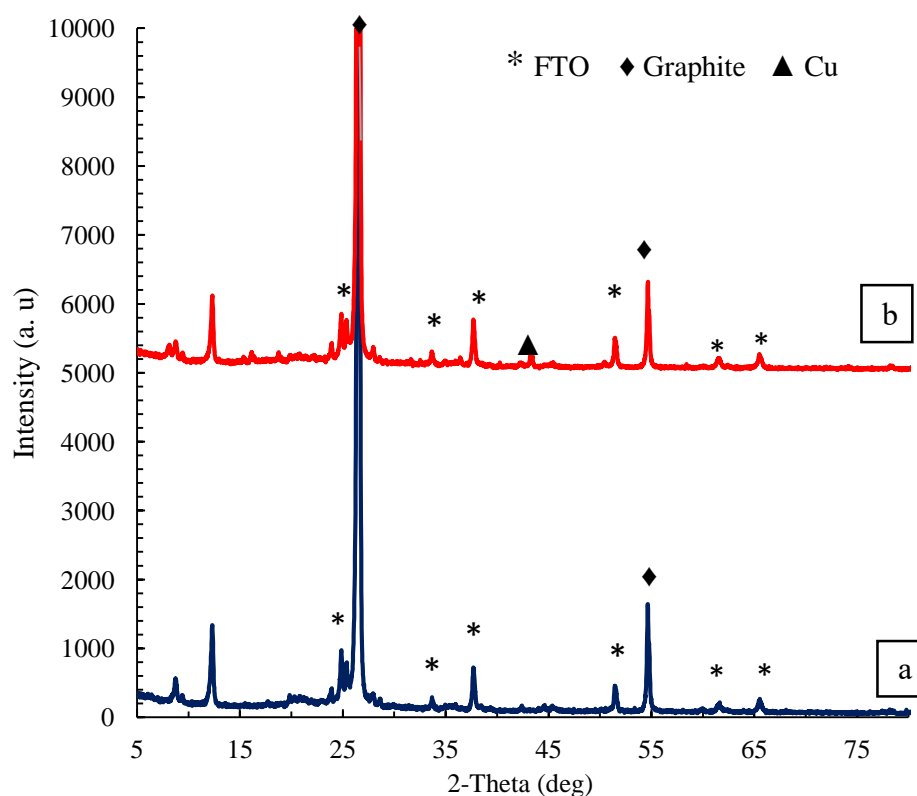


Figure 4.11: Measured XRD patterns for (a) FTO/Gr and (b) FTO/Gr-Cu.

Table 4.3: Analysis of XRD pattern of FTO/Gr and FTO/Gr-Cu electrodes.

Electrode	$2\theta^\circ$	FWHM	Species	Particle size (nm)	d (Å)	(hkl)
FTO/Gr	26.58	0.20	Graphite	-	3.353	(002)
	54.72	0.20	Graphite	-	1.6775	(004)
FTO/Gr-Cu	26.58	0.20	Graphite	-	3.3537	(002)
	54.72	0.20	Graphite	-	1.6775	(004)
	43.38	0.24	Cu	37.22	1.6775	(111)

XRD pattern for FTO/Gr-Cu indicates successful incorporation of small amount of Cu with graphite. This modification gives stability for Cu nanoparticles deposited on FTO/Gr electrode. Although the electrode analysis was done after one month of preparation (due to lack of instruments

in our university), that analysis shows that Cu nanoparticles didn't react with the air oxygen.

4.2.1.4 XPS Analysis

Figure 4.12 shows XPS spectra of FTO/Gr-Cu. Peak at binding energy 284.84 eV is well known to be related to C 1s binding energy in graphite C-C [176, 177]. Binding energy at 534.09 eV is corresponding to C-OH [178]. Binding energy peak at 935.08 eV is related to Cu 2p [168].

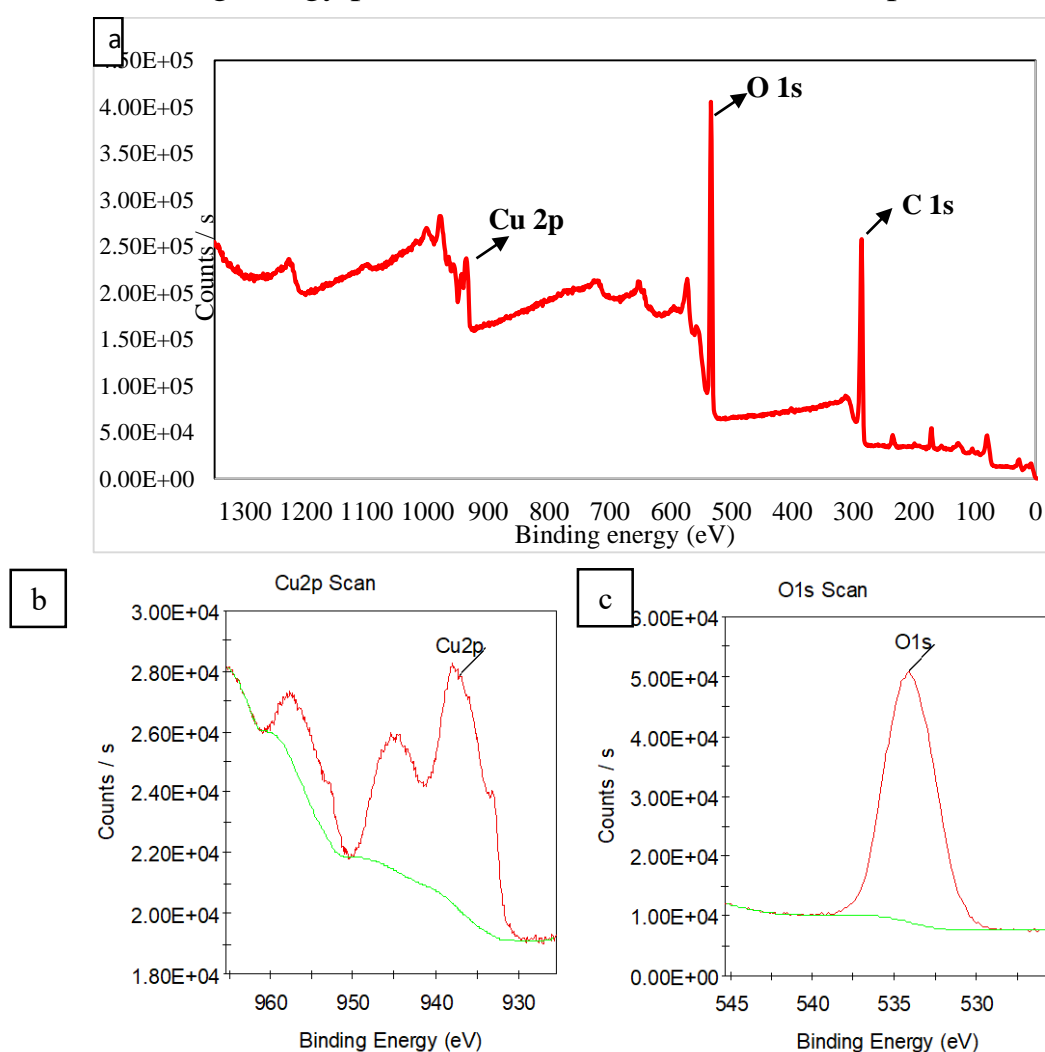
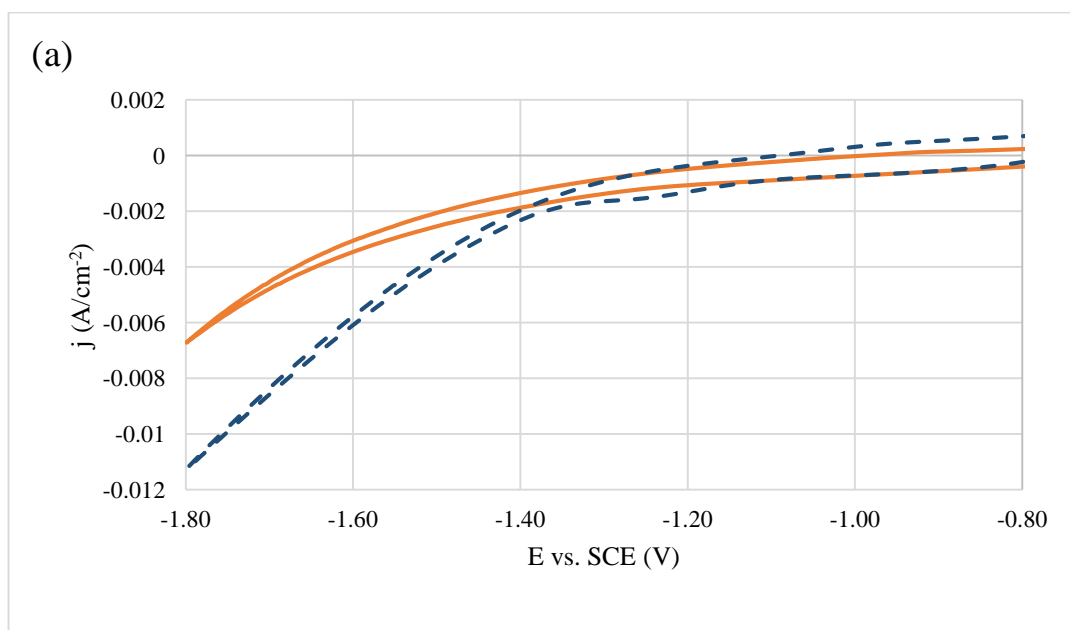


Figure 4.12: Measured XPS spectra for FTO/Gr-Cu, (a) complete spectrum, (b) copper peak and (c) oxygen peak.

4.2.1.5 Cyclic Voltammetry Investigations

Cyclic voltammograms obtained for the reduction of nitrate, using FTO/Gr and FTO/Gr-Cu as the working electrodes are shown in Figures 4.13 (a) and (b), respectively. The cyclic voltammograms show an increase in reduction current for FTO/Gr electrode between -1.40 V to -1.80 V, in the working solution (0.05 M Na₂SO₄ + 200 mg/L NO₃⁻) compared with the blank (0.05 M Na₂SO₄). At -1.60 V current density was 6.00 mA/cm² and 10.60 mA/cm², for FTO/Gr and FTO/Gr-Cu electrodes, respectively. This confirms the effectiveness of the modified electrode FTO/Gr-Cu in nitrate reduction. This may be due to high number of active sites on the electrode surface and better conductivity of Graphite-Cu composite.



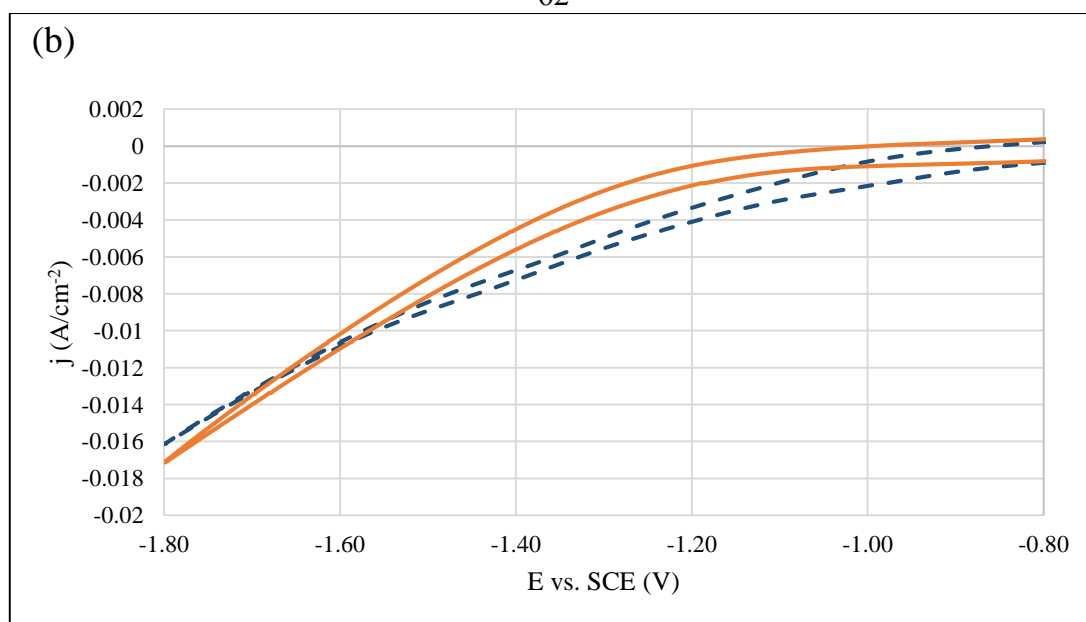


Figure 4.13: Cyclic voltammograms on (a) FTO/Gr and (b) FTO/Gr-Cu in ——— 0.05 M Na_2SO_4 and in - - - - 0.05 M Na_2SO_4 + 200 mg/L NO_3^- . Scan rate 20 mVs^{-1} .

4.2.2 Electroreduction of Nitrate

4.2.2.1 Electroreduction Experiments

Nitrate electroreduction experiments were conducted for two hours of electrolysis at -1.80 V using FTO/Gr and FTO/Gr-Cu electrodes.

4.2.2.1.1 Effect of Electrode Type

Figure 4.14 shows that the new modified electrode FTO/Gr-Cu has slightly higher nitrate conversion percentage (25.69%) compared with FTO/Gr (24%), after two hours of electrolysis.

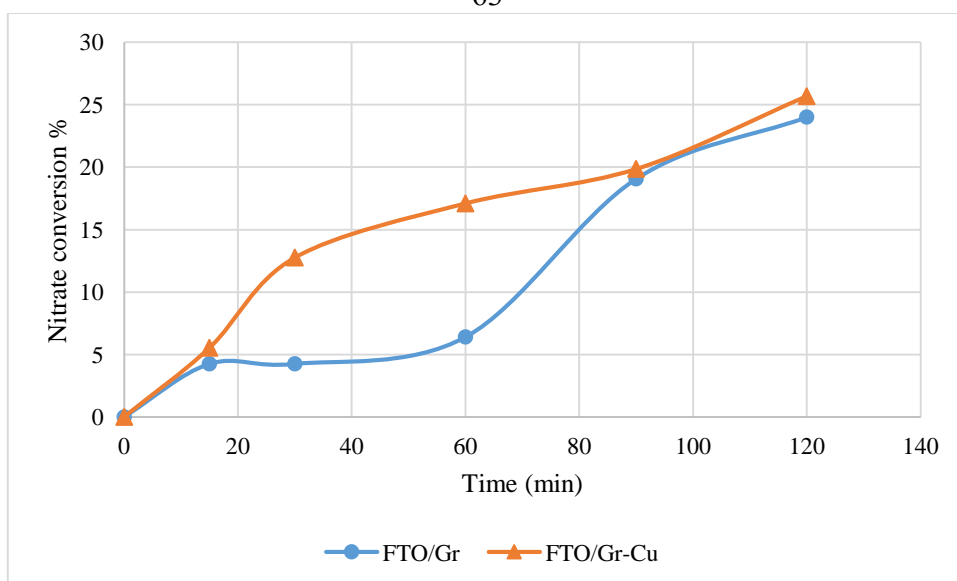
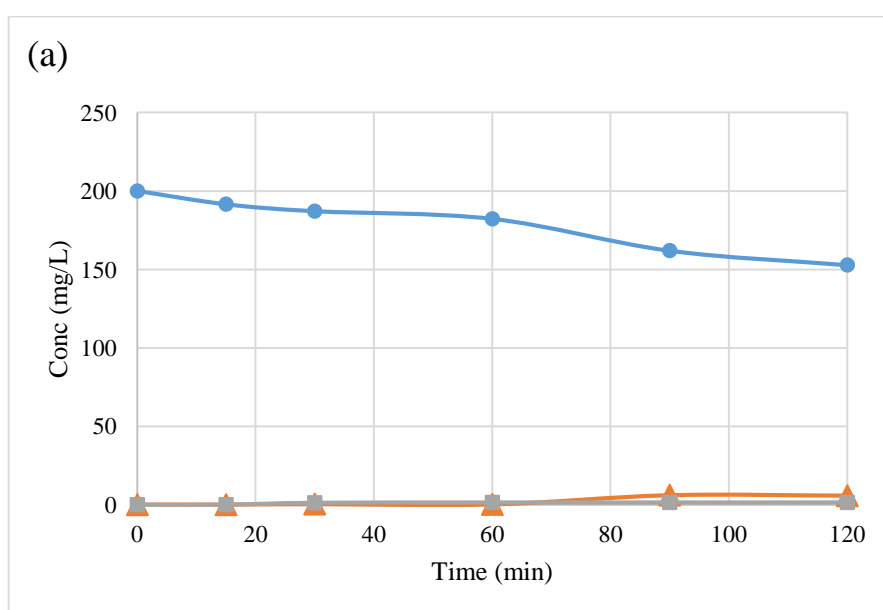


Figure 4.14: Percentage of nitrate conversion on ● FTO/Gr, and ▲ FTO/Gr-Cu vs. electrolysis time. Experiments were conducted using (70 mL; 0.05 M Na₂SO₄ + 200 mg/L NO₃⁻), at: 25 ± 1 °C, intrinsic pH, D = 0.75 cm, 2 h, and -1.80 V vs. SCE.

Little amount of NO₂⁻ was observed for the two system as shown in Figure 4.15. The FTO/Gr had 1.30 mg/L after 2 h and FTO/Gr-Cu electrode had 6.30 mg/L NO₂⁻ in the same time of electrolysis.



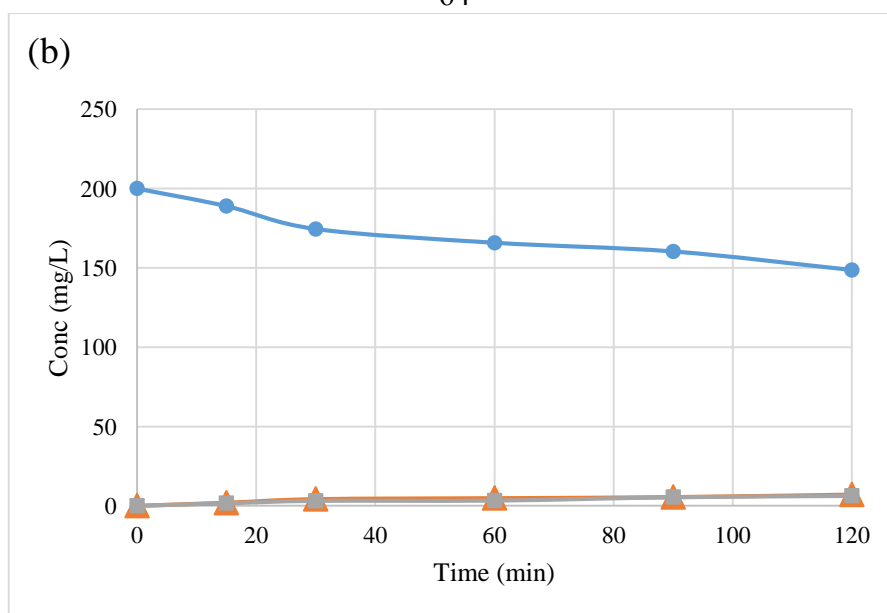


Figure 4.15: Variation of ● nitrate, ■ nitrite and ▲ ammonium concentration vs. electrolysis time on (a) FTO/Gr, and (b) FTO/Gr-Cu electrodes. Experiments were conducted using (70 mL; 0.05 M Na₂SO₄ + 200 mg/L NO₃⁻), at: 25 ± 1 °C, intrinsic pH, D = 0.75 cm, 2 h, and -1.80 V vs. SCE.

Table 4.4: Selectivity for ammonium, nitrite and nitrogen on FTO/ Gr, and FTO/Gr-Cu. Experiments were conducted using (70 mL; 0.05 M Na₂SO₄ + 200 mg/L NO₃⁻) at: 25 ± 1 °C, intrinsic pH, D = 0.75 cm, 2 h, and -1.80 V vs. SCE.

Electrode	NO ₃ ⁻ conversion% (Based on mg L ⁻¹ Conc.)	S%		
		(Based on molar Conc.)		
		NH ₄ ⁺	NO ₂ ⁻	N ₂
FTO/Gr	24	40.91	3.68	55.41
FTO/Gr-Cu	25.69	46.78	16.19	37.03

Table 4.4 shows nitrate conversion percentage and selectivity for different products after two hours of electrolysis, for FTO/Gr and FTO/Gr-Cu electrodes. Modification of the electrode surface by graphite slightly increases its efficiency in nitrate reduction. The modified electrode FTO/Gr electrode yields higher N₂ selectivity than for FTO/Gr-Cu electrode.

4.3 FTO/MWCNT Electrodes

4.3.1 Characterization of the Electrode

4.3.1.1 SEM Analysis

Figure 4.16, show SEM image for surface and cross section of FTO/MWCNT (a) and (a'), (b) FTO/MWCNT-Cu and (c) FTO/MWCNT-Cu electrode that was used for 2 h of electrolysis at -1.80 V. Tubular structure of the MWCNTs is clearly visible in the modified electrodes.

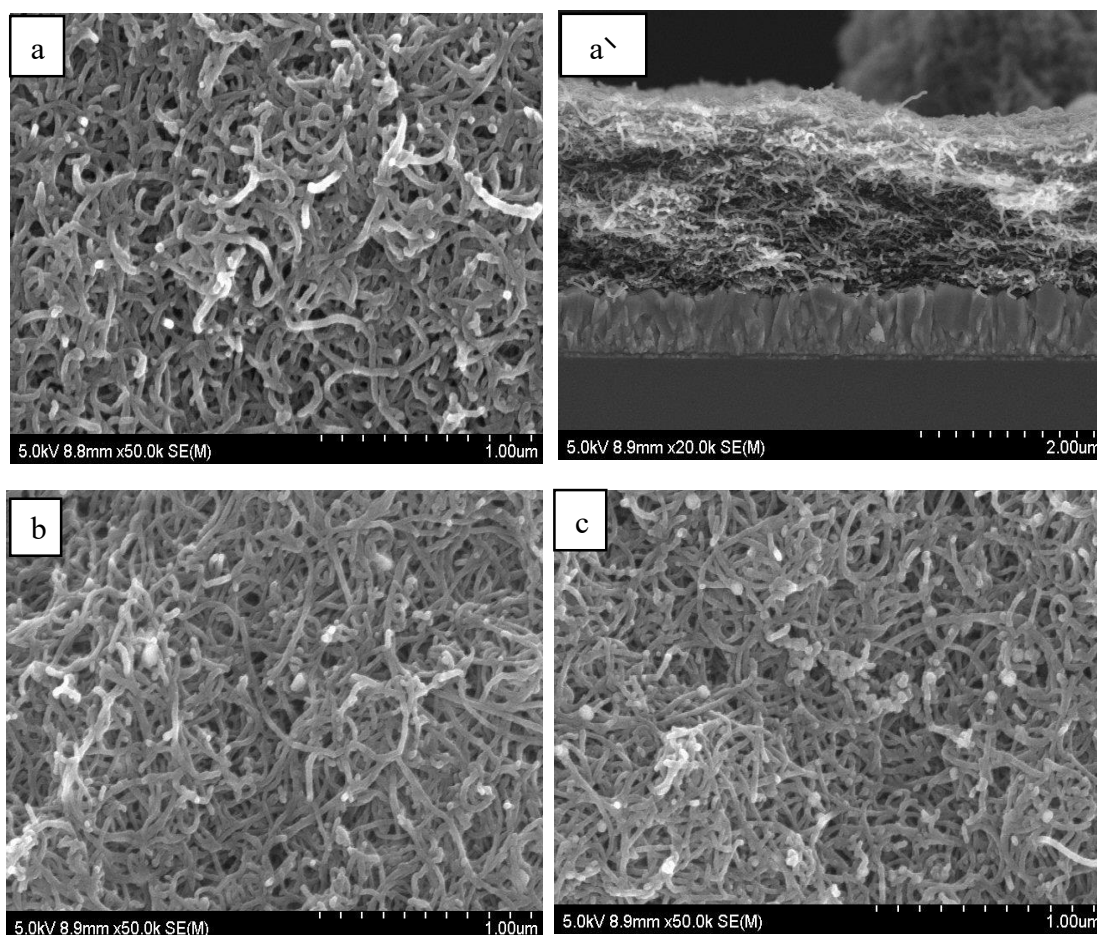


Figure 4.16: SEM images for (a) FTO/MWCNT, (b) FTO/MWCNT-Cu and (c) used FTO/MWCNT-Cu.

Thickness of MWCNT on FTO surface was found from the cross section image to be $\sim 1.66 \mu\text{m}$.

4.3.1.2 EDS Analysis

Elemental analysis of FTO/MWCNT-Cu electrode before it was used in the electroreduction experiment, and after using, are shown in Table 4.5. It can be seen that the electrode contains 35.23 weight % of Cu and after using copper content was decreased to 31.52 weight %. This revealed the good stability of the modified electrode FTO/MWCNT-Cu.

Table 4.5: Elemental analysis of FTO/MWCNT-Cu (a) before and after use (b).

(a)			(b)		
Element	Weight%	Atomic%	Element	Weight%	Atomic%
C K	57.48	83.88	C K	49.11	76.23
O K	2.97	4.26	O K	12.68	10.6
Cu L	35.23	11.85	Cu L	31.52	10.20
			Sn L	6.69	2.97
Totals	100.00		Totals	100.00	

4.3.1.3 XRD Analysis

XRD patterns of FTO/MWCNT and FTO/MWCNT-Cu before and after it have been used is given in Figure 4.17. Signals appear in the XRD pattern at $2\theta = 26.56^\circ, 33.76^\circ, 37.68^\circ, 51.56^\circ, 61.68^\circ$ and 65.68° are related to FTO substrate (JCPDS, 41-1445). Signals related to MWCNT_s observed at 26.1° is associated with (002) plane (JCPDS, 01-0646) [179-181]. XRD pattern of

the electrode FTO/MWCNT-Cu shows signals related to Cu (JCPDS, 65-9743) [165, 166], CuO (JCPDS, 45-0937) [163, 164], and Cu₂O (JCPDS, 03-0879) [164, 182, 183], analysis of signals related to Cu and Cu compounds in the electrodes are presented in Table 4.6.

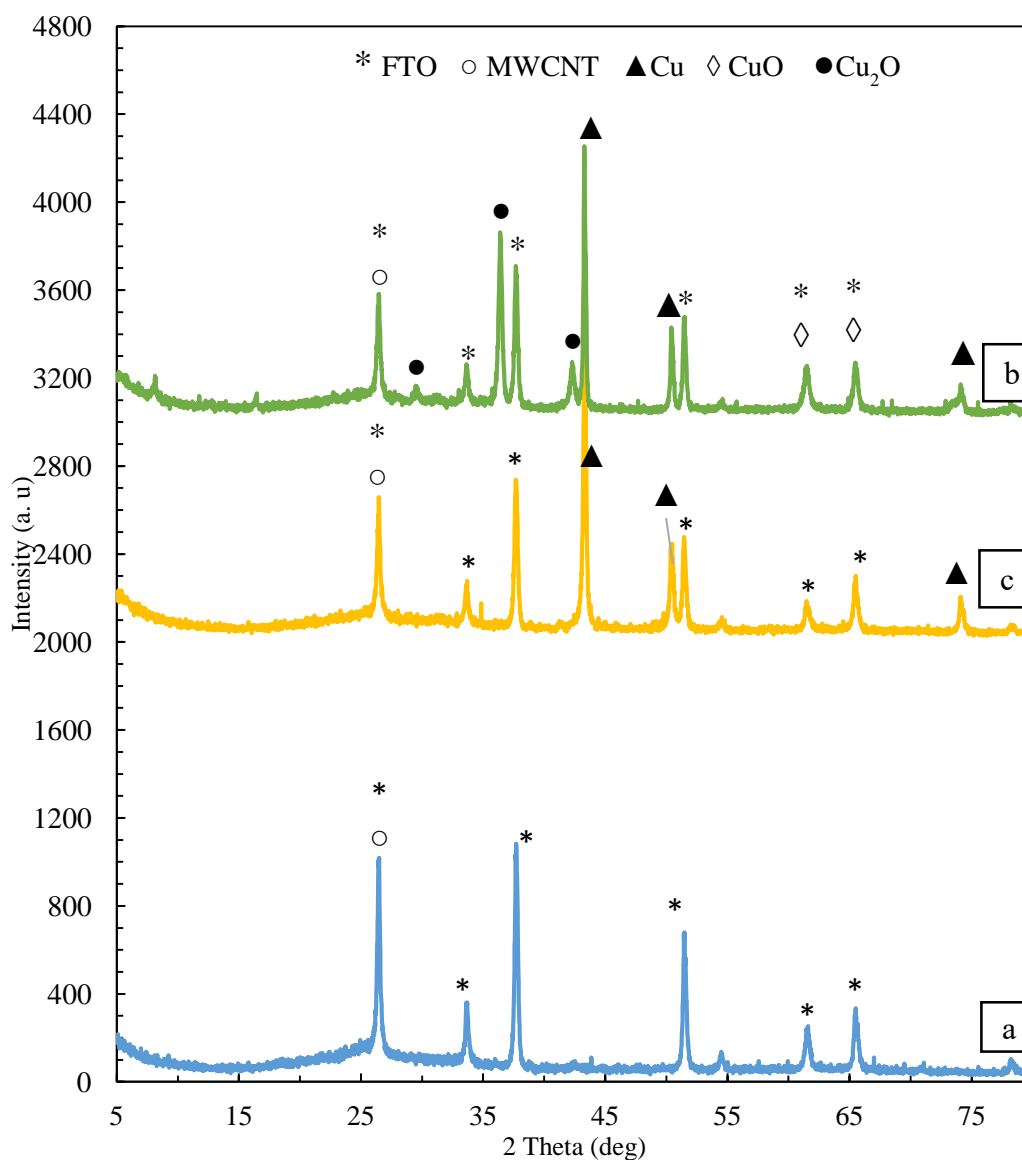


Figure 4.17: Measured XRD patterns for (a) FTO/MWCNT, (b) fresh FTO/MWCNT-Cu and (c) used FTO/MWCNT-Cu.

The signals of Cu are stronger than other signal of CuO or Cu₂O indicating that nanocomposite is mainly composed of metallic Cu. While XRD pattern

of the electrode after it have been used in electrolysis for 2 h, only show signals related to Cu nanoparticles. This is another indication of the stability of the prepared electrode compared to other in literature, since it's known that corrosion of copper occurred at pH higher than 8 [6].

Table 4.6: XRD analysis for Cu and related compounds in fresh and used FTO/MWCNT-Cu electrode.

Electrode	$2\theta^\circ$	FWHM	Species	Particle size (nm)	d (Å)	(hkl)
FTO/MWCNT-Cu	29.54	0.40	Cu ₂ O	21.46	3.021	(110)
	36.42	0.28	Cu ₂ O	31.21	2.46	(111)
	42.3	0.44	Cu ₂ O	20.23	2.134	(200)
	43.28	0.16	Cu	55.82	2.088	(111)
	50.42	0.20	Cu	45.88	1.808	(200)
	61.46	0.36	CuO	26.83	1.507	(113)
	65.48	0.36	CuO	27.42	1.424	(022)
	74.14	0.28	Cu	37.16	1.277	(220)
FTO/MWCNT-Cu **used	43.41	0.20	Cu	44.67	2.084	(111)
	50.53	0.28	Cu	32.78	1.806	(200)
	74.21	0.32	Cu	32.53	1.277	(220)

4.3.1.4 XPS Analysis

Figure 4.18 and Figure 4.19 show XPS spectra of the modified FTO/MWCNT-Cu with high resolution spectra of Cu 2p and O 1s included. The full-scale XPS spectrum of the electrode FTO/MWCNT-Cu, show that the Cu, O and C elements can detected.

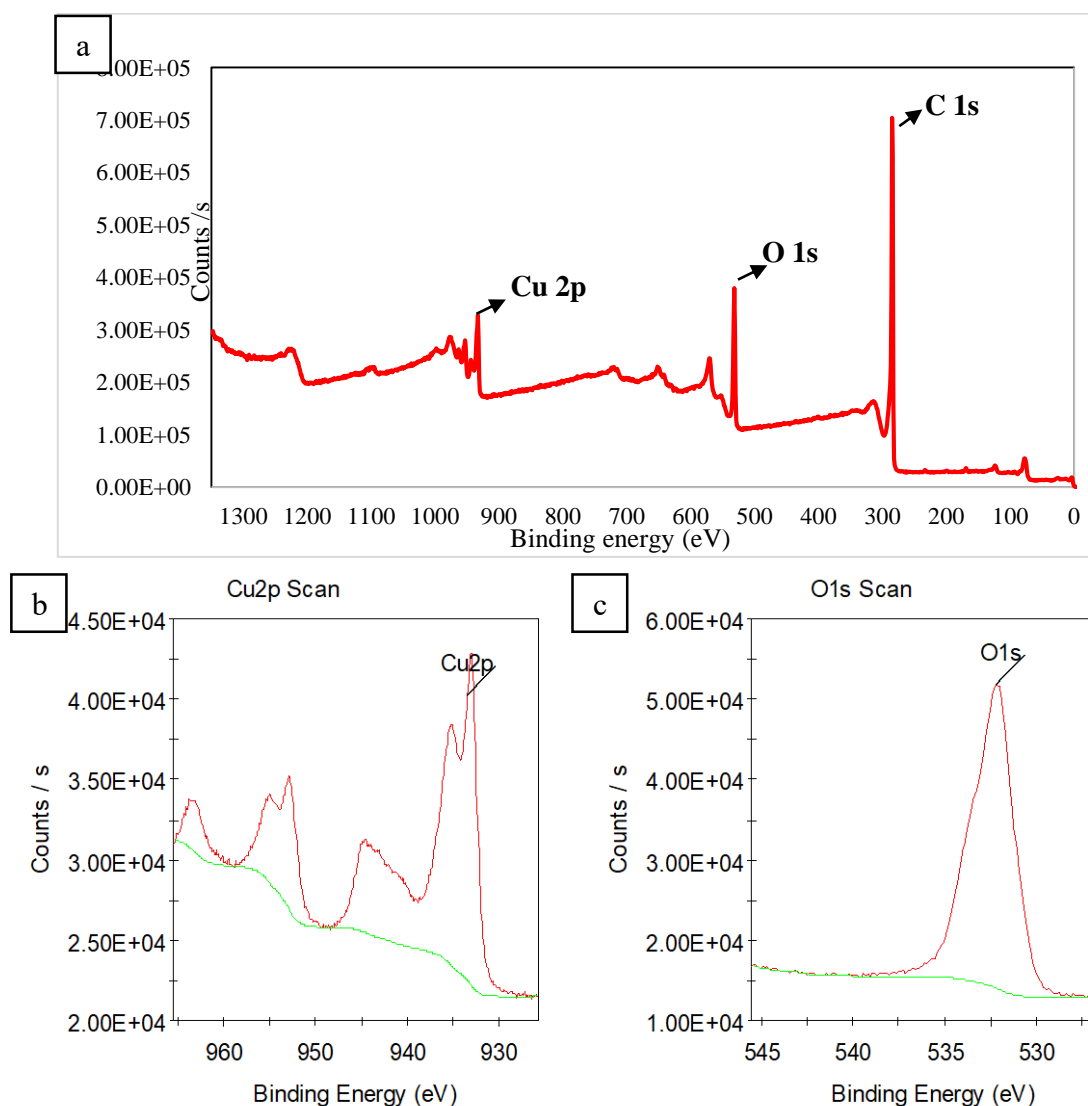


Figure 4.18: Measured XPS spectra for fresh FTO/MWCNT-Cu electrode, (a) complete spectrum, (b) copper peak and (c) oxygen peak.

XPS spectra measured for fresh FTO/MWCNT-Cu electrode show peaks of Cu 2p at 933.37 eV, O 1s at 532.19 eV and C 1s at 284.8 eV. While after the electrode was used for 2 h of electrolysis the peaks are almost found at the same positions. Cu 2p found at 933.08 eV, O 1s and C 1s at 284.82 eV. The peak of Cu 2p spectra for the two electrodes fits to Cu $2P^{3/2}$, indicating

possible of presence of Cu(0), Cu(I) and Cu(II) or some of them on the prepared electrode, in congruence with literature [168, 170].

The peak of C 1s peak at 284.82 eV is related to MWCNTs [184, 185]. The O 1s binding energy at 532.06 eV can be assigned to hydroxide, oxide metal species, adsorbed water and adsorbed oxygen on the electrode surface [186-189]. Here this energy may be due to functionalized group on MWCNT surface.

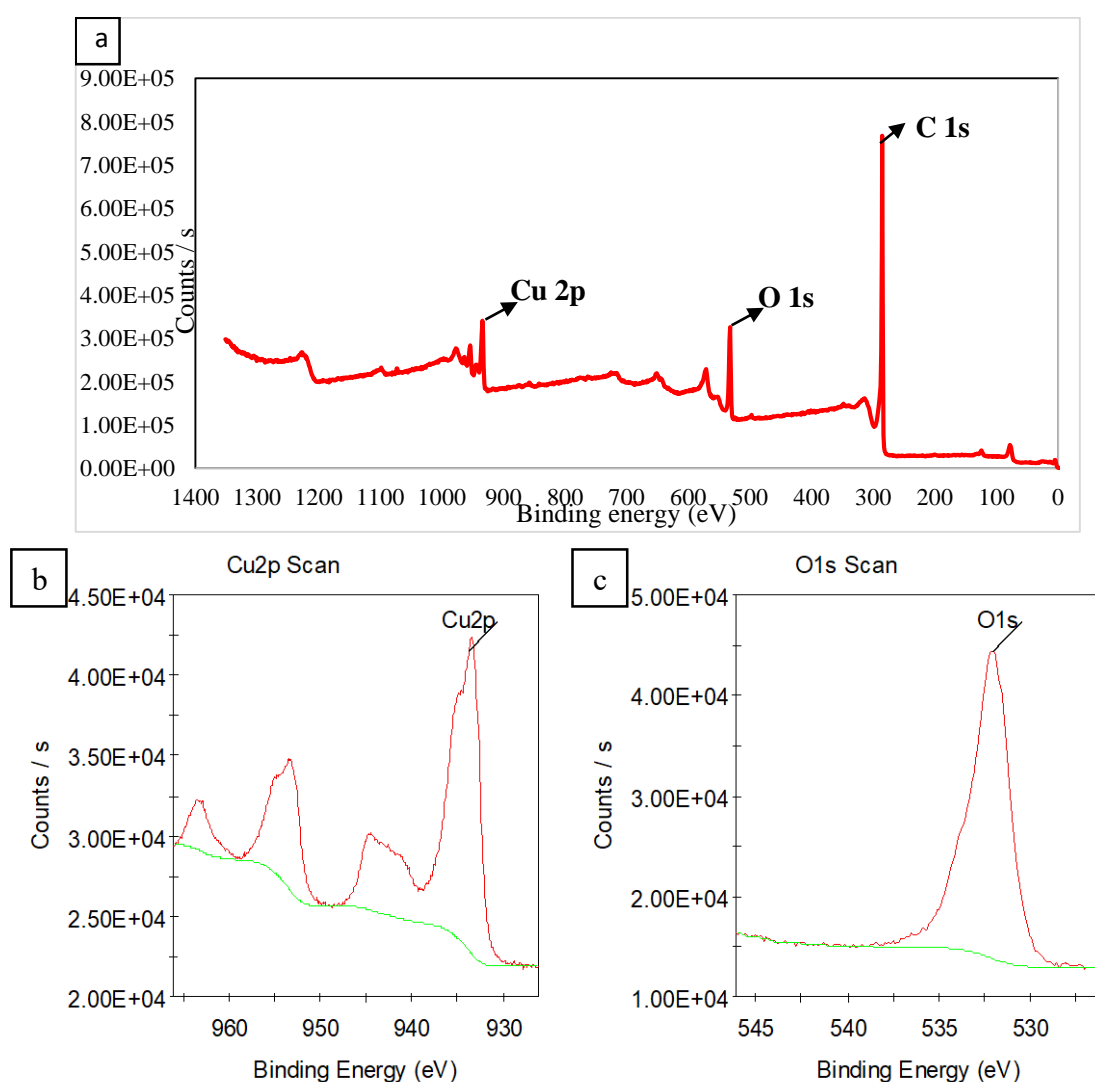


Figure 4.19: Measured XPS spectra for used FTO/MWCNT-Cu electrode, (a) complete spectrum, (b) copper peak and (c) oxygen peak.

4.3.1.5 Cyclic Voltammetry Investigations

Cyclic voltammograms for FTO/MWCNT and FTO/MWCNT-Cu are shown in Figure 4.20. The cyclic voltammograms show increased cathodic current for FTO/MWCNT with nitrate solution, compared with the Na_2SO_4 electrolyte only in the voltage range -1.26 V to -1.80 V, which confirms the nitrate reduction. The current density at -1.60 V is 5.60 mA/cm^2 and 18.60 mA/cm^2 for FTO/MWCNT and FTO/MWCNT-Cu, respectively. This suggested high electrochemical activity of the modified electrode FTO/MWCNT-Cu toward nitrate reduction.

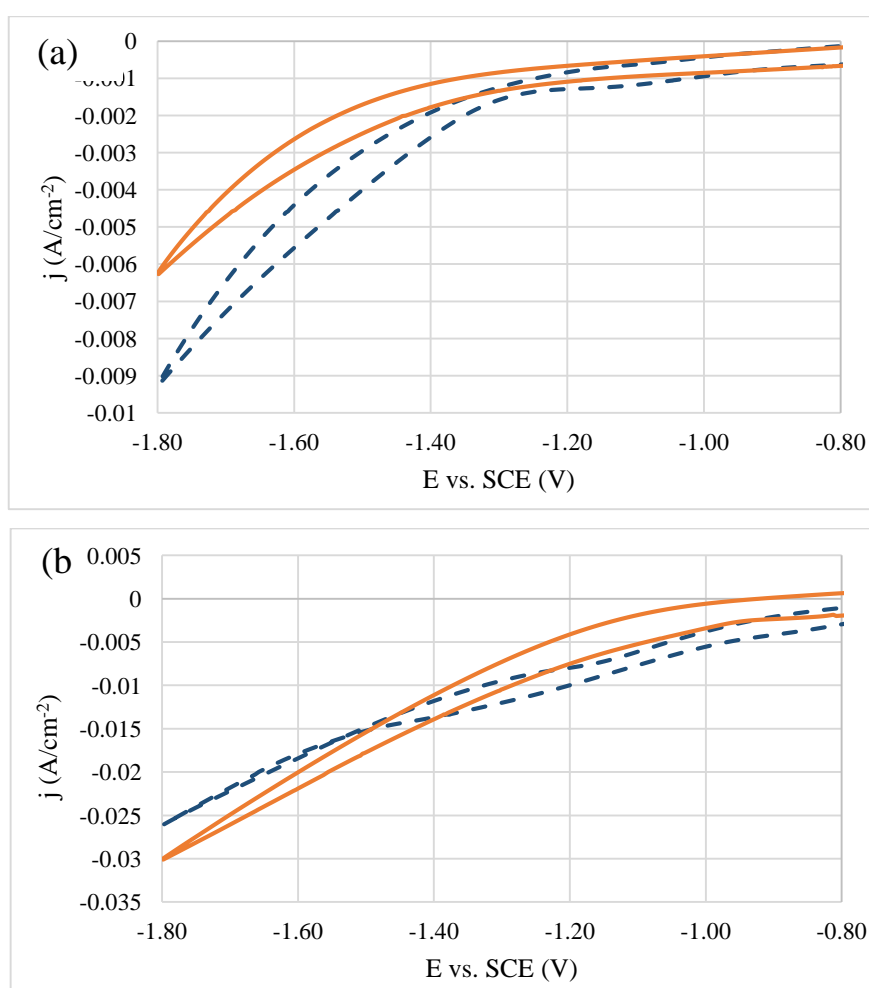


Figure 4.20: Cyclic voltammograms for (a) FTO/MWCNT and (b) FTO/MWCNT-Cu in — 0.05 M Na_2SO_4 and in - - - 0.05 M Na_2SO_4 + 200 mg/L NO_3^- . Scan rate 20 mVs^{-1} .

The higher cathodic current in the voltammogram of the electrode FTO/ MWCNT-Cu, indicates efficient reduction of NO_3^- on the electrode surface. This improvement could be due to high number of active sites and better conductivity of MWCNT-Cu composite.

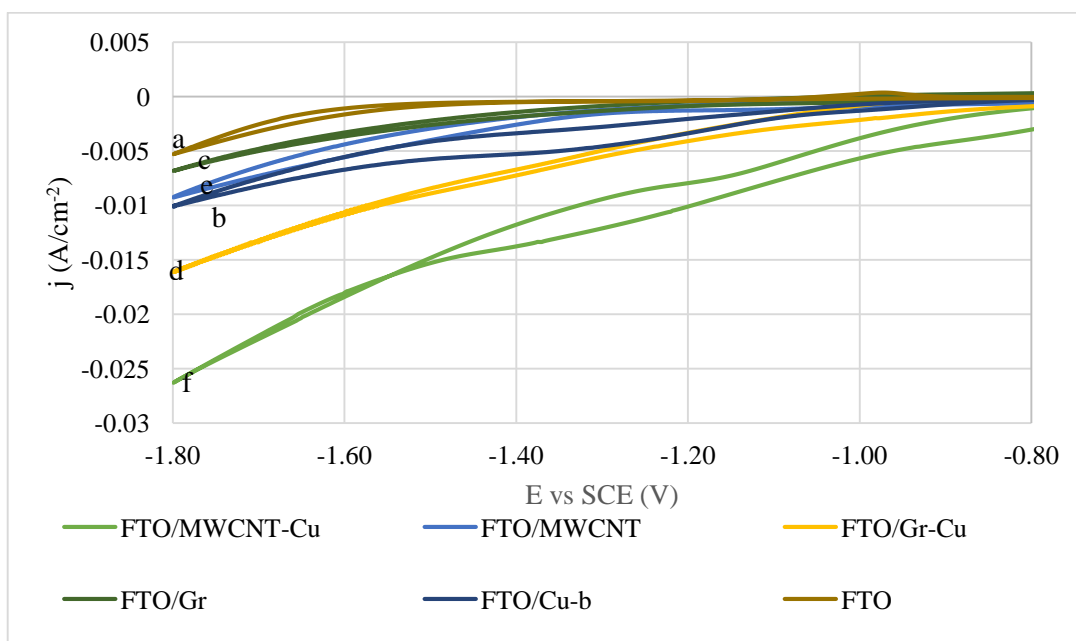


Figure 4.21: Cyclic voltammograms for (a) FTO, (b) FTO/Cu-b, (c) FTO/Gr, (d) FTO/Gr-Cu, (e) FTO/MWCNT and (f) FTO/MWCNT-Cu in 0.05 M Na_2SO_4 + 200 mg/L NO_3^- . Scan rate 20 mVs⁻¹.

For comparison of the FTO/MWCNT-Cu electrode, with all prepared electrodes, cyclic voltammograms are shown in Figure 4.21. The Figure shows the cyclic voltammograms for reduction of nitrate at (a) FTO, (b) Cu, (c) FTO/Cu-b, (d) FTO-Gr, (e) FTO/Gr-Cu, (f) FTO/MWCNT and (g) FTO/MWCNT-Cu. Figure 4.21 show that FTO/MWCNT-Cu electrode has the higher current densities at all reduction potential ranges, which indicates efficient nitrate reduction by this electrode. Therefore, the electrode

efficiency has been investigated in nitrate reduction under different conditions.

4.3.2 Electroreduction of Nitrate

4.3.2.1 Electroreduction Experiments

Nitrate electroreduction experiments were conducted for two hours of electrolysis at -1.80 V using FTO/MWCNT and FTO/MWCNT-Cu electrodes.

4.3.2.1.1 Effect of electrode Type

Figure 4.22 shows percentage of nitrate conversion vs. time, on FTO/MWCNT-Cu electrode. To pinpoint the value of the Cu particles, the FTO/MWCNT (with no Cu) has been studied as a control electrode.

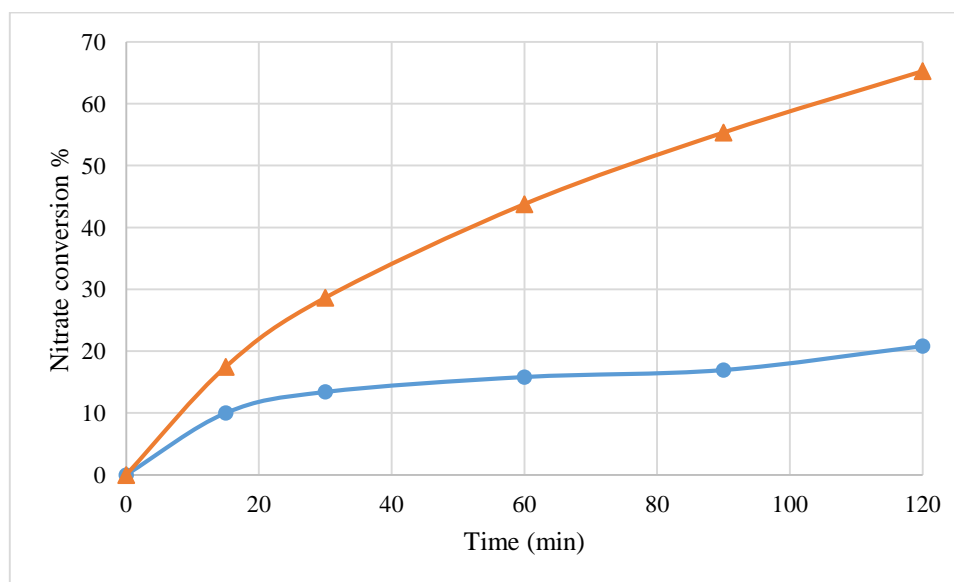
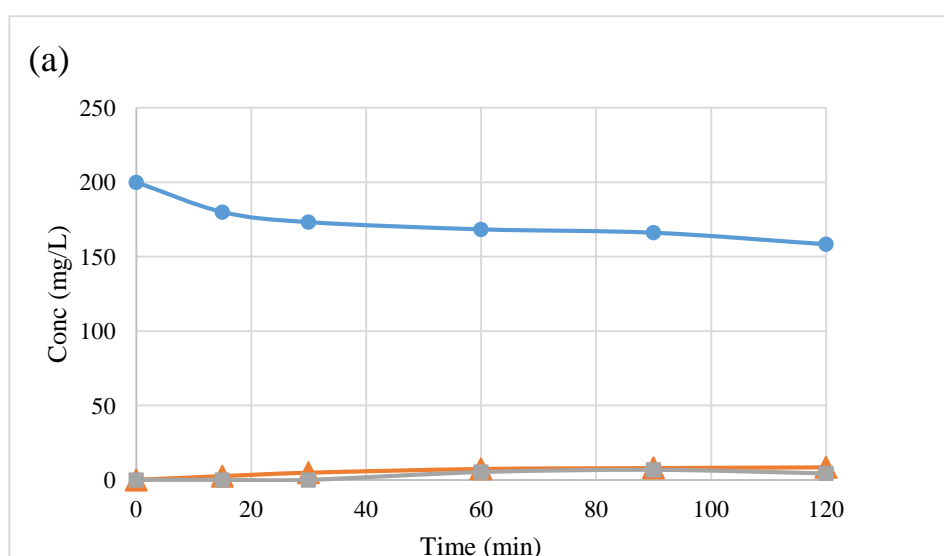


Figure 4.22: Percentage of nitrate conversion on ● FTO/MWCNT and ▲ FTO/MWCNT-Cu vs. electrolysis time. Experiments were conducted using (70 mL; 0.05 M Na₂SO₄ + 200 mg/L NO₃⁻), at: 25 ± 1 °C, intrinsic pH, D = 0.75 cm, 2 h and -1.80 V vs. SCE.

About 20.83% and 65.37% of nitrate was converted in two hours of electrolysis at -1.80 V by FTO/MWCNT and FTO/MWCNT-Cu, respectively. This can be attributed to the difference in electrode charge transfer efficiency, as described above. This confirms the added value for using Cu in the composite electrode.

Variation in concentrations of nitrate, nitrite and ammonium ions, during nitrate electroreduction with FTO/MWCNT and FTO/MWCNT-Cu electrodes are shown in Figures 4.23 (a) and (b) respectively. Selectivity values for nitrite, ammonium and nitrogen, after two hours of electrolysis, on FTO/MWCNT and FTO/MWCNT-Cu are given in Table 4.7.

After two hours of nitrate electroreduction, concentration of Cu in the working solution was measured and found to be 0.80 mg/L, which is far lower the permeisable limit (2 mg/L) according to WHO [190].



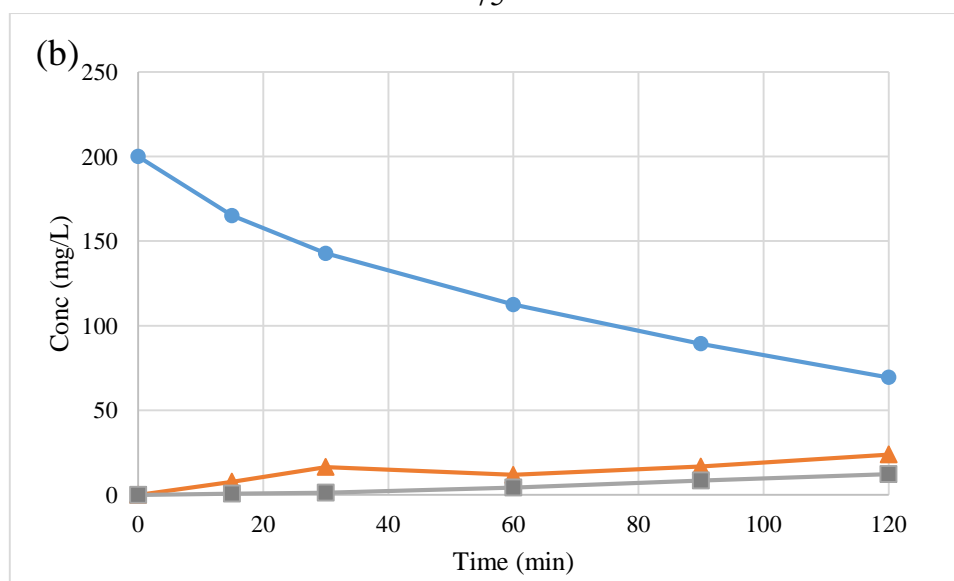


Figure 4.23: Variation in concentration of ● nitrate, ■ nitrite and ▲ ammonium on (a) FTO/MWCNT and (b) FTO/MWCNT-Cu. Experiments were conducted using (70 mL; 0.05 M Na₂SO₄ + 200 mg/L NO₃⁻) at: 25 ± 1 °C, intrinsic pH, D = 0.75 cm, 2 h, and -1.80 V vs. SCE.

Table 4.7: Selectivity for ammonium, nitrite and nitrogen on FTO/WCNT and FTO/MWCNT-Cu. Experiments were conducted using (70 mL; 0.05 M Na₂SO₄ + 200 mg/L NO₃⁻) at: 25 ± 1 °C, intrinsic pH, D = 0.75 cm, 2 h, and -1.80 V vs. SCE.

Electrode	NO ₃ ⁻ conversion% (Based on mg L ⁻¹ Conc.)	S% (Based on molar Conc.)		
		NH ₄ ⁺	NO ₂ ⁻	N ₂
FTO/MWCNT	20.83	72.68	14.49	12.83
FTO/MWCNT-Cu	65.27	62.55	13.60	23.85

The significant importance of this modified electrode FTO/MWCNT-Cu in the electrode stability, selectivity for nitrogen, as well as the kinetics are clear. As the new modified FTO/MWCNT-Cu has the best nitrate conversion

efficiency relative to other electrodes in this research. The all following sections in the study have been restricted to the FTO/MWCNT/Cu electrode.

4.3.2.2 Parameter Effects on FTO/MWCNT-Cu Efficiency

4.3.2.2.1 Effect of Applied Voltage

Figure 4.24 shows percentage of nitrate conversion at different applied potentials. As shown in the figure, percentage of nitrate conversion was 52.88%, 65.27% and 67.16% in two hours, at -1.50 V, -1.80 V and -2.10 V vs. SCE, respectively.

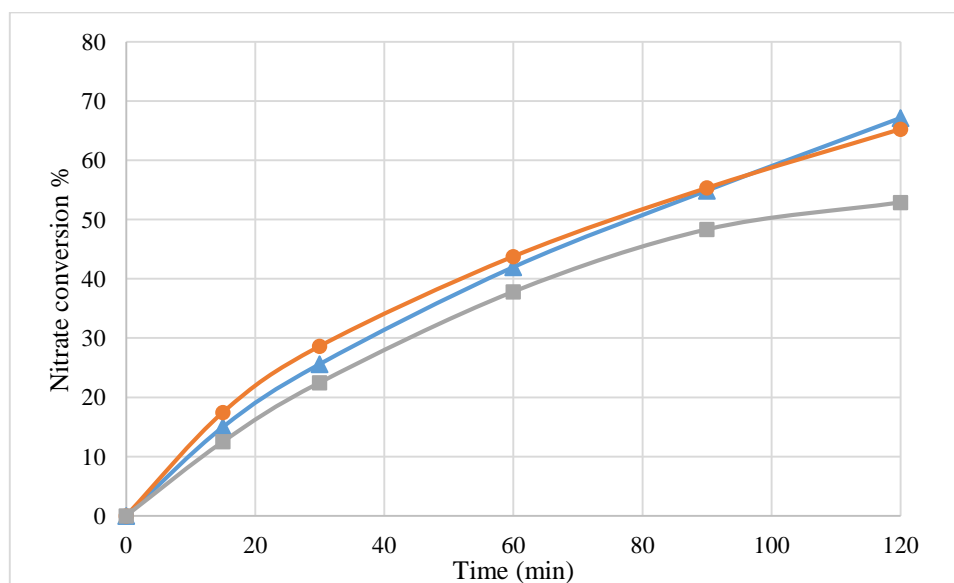


Figure 4.24: Percentage of nitrate conversion at (■ -1.50 V, ● -1.80 V, and ▲ -2.10 V) vs. SCE against electrolysis time, on FTO/MWCNT-Cu electrode. Experiments were conducted using (70 mL; 0.05 M Na_2SO_4 + 200 mg/L NO_3^-), at: 25 ± 1 °C, intrinsic pH, $D = 0.75$ cm, and 2 h.

Percentage of nitrate conversion slightly increases by increasing the applied voltage. This may be due to the increase of electromotive force for electrons by cathode at higher voltage. The catalytic activity of the electrode depends much on its composition and the distribution of the charge on its surface.

The applied potential -1.80 V was used in all next experiments, since there is a small difference in nitrate electroreduction efficiency when applying -2.10 V. Also, this voltage (-1.80 V) is a better choice for economic purposes. In fact the voltage used in some literature is very high compared to this value [28, 85, 191]. This shows the value of the electrode used here.

4.3.2.2.2 Effect of Electrolyte Type

The percentage of nitrate conversion vs. time using 0.05 M Na_2SO_4 and 0.075 M NaCl as electrolyte is shown in Figure 4.25. The percentage of nitrate conversion when 0.05 M Na_2SO_4 was used is slightly higher than the percentage when 0.075 M NaCl was used as in the values, 65.27% and 62.48% respectively.

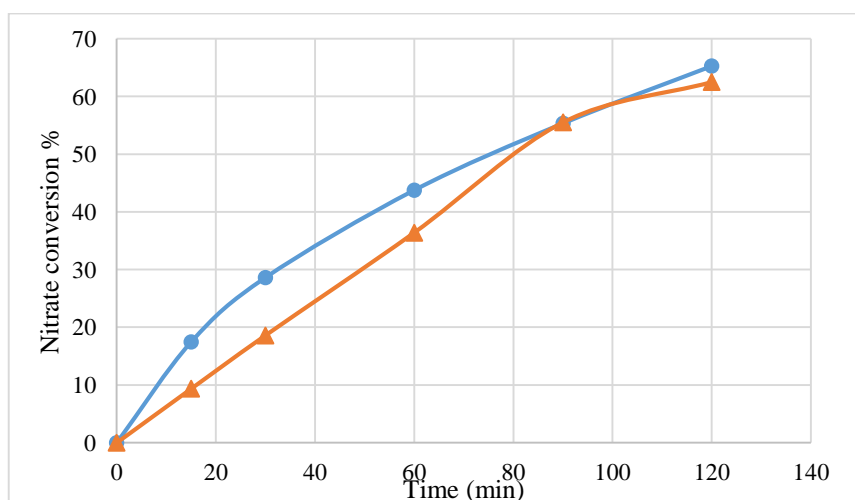


Figure 4.25: Percentage of nitrate conversion using (● 0.05 M Na_2SO_4 and ▲ 0.075 M NaCl) as electrolyte, vs. electrolysis time, on FTO/MWCNT-Cu electrode. Experiments were conducted using (70 mL; 200 mg/L NO_3^-), at: 25 ± 1 °C, intrinsic pH, $D = 0.75$ cm, 2 h and -1.80 V) vs. SCE.

Percentage of nitrate conversion dropped to 29.13%, when the same experiment was done in tap water without the presence of electrolyte. The similarity in the effectiveness of NaCl and Na₂SO₄ in nitrate conversion may be related to high conductivity of both.

Figures 4.26, show variation in nitrate, ammonium and nitrate concentration vs. electrolysis time, when 0.05 M Na₂SO₄ and 0.075 M NaCl were used as electrolyte, respectively. As is shown in Figure 4.26 (b), in the presence of NaCl, a linear depletion of nitrate concentration occurred during the first 90 min of electroreduction. Loss of linearity after that happened because of change in kinetics of the process due to side reactions that may happened.

The selectivity for ammonium, nitrite and nitrogen after two hours of electrolysis in the presence of NaCl and Na₂SO₄, have been calculated from equations 4.2, 4.3 and 4.4. Results are shown in Table 4.8.

Table 4.8: Selectivity for ammonium, nitrite and nitrogen on FTO/MWCNT-Cu, in the presence of 0.075 M NaCl and 0.05 M Na₂SO₄. Experiments were conducted using (70 mL; 200 mg/L NO₃⁻) at: 25 ± 1 °C, intrinsic pH, D = 0.75 cm, 2 h, and -1.80 V vs. SCE.

Electrolyte	NO ₃ ⁻ conversion% (Based on mg L ⁻¹ Conc.)	S% (Based on molar Conc.)		
		NH ₄ ⁺	NO ₂ ⁻	N ₂
0.075 M NaCl	62.48	70.79	4.18	25.03
0.05 M Na ₂ SO ₄	65.27	62.55	13.60	23.85

Results show that both electrolytes are suitable for nitrate electroreduction. Therefore, Na₂SO₄ was used as electrolyte in the next experiments. However, earlier studies were made on both electrolytes. [61, 73, 89, 192], in this work

the Na_2SO_4 was used due to its higher conductance than NaCl [193]. It is recommended to use NaCl electrolyte in future studies on the same electrode used here.

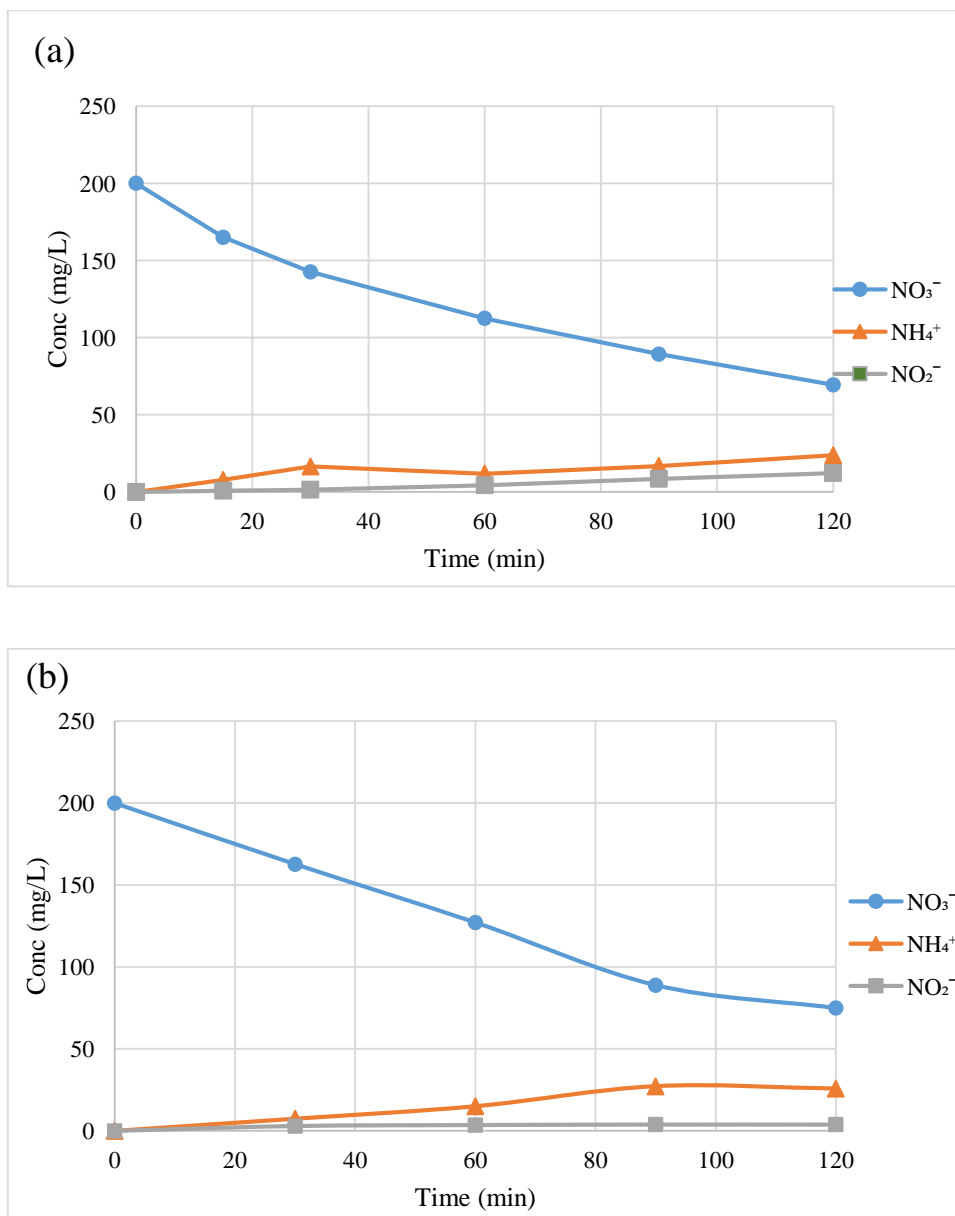


Figure 4.26: Variation in concentration of ● nitrate, ■ nitrite and ▲ ammonium on FTO/MWCNT-Cu, in (a) the presence of 0.075 M NaCl and (b) 0.05 M Na_2SO_4 . Experiments were conducted using (70 mL; 200 mg/L NO_3^-) at: 25 ± 1 °C, intrinsic pH, $D = 0.75$ cm, 2 h, and -1.80 V vs. SCE.

4.3.2.2.3 Effect of Electrolyte Concentration

Figure 4.27 indicates the variation of nitrate conversion with various electrolyte (Na_2SO_4) concentrations. By increasing electrolyte concentrations, a substantial increase in nitrate reduction was observed. Values 45.46%, 65.27%, and 74.52% of nitrate conversion, in the presence of 0.025 M, 0.05 M and 0.10 M of Na_2SO_4 respectively, within two hours of electrolysis. This tendency agrees with literature [115]. This may be due to the increase in conductivity of the working solutions, which leads to increase in charge transfer between electrodes. Electrolyte concentration of 0.05 M was used in all the next experiments.

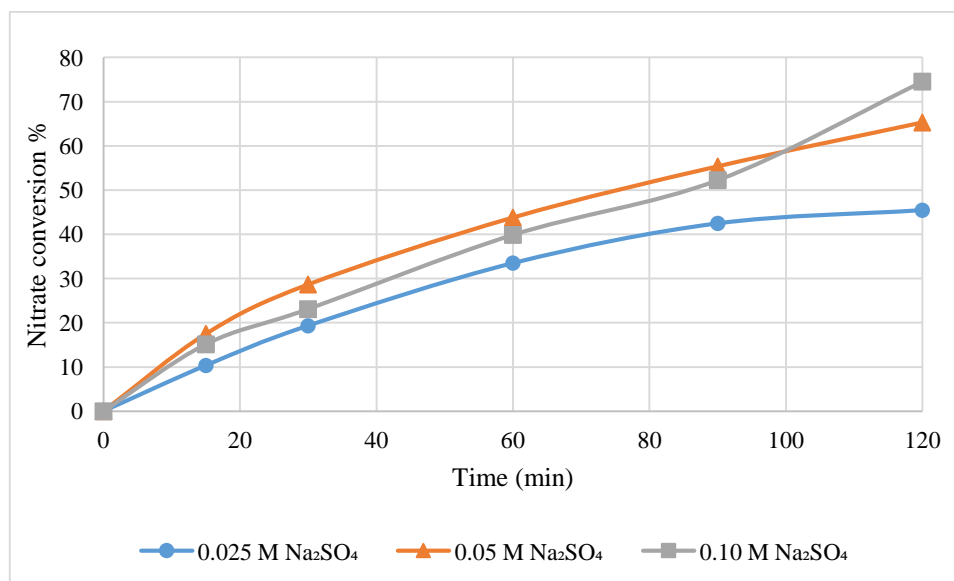


Figure 4.27: Percentage of nitrate conversion at (● 0.025 M Na_2SO_4 , ▲ 0.05 M Na_2SO_4 and ■ 0.10 M Na_2SO_4) vs electrolysis time, on FTO/MWCNT-Cu electrode. Experiments were conducted using (70 mL; 200 mg/L NO_3^-), at: 25 ± 1 °C, intrinsic pH, D = 0.75 cm, 2 h, and -1.80 V vs. SCE.

4.3.2.2.4 Effect of Solution Stirring

The effect of stirring the working solution on nitrate reduction was studied, as shown in Figure 4.28 without stirring, the percent of nitrate conversion decreased by 10.75%, when the same nitrate electroreduction experiment on FTO/MWCNT-Cu was conducted under the same conditions for 2 h. Such a tendency is not unexpected, as stirring increases the mass transfer to the electrode surface within the electrolysis experiment [21]. Therefore, all experiments were performed here using stirring as stated in the Experimental Sections.

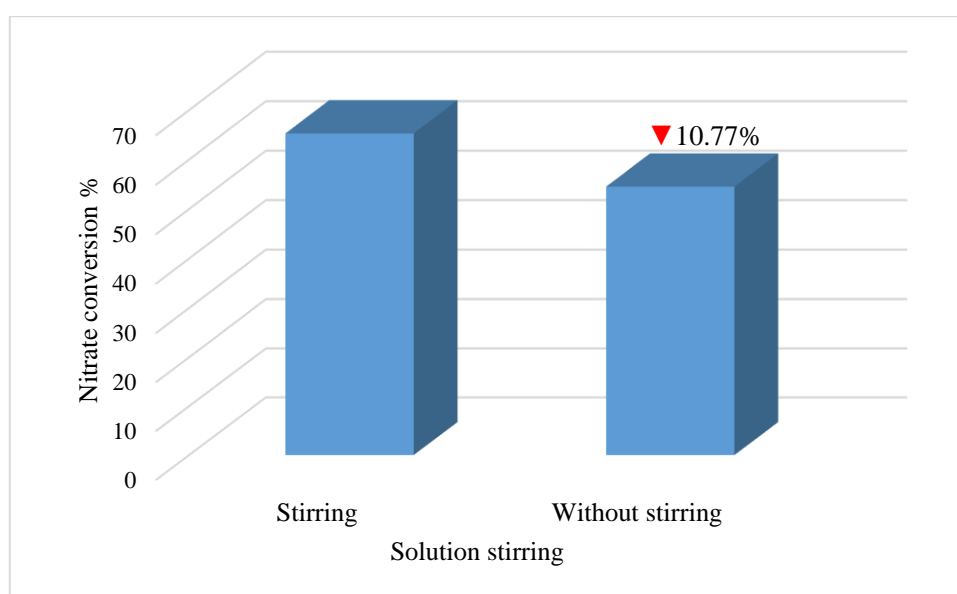


Figure 4.28: Effect of stirring the working solution on nitrate conversion percent using FTO/MWCNT-Cu electrode. Experiments were conducted using (70 mL; 0.05 M Na₂SO₄ + 200 mg/L NO₃⁻), at: 25 ± 1 °C, intrinsic pH, D = 0.75 cm, 2 h, and -1.80 V vs. SCE.

4.3.2.2.5 Effect of Distance between Electrodes

Effect of distance between electrodes (D) on nitrate electroreduction was studied. Figure 4.29 show that nitrate reduction was more efficient when

($D = 0.75$ cm). This slight increase in the conversion of nitrate, by reducing the distance between the electrodes, is due to improvement of the charge transfer between them. Therefore, we have used the distance ($D = 0.75$ cm) throughout this work as stated earlier in the Experimental Sections.

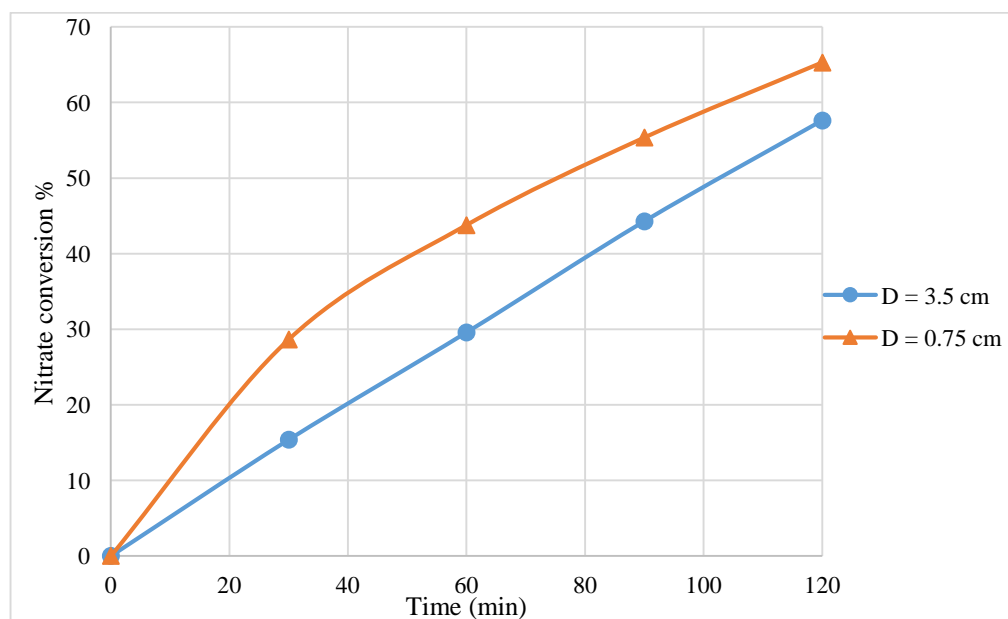


Figure 4.29: Percentage of nitrate conversion on FTO/MWCNT-Cu electrode at (● $D = 3.5$ cm and ▲ $D = 0.75$ cm) vs. electrolysis time on FTO/MWCNT-Cu electrode. Experiments were conducted using (70 mL; 0.05 M Na_2SO_4 + 200 mg/L NO_3^-), at: 25 ± 1 °C, intrinsic pH, 2 h, and -1.80 V vs. SCE.

4.3.2.2.6 Effect of Temperature

The effect of temperature on nitrate electroreduction by FTO/MWCNT-Cu electrode has been investigated in the (10-35) °C range. The results are shown in Figure 4.30. As seen, the percentage of nitrate conversion at 10 °C and 35 °C, were 65.27% and 74.79% respectively. This slight improvement in the conversion of nitrate by raising the temperature, is attributed to the

increase in the rate of diffusion of nitrate to the electrode surface from the bulk of the solution [112].

However, the results show no significant effect of temperature on electroreduction. Temperature effect on electroreduction was rarely studied in previous works. A narrow temperature range was studied here as temperature has only small effect on nitrate electroreduction process. Unless otherwise stated, the temperature 25 ± 1 °C was used throughout this work, as stated in Experimental Sections.

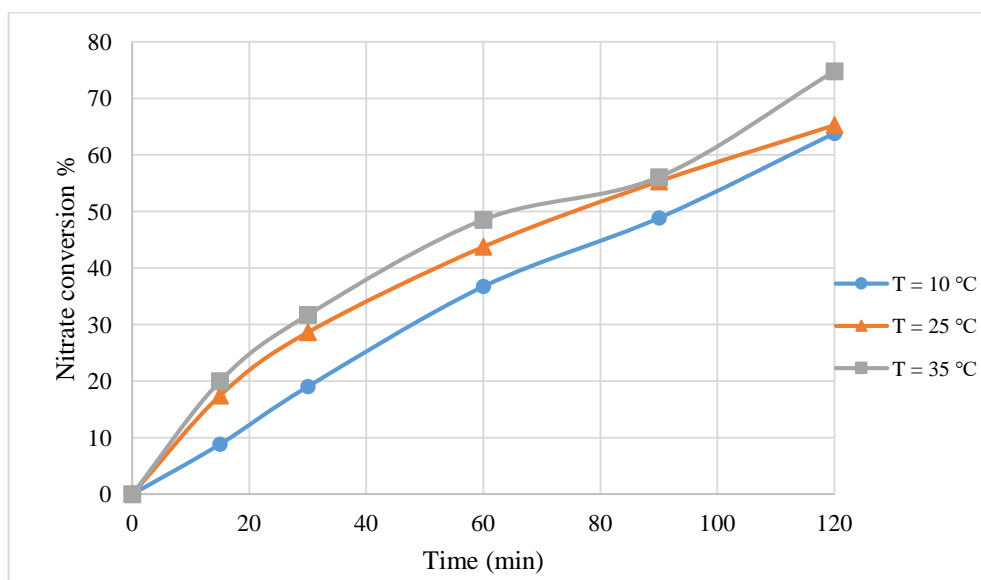


Figure 4.30: Nitrate conversion percent at (● 10 °C, ▲ 25 °C and ■ 35 °C) vs. the electrolysis time on FTO/MWCNT-Cu electrode. Experiments were conducted using (70 mL; 0.05 M Na₂SO₄ + 200 mg/L NO₃⁻), at: intrinsic pH, D = 0.75 cm, 2 h, and -1.80 V vs. SCE.

4.3.2.2.7 Effect of Initial Nitrate Concentration

Effect of variation of initial nitrate concentration during a potentiostatic electrolysis at -1.80 V is reported in Figure 4.31. As shown, when nitrate concentration was increased from 200 mg/L to 600 mg/L and 1000 mg/L,

the amounts of nitrate removal and nitrate conversion percentage values were (130.54 mg, 65.27%), (189.60 mg, 38.98%) and (316 mg, 31.60%), respectively. While the conversion percentage decreases with increased nitrate concentration, the absolute removal increases. This shows the practical value of this study to treat waters with high nitrate contamination.

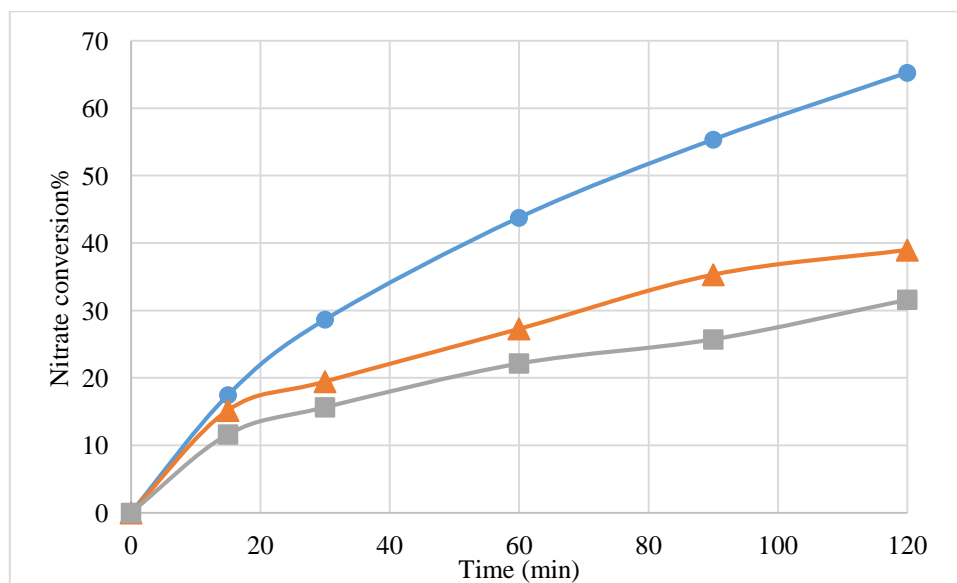


Figure 4.31: Percentage of nitrate conversion vs. the electrolysis time on FTO/MWCNT-Cu electrode, using different initial concentrations of NO_3^- (● 200 mg/L, ▲ 600 mg/L and ■ 1000 mg/L). Experiments were conducted using (70 mL; 0.05 M Na_2SO_4), at: 25 ± 1 °C, intrinsic pH, $D = 0.75$ cm, 2 h, and -1.80 V vs. SCE.

4.3.2.2.8 Effect of Initial pH

Effect of the variation of the initial pH of the working solution (0.05 M $\text{Na}_2\text{SO}_4 + 200$ mg/L NO_3^-), which was 5.40 to more acidic medium, or to basic medium, on nitrate electroreduction have been studied. Figure 4.32 summarizes the results. The Figure shows that changing the initial pH

of the working solution affect the percentage of nitrate conversion within two hours of electrolysis.

Results show that nitrate electroreduction by the prepared electrode FTO/MWCNT-Cu is effective at various pH ranges; acidic or basic media. Also, nitrate electroreduction at the intrinsic pH (5.40) is effective, this is an added value for the prepared electrode from this work, since natural waters have close pH values.

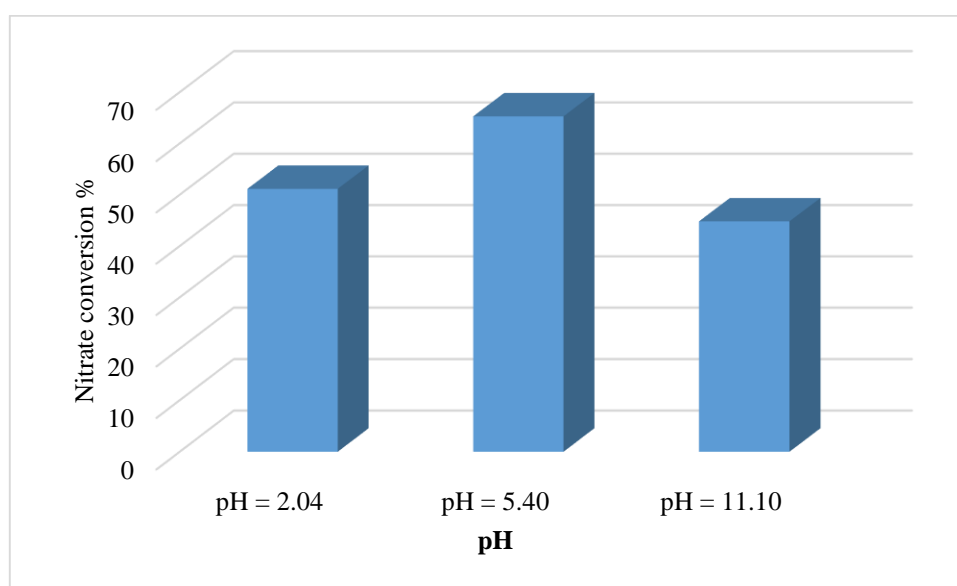


Figure 4.32: Variation of percentage of nitrate conversion against the intrinsic pH on FTO/MWCNT-Cu, for (70 mL; 0.05 M Na_2SO_4 + 200 mg/L NO_3^-). Experiments were conducted at: 25 ± 1 °C, $D = 0.75$ cm, 2 h, and -1.80 V vs. SCE.

4.3.2.3 Kinetics of Nitrate Electroreduction

To find out the rate order and rate constant of nitrate electroreduction process on FTO/MWCNT-Cu electrode, common integrated rate laws were used. Laws of zero order kinetic model, first-order kinetic model and second-order kinetic model were used to test the experimental data.

Integrated formula of these laws are given in equations 4.5, 4.6 and 4.7, respectively [194-196].

$$\text{Zero order reaction: } [C]_t = -kt + [C]_o \dots\dots\dots (4.5)$$

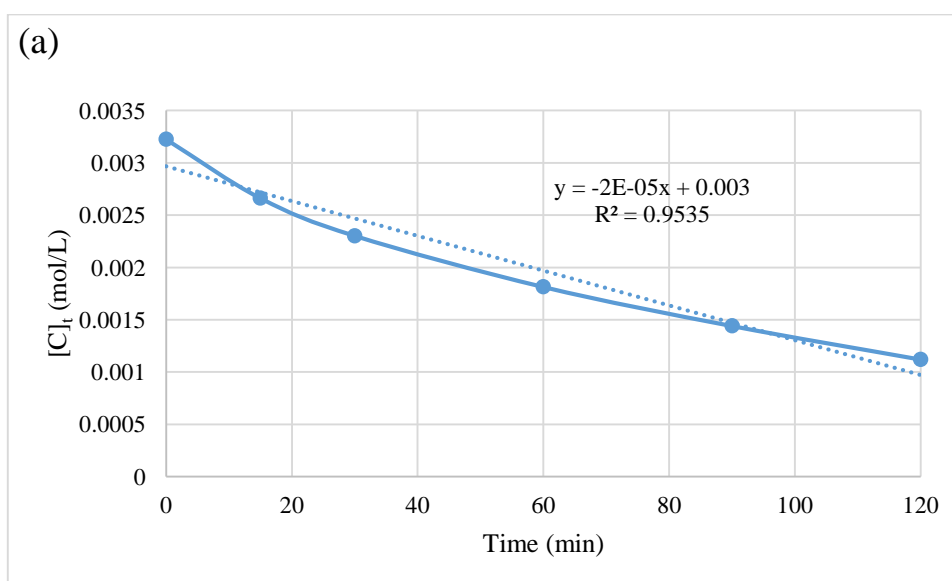
$$\text{First order reaction: } \ln [C]_t = -kt + \ln [C]_o \dots\dots\dots (4.6)$$

$$\text{Second order reaction: } 1/[C]_t = kt + 1/[C]_o \dots\dots\dots (4.7)$$

Where $[C]_o$ is the initial molar concentration of nitrate, $[C]_t$ is the molar concentration of nitrate at time t (min) and k is the rate constant.

In order to quantify the applicability of zero-rate law, first-rate law and second- rate law, linear plots of $[C]_t$ vs. t , $\ln [C]_t$ vs. t , and $1/[C]_t$ vs. t were used to check the fit of the above models respectively. If any of these models is applicable, it should give a linear relationship, from which the rate constant and their correlation coefficients (R^2) can be determined.

Results of investigations of these models on nitrate electroreduction on FTO/MWCNT-Cu electrode are shown in Figure 4.33 (a, b and c) respectively.



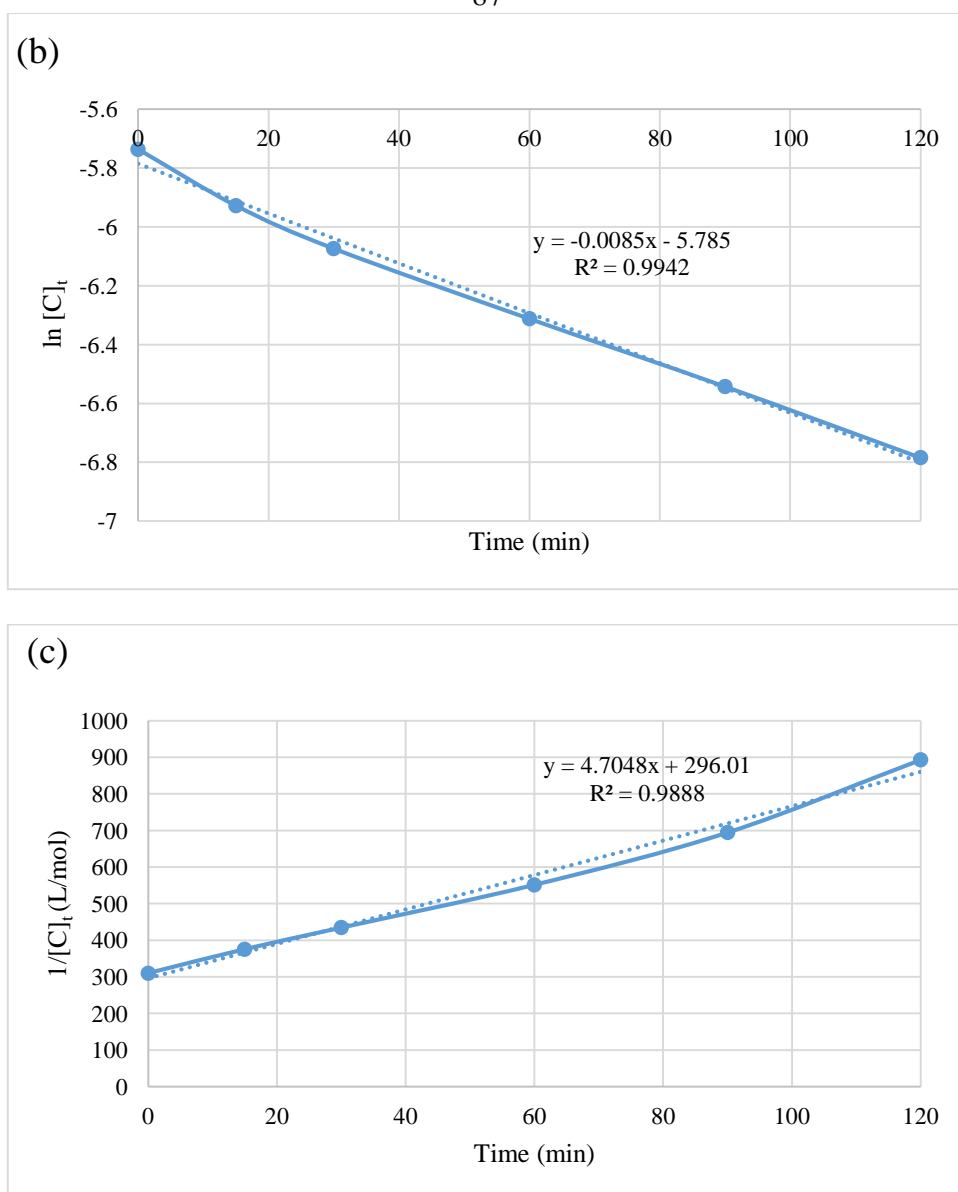


Figure 3.33: Kinetics of nitrate electroreduction according to (a) the zero-order law, (b) the first-order law and (c) to the second-order law by FTO/MWCNT-Cu electrode. Experiments were conducted using (70 mL; 0.05 M Na_2SO_4 + 200 mg/L NO_3^-), at: 25 ± 1 °C, intrinsic pH, $D = 0.75$ cm, 2 h and -1.80 V vs. SCE.

The correlation coefficients for the zero-order, first-order and second-order model are found to be 0.95, 0.99 and 0.98 respectively. The correlation coefficient values (R^2) of the first-order model is slightly greater than those obtained for the zero-order and second-order model. Thus, this indicates that

the first-order kinetic model might be more suitable to describe the kinetic of nitrate electroreduction process on FTO/MWCNT-Cu electrode. Literature also showed that, the nitrate electroreduction obeyed the first order kinetic [101].

Because of the small differences in R^2 values for the three rate laws, another attempt to find the rate order and constant was made using the method of initial rate law [197]. Three electroreduction experiments with different initial concentrations of nitrate (200 mg/L, 600 mg/L and 1000 mg/L) was studied. The general formula of the reaction rate is given in equation (4.8) [198, 199].

$$\text{Rate}_{\text{initial}} = k [C]_o^n \quad \dots\dots\dots (4.8)$$

Using the natural logarithms of both sides of equation (4.8) [198, 199] gives:

$$\ln \text{Rate}_{\text{initial}} = \ln k + n \ln [C]_o \quad \dots\dots\dots (4.9)$$

Where n is the order of the reaction. Initial rate for three different experiments with different initial nitrate concentration was found. Initial rate of each reaction equals the slope of a tangent at initial time to the curve result from plotting nitrate concentration vs. time (Figure 4.34). From the plot of $\ln \text{Rate}_{\text{initial}}$ vs. $\ln [C]_o$ (Figure 4.35), the slope was found to be (0.76), which is equal to the order of the reaction (n), and the rate constant was found from the intercept which is equal to $\ln k$ to be $4.53 \times 10^{-2} \text{ min}^{-1}$.

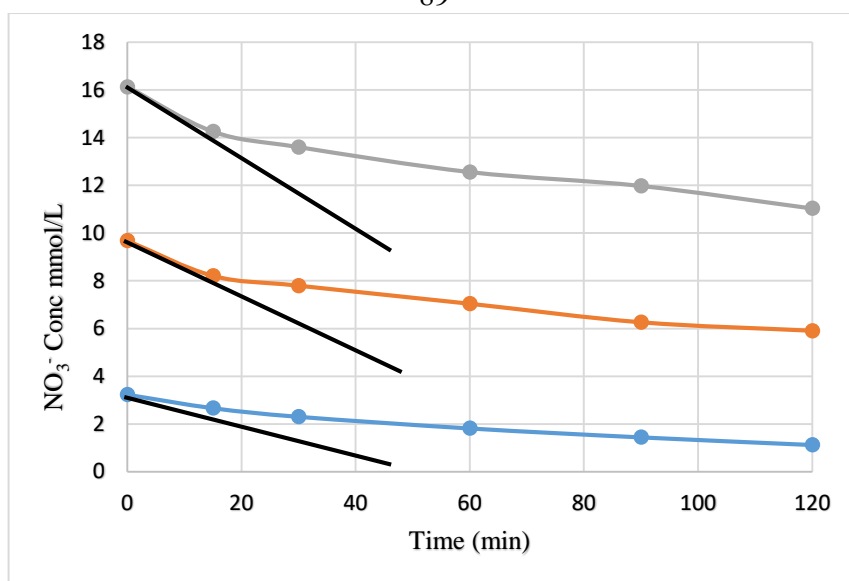


Figure 4.34: Effect of initial concentration of nitrate on initial rate of electroreduction. Experiments were conducted using FTO/MWCNT-Cu electrode, (70 mL; 0.05 M Na₂SO₄), at 25 ± 1 °C, intrinsic pH, $D = 0.75$ cm, 2 h, and -1.80 V vs. SCE.

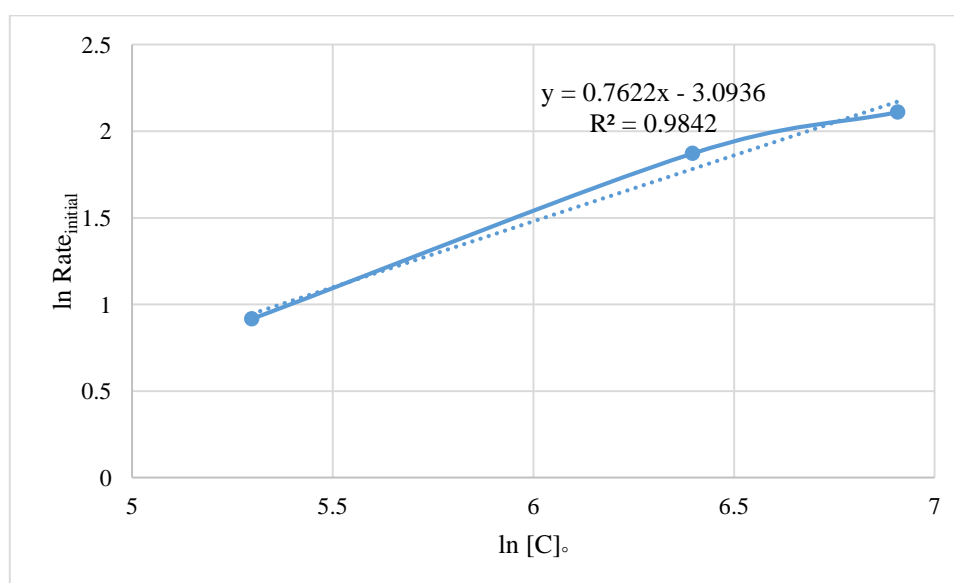


Figure 4.35: Plot of $\ln \text{Rate}_{\text{initial}}$ vs. $\ln [C]_0$ on FTO/MWCNT-Cu electrode. Experiments were conducted using (70 mL; 0.05 M Na₂SO₄), at 25 ± 1 °C, intrinsic pH, $D = 0.75$ cm, 2 h, and -1.80 V vs. SCE.

It should be noted that the logarithmic method does not tell surely if the reaction is first or second order despite the value for R^2 . However, based on higher R^2 value, the reaction is closer to but not a first order. This is

consistent with the initial rate method findings, where the reaction rate is not first order as well, but is 0.76. This value is comparable to those in literature as Table 4.9 shows. Values of ($n < 1$) reveals that nitrate is adsorbed at the electrode surface and reduced, as well as co-adsorption of other species occurs [139]. The rate constant value is therefore preferentially obtained from the initial rate method as $4.53 \times 10^{-2} \text{ min}^{-1}$.

Table 4.9: Comparison of order and rate constant of nitrate electroreduction values for FTO/MWCNT-Cu electrode with literature.

Electrode	Order of the reaction (n)	Rate constant	Initial NO_3^- Con	Ref.
CuPc/CNT*	0.78	15.03 sec^{-1}	1 M	[128]
Pd/Cu	0.70	-	0.1 M	[200]
Cu/Graphite	0.88	$0.75 \times 10^{-4} \text{ sec}^{-1}$	1 M	[201]
Pd/Cu/Graphite	0.87	$2.23 \times 10^{-4} \text{ sec}^{-1}$	1 M	[201]
FTO/MWCNT-Cu	0.76	$7.55 \times 10^{-4} \text{ sec}^{-1}$	$3.22 \times 10^{-3} \text{ M}$	This work

* Copper phthalocyanine supported on functionalised multi-walled carbon.

Reaction rate constant indicates the efficiency of nitrate electroreduction [202]. Table 4.9 shows that reaction of nitrate electroreduction in this work occurs more efficiently than in literature.

4.3.2.4 Prolonged Electroreduction Time

Variation of concentration of nitrate, nitrite, and ammonium during 7 hours of electrolysis by FTO/MWCNT-Cu electrode, at -1.80 V vs. SCE, are shown in Figure 4.36.

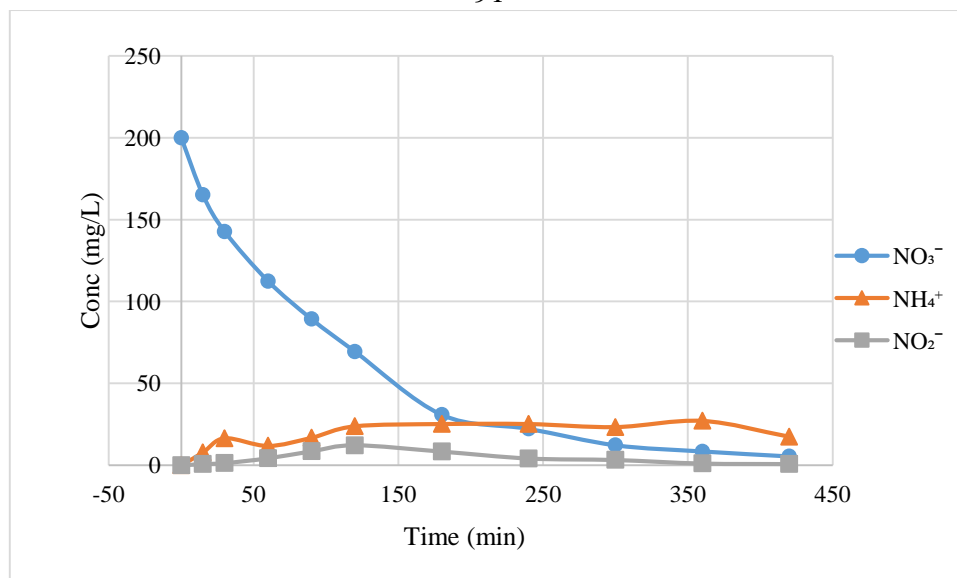


Figure 4.36: Variation of the concentration of nitrate, nitrite and ammonium against the electrolysis time on FTO/MWCNT-Cu. Experiments were conducted using (70 mL; 0.05 M Na₂SO₄ + 200 mg/L NO₃⁻) at: 25 ± 1 °C, intrinsic pH, D = 0.75 cm, and -1.80 V vs. SCE. After 200 min of electrolysis, nitrate concentration in the working solution reaches only about 25 mg/L. This concentration is about half the allowed nitrate concentration according to WHO (50 mg/L). Almost 100% of nitrate was converted after 300 min of electrolysis. Nitrite concentration increased in the working solution and began to decrease after 130 min of electrolysis, and at the end of the experiment no nitrite was found in the solution. The concentration of ammonium ion started to decrease within the last hour of electrolysis.

Table 4.10: Selectivity for ammonium, nitrite and nitrogen on FTO/MWCNT-Cu. Experiments were conducted using (70 mL; 0.05 M Na₂SO₄ + 200 mg/L NO₃⁻) at: 25 ± 1 °C, intrinsic pH, D = 0.75 cm, -1.80 V vs. SCE, and different time of electrolysis (2 h, 3 h and 7 h).

Time	NO ₃ ⁻ conversion% (Based on mg L ⁻¹ Conc.)	S%		
		(Based on molar Conc.)		
		NH ₄ ⁺	NO ₂ ⁻	N ₂
2 h	65.27	62.55	13.60	23.85
3 h	87.62	53.61	7.11	39.28
7 h	97.28	34.69	0.00	65.31

As shown in Table 4.10, selectivity of nitrogen increases by increasing the time of electrolysis. After seven hours of electrolysis, selectivity for ammonium, and nitrogen, were 34.69% and 65.31% respectively. The high selectivity for nitrogen gas is another evidence for the efficiency of our new modified electrode FTO/MWCNT-Cu.

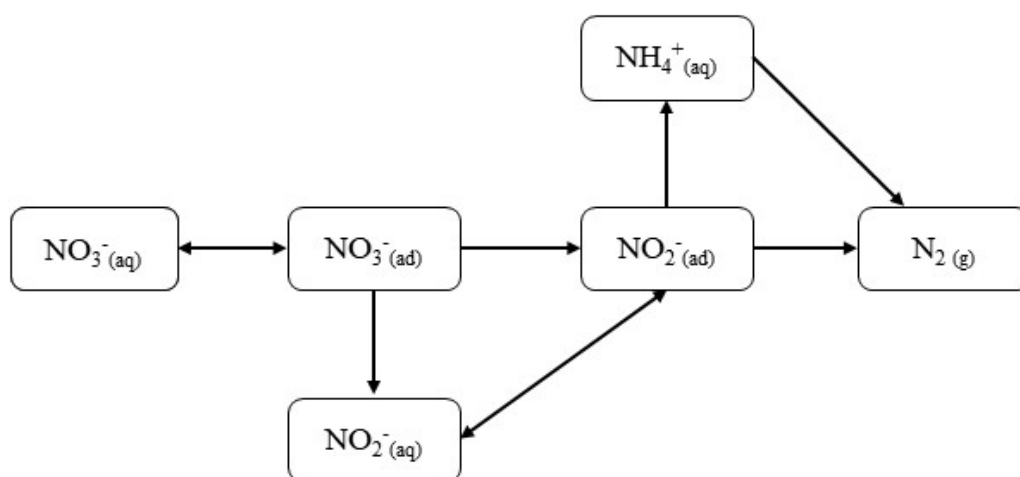


Figure 4.37: Simplified scheme for nitrate electrochemical pathways on FTO/MWCNT-Cu electrode.

Electroreduction of nitrate ions is a complex reaction that occurs at a multi-step reaction mechanism [97, 139, 203]. Figure 4.37 shows simplified scheme of the main steps in nitrate electrolysis on FTO/MWCNT-Cu electrode. Nitrate electroreduction requires an initial adsorption step of nitrate at the cathode surface [204]. So, enhancing mass transfer and increasing electrode surface area is important to increase the efficiency of nitrate electroreduction [111, 139, 200, 205, 206]. This proves one of the basic assumptions made in this work for the new modified FTO/MWCNT-Cu electrode.

Adsorption of nitrate ion on the electrode surface is one step. Then, an electron transfer occurs to yield nitrite NO_2^- , as described earlier [204]. The nitrate reacts in various routes to other products including nitrogen gas or ammonia [208, 207, 117].

In the electroreduction process, the major semi-stable intermediate is nitrite [208, 207, 117]. Variation in nitrite concentration shown in Figure 4.36, confirms that nitrite is an intermediate product. The nitrite may yield ammonia in through intermediates, such as the nitrous oxide (N_2O) and nitric oxide (NO), which finally yields nitrogen [209].

4.3.2.5 Alkalinity Change during Process

Figure 4.38 shows pH changes of the working solutions during 5 hours of electrolysis, increasing pH is expected to be due to formation of hydroxyl group result from conversion of nitrate to nitrite, ammonia and nitrogen

[28, 210]. The pH value increases during the reaction after 120 min of electrolysis get a stable value $\sim 10.9 \pm 0.2$.

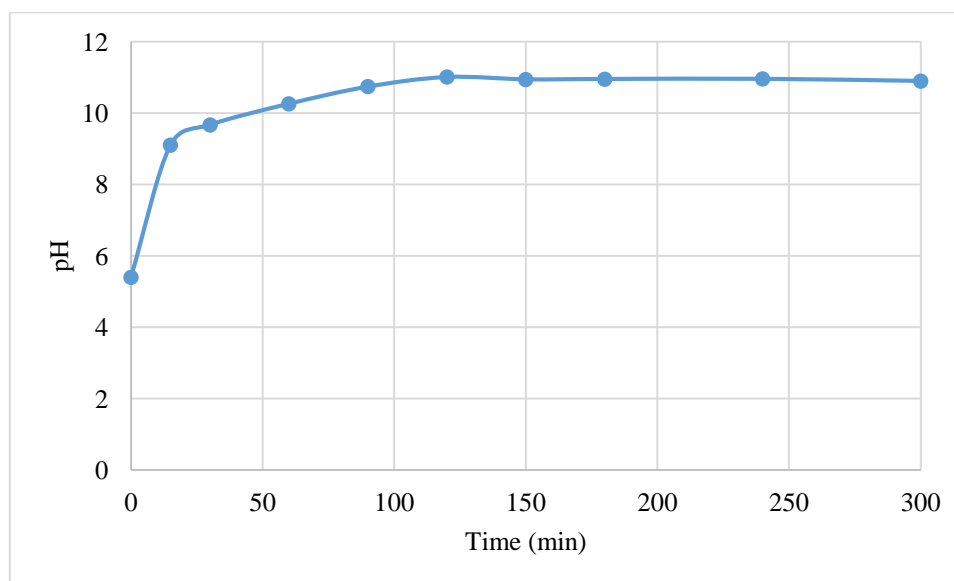


Figure 4.38: pH changes during five hours of electrolysis. Experiment was conducted using (70 mL; 0.05 M Na_2SO_4 + 200 mg/L NO_3^-) at: 25 ± 1 °C, intrinsic pH, $D = 0.75$ cm, -1.80 V vs. SCE.

4.3.2.6 Stability and Reuse of the Electrode

Result of three consecutive potentiostatic electroreduction experiments at -1.80 V, using the same electrode FTO/MWCNT-Cu, are shown in Figure 4.39. As is shown in the figure, the percentage of nitrate conversion obtained by using the same electrode for two hours, was almost the same ($65 \pm 2\%$) in all three experiments. This implies the stability and efficiency of the modified electrode (FTO/MWCNT-Cu).

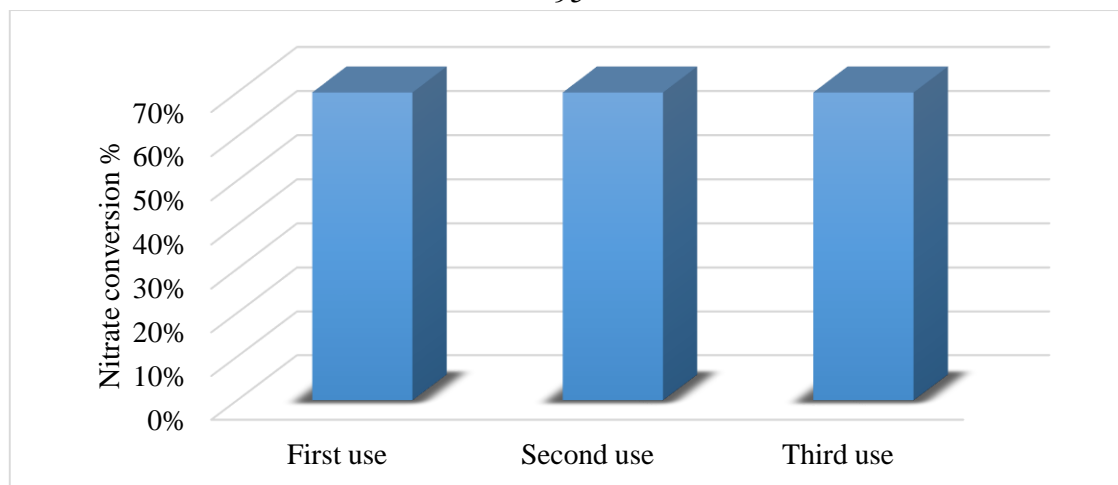


Figure 4.39: Percentage of nitrate conversion for three consecutive times (2 h each), using the same electrode (FTO/MWCNT-Cu). Experiments were conducted using (70 mL; 0.05 M Na₂SO₄ + 200 mg/L NO₃⁻), at: 25 ± 1 °C, intrinsic pH, D = 0.75 cm, and -1.80 V vs. SCE.

Comparison of nitrate electroreduction performance of this modified electrode, with other reported materials, is given in Table 4.11. Results show the effectiveness of FTO/MWCNT-Cu electrode compared with literature. In literature, the main selectivity for nitrate electroreduction by Cu electrode was for NH₄⁺ (reaching 97% after 250 h of electrolysis) and the remaining as NO₂⁻ [100]. The FTO/MWCNT-Cu electrode here shows complete removal of nitrate in 7 h, with 34.7% NH₄⁺ and 65.3% nitrogen. Our electrode thus shows higher efficiency and selectivity than literature systems. In some literature, longer times of 250 h [100] or 48 h [201] were needed for complete removal of nitrate, compared to only 7 h here.

Maximum selectivity for nitrogen was recorded in literature to be (60 - 70%), this was achieved by bimetallic catalyst from Cu and Pd in ~48 h of electrolysis [201], while the FTO/MWCNT-Cu gave 65.35% selectivity of

nitrogen within only 7 h of electrolysis. Therefore, the catalyst described here combines both efficiency and selectivity compared to others.

These results show that the FTO/MWCNT-Cu electrode is strongly recommended to use in nitrate removal from aqueous solutions. Moreover, the electrolytic system used throughout this work was simple and the electrolyte used was not harmful, compared to others used in literature. Add to these advantages the working potential needed in our catalyst is only -1.80 V.

Table 4.11: Comparison between the present electrodes with reported ones in nitrate electroreduction.

Operation and configuration	Reaction media	Electrode material			Power supply	Time	NO ₃ ⁻ conversion/%	Final Products			Ref.
		Cathode	Anode	Reference				S%			
								NH ₄ ⁺	NO ₂ ⁻	N ₂	
Flow cell (2 mL/ min), with cation and anion exchange membrane.	Acetate and phosphate buffer (pH 4.8) + 3 g/L NO ₃ ⁻	Graphite/Ni/Cu	Pt	-	1.86 A	500 min	82	62	4	-	[6]
Undivided cell	0.1 M K ₂ SO ₄ + 150 ppm NO ₃ ⁻	Ti/BDD/Cu	BDD*	Ag/AgCl/KCl _(sat)	20 mA/cm ⁻²	5 h	57.46	-	-	-	[211]
Undivided batch electrochemical cell	2 g/ L Na ₂ SO ₄ + 25 mg/L NO ₃ ⁻ -N	Cu	Pt/Ti	-	20 mA/cm ⁻²	140 min	94.94	-	-	-	[115]
Two compartment cell separated by cationic exchange membrane	1 M NaOH + 0.1 M NO ₃ ⁻	Cu disk	Pt	Hg/HgO	-1.4 V	250 h	100	97	3	-	[100]
Bach undivided electrolytic cell	30 mmol dm ⁻³ NO ₃ ⁻ + 0.1 mol dm ⁻³ K ₂ SO ₄	Cu rotating cylinder	Pt	SCE	-1.2 V	1 h	92	86	-	-	[113]

H cell separated by parous glass fit	5 M HClO ₄ + 1 M NO ₃ ⁻	CuPc/CNT**	Pt/C	Ag/AgCl	-0.6 V	24 h	65	-	-	-	[128]
Batch electrochemical cell	500 mg/L NaCl + 3% w/w Na ₂ SO ₄ + 150 mg/L NO ₃ ⁻	Ti/Cu ₅ ZnOx***	Ti/RuO ₂ - IrO ₂	SCE	20 mA/cm ⁻²	6 h	92.3	-	-	33.7	[117]
Two compartment cell	1 M NaOH + 0.1 M NO ₃ ⁻	Cu ₇₀ Ni ₃₀ rotating disc	Pt	Hg/ HgO	-1.2 V	8 h	86.8	95.9	-	-	[120]
Batch electrochemical cell	0.1 M Na ₂ SO ₄ + 3.61 g/L KNO ₃	Ti/CNTs/Cu ₅ -Pd ₅	SCE	Hg/ Hg ₂ Cl ₂	-1.3 V	4 h	32.52	54.0	3.5	42.5	[119]
Batch electrochemical cell	1 M NaNO ₃ + 0.5 M NaOH	Pd-Cu/graphite (95% Pd + 5% Cu)	Pt	Hg/ HgO	-1.1 V	48 h	100	~1	29	70	[201]
Batch electrochemical cell	0.05 M Na ₂ SO ₄ + 200 mg/L NO ₃ ⁻	FTO/Cu-b FTO/Gr-Cu FTO/MWCNT-Cu	Pt Pt Pt	SCE SCE SCE	-1.8 V -1.8 V -1.8 V	2 h 2 h 2 h 7 h	93.90 25.69 65.27 97.28	63.3 46.8 62.6 34.7	7.14 16.2 13.6 0.00	29.6 37.0 23.8 65.3	This work

*Boron doped diamond.

** Copper phthalocyanine supported on functionalised multi-walled carbon nanotubes (CuPc/CNT).

*** Cu/Zn atomic % 5.37:1.

Chapter Five
Conclusion

Chapter Five

Conclusion

5.1 Conclusion

Different electrodes have been modified, characterized and used for nitrate electroreduction. The following conclusions were drawn from this study:

1. Electrodeposition of Cu on FTO surface by potentiostatic method gave better adhesion between the deposited film and FTO surface, compared with deposition by CV method.
2. Thin film of Cu on FTO was more stable when deposited from acidic solution than from neutral solution, as shown by XRD analysis.
3. FTO has been used here for the first time as substrate for electrodes in nitrate electroreduction. FTO sheet showed low rate for nitrate conversion with high selectivity for nitrogen.
4. FTO/Cu-b electrode showed higher efficiency in nitrate electroreduction compared with Cu sheet, which shows the special importance of Cu nanoparticles.
5. Modification of FTO surface by graphite thin film increased the efficiency of nitrate electroreduction.
6. Small amount of highly stable Cu was loaded on the surface of FTO/Gr electrode by electrodeposition.
7. FTO/Gr-Cu electrode was prepared successfully for the first time here.
8. FTO/MWCNT-Cu electrode was successfully fabricated, for the first time, via a simple method.

9. Characterization of MWCNT-Cu nanocomposite by transmission electron microscopy could not be made and is recommended.
10. The main product for nitrate electroreduction by almost all the prepared electrodes after 2 h of electrolysis was NH_4^+ .
11. Voltammetric tests of nitrate reduction showed highest catalytic activity for the FTO/MWCNT-Cu electrode.
12. Among different electrodes, the modified electrode FTO/MWCNT-Cu showed the best performance for nitrate electroreduction, and was used for studying the effects of different parameters on nitrate electroreduction.
13. Electrolysis carried out at low over potentials ($E = -1.80 \text{ V vs. SCE}$) with FTO/MWCNT-Cu showed a fairly rapid decay of nitrate concentration, confirming the high performance of the electrode.
14. FTO/MWCNT-Cu electrode is stable and retains its catalytic activity in a durability test.

5.2 Future Suggestions

It is recommended to investigate the following:

1. Studying the effect of Cu amount on the FTO/Cu electrodes on the efficiency of nitrate electroreduction.
2. Using the FTO/Glass substrates for deposition of bimetallic system such as Ni/Cu or Pd/Cu to modify other electrodes.
3. Deposition of Ni on FTO/Gr electrode before Cu deposition on its surface.

4. Conducting nitrate electroreduction experiments on real samples by FTO/MWCNT-Cu electrode.
5. Studying the mechanism of nitrate electroreduction on FTO/MWCNT-Cu electrode.
6. Studying current efficiency of nitrate electroreduction on FTO/MWCNT-Cu electrode.
7. Conducting nitrate electroreduction experiments by the prepared electrodes using $\text{NaCl}_{(\text{aq})}$ as electrolyte.
8. Studying nitrate electroreduction using H-electrochemical cell with cation exchange membrane, by FTO/MWCNT-Cu electrode.
9. Studying nitrate electroreduction using different counter electrodes.
10. Preparing a new electrode by electrodeposition of Cu on the surface of FTO/MWCNT electrode.
11. Fabrication of the prepared composite MWCNT-Cu on the surface of graphite felt to study the effect of substrate on the electroreduction process.
12. Preparation of MWCNT/Cu-Pd nanocomposite in order to prepare
13. a new modified electrode on FTO substrate.
14. Designing a pilot-plant scale continuous-flow reactor for nitrate electroreduction based on the FTO/MWCNT-Cu electrode described here.

References

1. Cabello, P., M.D. Roldan, and C. Moreno-Vivian, *Nitrate reduction and the nitrogen cycle in archaea*. **Microbiology**, 2004. **150**(11): p. 3527-3546.
2. Galloway, J.N., F.J. Dentener, D.G. Capone, E.W. Boyer, R.W. Howarth, S.P. Seitzinger, G.P. Asner, C.C. Cleveland, P. Green, and E.A. Holland, *Nitrogen cycles: past, present, and future*. **Biogeochemistry**, 2004. **70**(2): p. 153-226.
3. Imsande, J. and B. Touraine, *N demand and the regulation of nitrate uptake*. **Plant physiology**, 1994. **105**(1): p. 3.
4. Smil, V., *Nitrogen cycle and world food production*. **World Agriculture**, 2011. **2**(1): p. 9-13.
5. Afzal, B.M., *Drinking water and women's health*. **Journal of midwifery & women's health**, 2006. **51**(1): p. 12-18.
6. Abdallah, R., F. Geneste, T. Labasque, H. Djelal, F. Fourcade, A. Amrane, S. Taha, and D. Floner, *Selective and quantitative nitrate electroreduction to ammonium using a porous copper electrode in an electrochemical flow cell*. **Journal of Electroanalytical Chemistry**, 2014. **727**: p. 148-153.
7. Zaqoot, H.A., M. Hamada, and S. Miqdad, *A comparative study of ANN for predicting nitrate concentration in groundwater wells in the southern area of Gaza Strip*. **Applied Artificial Intelligence**, 2018. **32**(7-8): p. 727-744.

8. Anayah, F.M. and M.N. Almasri, *Trends and occurrences of nitrate in the groundwater of the West Bank, Palestine*. **Applied Geography**, 2009. **29**(4): p. 588-601.
9. Zhou, Z., N. Ansems, and P. Torfs, *A global assessment of nitrate contamination in groundwater*. **International Groundwater Resources Assessment Center. Internship report**, 2015.
10. Vymazal, J., *Removal of nutrients in various types of constructed wetlands*. **Science of the total environment**, 2007. **380**(1-3): p. 48-65.
11. Yang, Y.-Y. and G.S. Toor, *Sources and mechanisms of nitrate and orthophosphate transport in urban stormwater runoff from residential catchments*. **Water research**, 2017. **112**: p. 176-184.
12. Burkart, M. and J. Stoner, *Nitrate in aquifers beneath agricultural systems*. **Water science and technology**, 2007. **56**(1): p. 59-69.
13. Rupert, M.G., *Decadal-scale changes of nitrate in ground water of the United States, 1988–2004*. **Journal of Environmental Quality**, 2008. **37**(5_Supplement): p. S-240-S-248.
14. Burow, K.R., B.T. Nolan, M.G. Rupert, and N.M. Dubrovsky, *Nitrate in groundwater of the United States, 1991– 2003*. **Environmental Science & Technology**, 2010. **44**(13): p. 4988-4997.
15. Casella, I.G. and M. Contursi, *An electrochemical and XPS study of the electrodeposited binary Pd–Sn catalyst: The electroreduction of nitrate ions in acid medium*. **Journal of Electroanalytical Chemistry**, 2006. **588**(1): p. 147-154.

16. Bockris, J.M. and J. Kim, *Electrochemical treatment of low-level nuclear wastes*. **Journal of applied electrochemistry**, 1997. **27**(6): p. 623-634.
17. Sobti, R. and S. Sharma, *Nitrate removal from ground water*. **EJ. Chem.**, 2011. **9**: p. 1667-1675.
18. Kapoor, A. and T. Viraraghavan, *Nitrate removal from drinking water*. **Journal of environmental engineering**, 1997. **123**(4): p. 371-380.
19. Mensinga, T.T., G.J. Speijers, and J. Meulenbelt, *Health implications of exposure to environmental nitrogenous compounds*. **Toxicological reviews**, 2003. **22**(1): p. 41-51.
20. Ward, M.H., T.M. DeKok, P. Levallois, J. Brender, G. Gulis, B.T. Nolan, and J. VanDerslice, *Workgroup report: drinking-water nitrate and health—recent findings and research needs*. **Environmental health perspectives**, 2005. **113**(11): p. 1607-1614.
21. Weyer, P., J. Kantamneni, X. Lu, M. Ward, and J. Cerhan, *Nitrate Ingestion from drinking water and diet and cancer risk*. **Epidemiology**, 2008. **19**(6): p. S55.
22. Fan, A.M. and V.E. Steinberg, *Health implications of nitrate and nitrite in drinking water: an update on methemoglobinemia occurrence and reproductive and developmental toxicity*. **Regulatory toxicology and pharmacology**, 1996. **23**(1): p. 35-43.

23. Pelley, J., *Nitrate eyed as endocrine disruptor*. 2003, ACS Publications.
24. Lundberg, J.O., M. Carlström, and E. Weitzberg, *Metabolic effects of dietary nitrate in health and disease*. **Cell metabolism**, 2018. **28**(1): p. 9-22.
25. Chan, T.Y., *Vegetable-borne nitrate and nitrite and the risk of methaemoglobinaemia*. **Toxicology letters**, 2011. **200**(1-2): p. 107-108.
26. Luk, G. and W. Au-Yeung, *Experimental investigation on the chemical reduction of nitrate from groundwater*. **Advances in environmental research**, 2002. **6**(4): p. 441-453.
27. Ayyasamy, P.M., K. Shanthi, P. Lakshmanaperumalsamy, S.-J. Lee, N.-C. Choi, and D.-J. Kim, *Two-stage removal of nitrate from groundwater using biological and chemical treatments*. **Journal of bioscience and bioengineering**, 2007. **104**(2): p. 129-134.
28. Talhi, B., F. Monette, and A. Azzouz, *Effective and selective nitrate electroreduction into nitrogen through synergistic parameter interactions*. **Electrochimica acta**, 2011. **58**: p. 276-284.
29. Ghafari, S., M. Hasan, and M.K. Aroua, *Bio-electrochemical removal of nitrate from water and wastewater—a review*. **Bioresource technology**, 2008. **99**(10): p. 3965-3974.
30. WHO, G., *Guidelines for drinking-water quality*. **World Health Organization**, 2011. **216**: p. 303-304.

31. Mikuška, P. and Z. Večeřa, *Simultaneous determination of nitrite and nitrate in water by chemiluminescent flow-injection analysis. Analytica chimica acta*, 2003. **495**(1-2): p. 225-232.
32. Matějů, V., S. Čížinská, J. Krejčí, and T. Janoch, *Biological water denitrification—a review. Enzyme and microbial technology*, 1992. **14**(3): p. 170-183.
33. Badea, G.E., *Electrocatalytic reduction of nitrate on copper electrode in alkaline solution. Electrochimica Acta*, 2009. **54**(3): p. 996-1001.
34. Ferro, S. and A. e Farmaceutiche, **Removal of Nitrates from industrial wastewater**. 2012.
35. Barrabés, N., J. Just, A. Dafinov, F. Medina, J. Fierro, J. Sueiras, P. Salagre, and Y. Cesteros, *Catalytic reduction of nitrate on Pt-Cu and Pd-Cu on active carbon using continuous reactor: The effect of copper nanoparticles. Applied Catalysis B: Environmental*, 2006. **62**(1-2): p. 77-85.
36. Panyor, L. and C. Fabiani, *Anion rejection in a nitrate highly rejecting reverse osmosis thin-film composite membrane. Desalination*, 1996. **104**(3): p. 165-174.
37. Clifford, D.A., **Ion exchange and inorganic adsorption. MCGRAW-HILL, INC.,(USA)**. 1194, 1990: p. 1990.
38. Schoeman, J. and A. Steyn, *Nitrate removal with reverse osmosis in a rural area in South Africa*. 2003.

39. Mani, K., *Electrodialysis water splitting technology*. **Journal of membrane science**, 1991. **58**(2): p. 117-138.
40. Aghapour, A.A., S. Nemati, A. Mohammadi, H. Nourmoradi, and S. Karimzadeh, *Nitrate removal from water using alum and ferric chloride: a comparative study of alum and ferric chloride efficiency*. **Environmental Health Engineering and Management Journal**, 2016. **3**(2): p. 69-73.
41. Clifford, D. and W. Weber. *A Nitrate-Removal Ion-Exchange Process With a Land-Disposable Regenerant*. in *Proceedings of the 1977 National Conference on Treatment and Disposal of Industrial Wastewaters and Residues April 26-28, 1977, Houston, Texas*, p. 216-225.
42. Rautenbach, R., W. Kopp, G. Van Opbergen, and R. Hellekes, *Nitrate reduction of well water by reverse osmosis and electrodialysis-studies on plant performance and costs*. **Desalination**, 1987. **65**: p. 241-258.
43. Inazu, K., M. Kitahara, and K.-i. Aika, *Decomposition of ammonium nitrate in aqueous solution using supported platinum catalysts*. **Catalysis today**, 2004. **93**: p. 263-271.
44. Prüsse, U., M. Hähnlein, J. Daum, and K.-D. Vorlop, *Improving the catalytic nitrate reduction*. **Catalysis Today**, 2000. **55**(1-2): p. 79-90.
45. Gao, W., N. Guan, J. Chen, X. Guan, R. Jin, H. Zeng, Z. Liu, and F. Zhang, *Titania supported Pd-Cu bimetallic catalyst for the reduction*

- of nitrate in drinking water. Applied Catalysis B: Environmental*, 2003. **46**(2): p. 341-351.
46. Ottley, C., W. Davison, and W. Edmunds, *Chemical catalysis of nitrate reduction by iron (II)*. *Geochimica et Cosmochimica acta*, 1997. **61**(9): p. 1819-1828.
47. Gauthard, F., F. Epron, and J. Barbier, *Palladium and platinum-based catalysts in the catalytic reduction of nitrate in water: effect of copper, silver, or gold addition*. *Journal of Catalysis*, 2003. **220**(1): p. 182-191.
48. Kaczur, J.J., D.W. Cawfield, and K.E. Woodard, *Process and apparatus for the removal of oxyhalide species from aqueous solutions*. 1992, Google Patents.
49. Kaczur, J.J., D.W. Cawfield, and K.E. Woodard Jr, *Process for the removal of oxynitrogen species for aqueous solutions*. 1994, Google Patents.
50. Kaczur, J.J. and D. Cawfield. *Oxyhalide and Oxynitrogen Specie Removal From Aqueous Solutions by Electrochemical Reduction*. in *8th Annual International Forum on Electrolysis in the Chemical Industry: Environmental Electrochemistry*”, Lake Buena Vista, FL. 1994.
51. Rutten, O., A. Van Sandwijk, and G. Van Weert, *The electrochemical reduction of nitrate in acidic nitrate solutions*. *Journal of applied electrochemistry*, 1999. **29**(1): p. 87-92.

52. Janssen, L., M. Pieterse, and E. Barendrecht, *Reduction of nitric oxide at a platinum cathode in an acidic solution*. **Electrochimica Acta**, 1977. **22**(1): p. 27-30.
53. Li, H.I., D.H. Robertson, J.Q. Chambers, and D.T. Hobbs, *Electrochemical reduction of nitrate and nitrite in concentrated sodium hydroxide at platinum and nickel electrodes*. **Journal of the Electrochemical Society**, 1988. **135**(5): p. 1154-1158.
54. Gootzen, J., P. Peeters, J. Dukers, L. Lefferts, W. Visscher, and J. Van Veen, *The electrocatalytic reduction of NO_3^- on Pt, Pd and Pt/Pd electrodes activated with Ge*. **Journal of electroanalytical chemistry**, 1997. **434**(1-2): p. 171-183.
55. Horanyi, G. and E. Rizmayer, *Electrocatalytic reduction of NO_2^- and NO_3^- ions at a platinized platinum electrode in alkaline medium*. **Journal of electroanalytical chemistry and interfacial electrochemistry**, 1985. **188**(1-2): p. 265-272.
56. Katsounaros, I., M. Dortsiou, and G. Kyriacou, *Electrochemical reduction of nitrate and nitrite in simulated liquid nuclear wastes*. **Journal of hazardous materials**, 2009. **171**(1-3): p. 323-327.
57. Dash, B.P. and S. Chaudhari, *Electrochemical denitrification of simulated ground water*. **Water research**, 2005. **39**(17): p. 4065-4072.
58. Bosko, M.L., M. Rodrigues, J.Z. Ferreira, E.E. Miró, and A.M. Bernardes, *Nitrate reduction of brines from water desalination*

- plants by membrane electrolysis. Journal of membrane science*, 2014. **451**: p. 276-284.
59. Ghazouani, M., H. Akrou, and L. Bousselmi, *Nitrate and carbon matter removals from real effluents using Si/BDD electrode. Environmental Science and Pollution Research*, 2017. **24**(11): p. 9895-9906.
60. Xu, D., Y. Li, L. Yin, Y. Ji, J. Niu, and Y. Yu, *Electrochemical removal of nitrate in industrial wastewater. Frontiers of environmental science & engineering*, 2018. **12**(1): p. 9.
61. Li, M., C. Feng, Z. Zhang, Z. Shen, and N. Sugiura, *Electrochemical reduction of nitrate using various anodes and a Cu/Zn cathode. Electrochemistry communications*, 2009. **11**(10): p. 1853-1856.
62. Pérez, G., A. Fernández-Alba, A. Urtiaga, and I. Ortiz, *Electro-oxidation of reverse osmosis concentrates generated in tertiary water treatment. Water research*, 2010. **44**(9): p. 2763-2772.
63. Sa, Y.J., C.W. Lee, S.Y. Lee, J. Na, U. Lee, and Y.J. Hwang, *Catalyst–electrolyte interface chemistry for electrochemical CO₂ reduction. Chemical Society Reviews*, 2020. **49**(18): p. 6632-6665.
64. Polatides, C. and G. Kyriacou, *Electrochemical reduction of nitrate ion on various cathodes–reaction kinetics on bronze cathode. Journal of Applied Electrochemistry*, 2005. **35**(5): p. 421-427.

65. Xiang, Y., D.-L. Zhou, and J.F. Rusling, *Electrochemical conversion of nitrate to ammonia in water using Cobalt-DIM as catalyst. Journal of Electroanalytical Chemistry*, 1997. **424**(1-2): p. 1-3.
66. Chebotareva, N. and T. Nyokong, *Metallophthalocyanine catalysed electroreduction of nitrate and nitrite ions in alkaline media. Journal of applied electrochemistry*, 1997. **27**(8): p. 975-981.
67. Paidar, M., I. Roušar, and K. Bouzek, *Electrochemical removal of nitrate ions in waste solutions after regeneration of ion exchange columns. Journal of Applied Electrochemistry*, 1999. **29**(5): p. 611-617.
68. Ureta-Zañartu, S. and C. Yáñez, *Electroreduction of nitrate ion on Pt, Ir and on 70: 30 Pt: Ir alloy. Electrochimica acta*, 1997. **42**(11): p. 1725-1731.
69. M cov , Z., K. Bouzek, and J. er k, *Electrocatalytic activity of copper alloys for NO_3^- reduction in a weakly alkaline solution. Journal of Applied Electrochemistry*, 2007. **37**(5): p. 557-566.
70. Haque, I.U. and M. Tariq, *Voltammetry of nitrate at solid cathodes. ECS Transactions*, 2009. **16**(18): p. 25.
71. Yoshida, M., *Process for preparing nitrogen by ammonium nitrate decomposition*. 1983, Google Patents.
72. Szpyrkowicz, L., S. Daniele, M. Radaelli, and S. Specchia, *Removal of NO_3^- from water by electrochemical reduction in different reactor*

- configurations. Applied Catalysis B: Environmental*, 2006. **66**(1-2): p. 40-50.
73. Li, W., C. Xiao, Y. Zhao, Q. Zhao, R. Fan, and J. Xue, *Electrochemical reduction of high-concentrated nitrate using Ti/TiO₂ nanotube array anode and Fe cathode in dual-chamber cell. Catalysis Letters*, 2016. **146**(12): p. 2585-2595.
74. Küngas, R., *Electrochemical CO₂ Reduction for CO Production: Comparison of Low-and High-Temperature Electrolysis Technologies. Journal of The Electrochemical Society*, 2020. **167**(4): p. 044508.
75. Rivera, F.F., C.P. de León, J.L. Nava, and F.C. Walsh, *The filter-press FM01-LC laboratory flow reactor and its applications. Electrochimica Acta*, 2015. **163**: p. 338-354.
76. Paidar, M., K. Bouzek, and H. Bergmann, *Influence of cell construction on the electrochemical reduction of nitrate. Chemical Engineering Journal*, 2002. **85**(2-3): p. 99-109.
77. Heitz, E., *D. Pletcher, FC Walsh: Industrial Electrochemistry*, 1995. **99**(4): p. 693-694.
78. Bard, A.J. and L.R. Faulkner, *Fundamentals and applications. Electrochemical Methods*, 2001. **2**(482): p. 580-632.
79. Vetter, K.J., *Electrochemical kinetics: theoretical aspects*. 2013: Elsevier.

80. Huang, H., M. Zhao, X. Xing, I. Bae, and D. Scherson, *In-situ infrared studies of the Cd-UPD mediated reduction of nitrate on gold*. **Journal of Electroanalytical Chemistry and Interfacial Electrochemistry**, 1990. **293**(1-2): p. 279-284.
81. Da Cunha, M., M. Weber, and F.C. Nart, *On the adsorption and reduction of NO_3^- ions at Au and Pt electrodes studied by in situ FTIR spectroscopy*. **Journal of Electroanalytical Chemistry**, 1996. **414**(2): p. 163-170.
82. De, D., E.E. Kalu, P.P. Tarjan, and J.D. Englehardt, *Kinetic Studies of the Electrochemical Treatment of Nitrate and Nitrite Ions on Iridium-Modified Carbon Fiber Electrodes*. **Chemical Engineering & Technology: Industrial Chemistry-Plant Equipment-Process Engineering-Biotechnology**, 2004. **27**(1): p. 56-64.
83. Hsieh, S.-J. and A.A. Gewirth, *Nitrate reduction catalyzed by underpotentially deposited Cd on Au (111): Identification of the electroactive surface structure*. **Langmuir**, 2000. **16**(24): p. 9501-9512.
84. Abuzaid, N.S., Z. Al-Hamouz, A.A. Bukhari, and M.H. Essa, *Electrochemical treatment of nitrite using stainless steel electrodes*. **Water, Air, and Soil Pollution**, 1999. **109**(1-4): p. 429-442.
85. Seetharam, B.N., T. Brahmaiah, U.I. Basha, H. Murthy, and J.N. Kalkur, *Effect of Operational Parameters on Nitrate Removal from the Simulated Groundwater Using Electrochemical Method*.

86. Dima, G., G. Beltramo, and M. Koper, *Nitrate reduction on single-crystal platinum electrodes*. *Electrochimica acta*, 2005. **50**(21): p. 4318-4326.
87. Hristovski, K.D. and J. Markovski, *Engineering metal (hydr) oxide sorbents for removal of arsenate and similar weak-acid oxyanion contaminants: A critical review with emphasis on factors governing sorption processes*. *Science of The Total Environment*, 2017. **598**: p. 258-271.
88. Da Cunha, M., M. Weber, and F. Nart, *On the adsorption and reduction of NO_3^- ions at Au and Pt electrodes studied by in situ FTIR spectroscopy*. *Journal of Electroanalytical Chemistry*, 1996. **414**(2): p. 163-170.
89. Wang, L., M. Li, X. Liu, C. Feng, F. Zhou, N. Chen, and W. Hu, *Mechanism and effectiveness of Ti-based nano-electrode for electrochemical denitrification*. *International Journal of Electrochemical Science*, 2017. **12**(3): p. 1992-2002.
90. Ma, X., M. Li, C. Feng, W. Hu, L. Wang, and X. Liu, *Development and reaction mechanism of efficient nano titanium electrode: Reconstructed nanostructure and enhanced nitrate removal efficiency*. *Journal of Electroanalytical Chemistry*, 2016. **782**: p. 270-277.
91. Cuibus, F.M., A. Ispas, A. Bund, and P. Ilea, *Square wave voltammetric detection of electroactive products resulting from*

- electrochemical nitrate reduction in alkaline media. Journal of Electroanalytical Chemistry*, 2012. **675**: p. 32-40.
92. Casella, I.G. and M. Contursi, *Highly dispersed rhodium particles on multi-walled carbon nanotubes for the electrochemical reduction of nitrate and nitrite ions in acid medium. Electrochimica Acta*, 2014. **138**: p. 447-453.
93. Shen, J., Y.Y. Birdja, and M.T. Koper, *Electrocatalytic nitrate reduction by a cobalt protoporphyrin immobilized on a pyrolytic graphite electrode. Langmuir*, 2015. **31**(30): p. 8495-8501.
94. Wang, Q., X. Zhao, J. Zhang, and X. Zhang, *Investigation of nitrate reduction on polycrystalline Pt nanoparticles with controlled crystal plane. Journal of Electroanalytical Chemistry*, 2015. **755**: p. 210-214.
95. Abdallah, R., H. Djelal, A. Amrane, W. Sayed, F. Fourcade, T. Labasque, F. Geneste, S. Taha, and D. Floner, *Dark fermentative hydrogen production by anaerobic sludge growing on glucose and ammonium resulting from nitrate electroreduction. international journal of hydrogen energy*, 2016. **41**(12): p. 5445-5455.
96. Katsounaros, I., M. Dortsiou, C. Polatides, S. Preston, T. Kypraios, and G. Kyriacou, *Reaction pathways in the electrochemical reduction of nitrate on tin. Electrochimica Acta*, 2012. **71**: p. 270-276.
97. De Groot, M. and M. Koper, *The influence of nitrate concentration and acidity on the electrocatalytic reduction of nitrate on platinum. Journal of Electroanalytical Chemistry*, 2004. **562**(1): p. 81-94.

98. Ota, K.-i., G. Kreysa, and R.F. Savinell, **Encyclopedia of applied electrochemistry**. 2014: Springer New York.
99. Khomutov, N. and U. Stamkulov, *Nitrate reduction at various metal electrodes*. **Sov. Electrochem**, 1971. **7**: p. 312-316.
100. Reyter, D., D. Bélanger, and L. Roué, *Study of the electroreduction of nitrate on copper in alkaline solution*. **Electrochimica Acta**, 2008. **53**(20): p. 5977-5984.
101. Reyter, D., D. Bélanger, and L. Roué, *Optimization of the cathode material for nitrate removal by a paired electrolysis process*. **Journal of hazardous materials**, 2011. **192**(2): p. 507-513.
102. Bard, A., **Standard potentials in aqueous solution**. 2017: Routledge.
103. Pourbaix, M., *Atlas of electrochemical equilibria in aqueous solution*. **NACE**, 1974. **307**.
104. Bard, A.J. and J. Ketelaar, *Encyclopedia of Electrochemistry of the Elements*. **Journal of The Electrochemical Society**, 1974. **121**(6): p. 212C.
105. Li, H.I., D.H. Robertson, J.Q. Chambers, and D.T. Hobbs, *Electrochemical reduction of nitrate and nitrite in concentrated sodium hydroxide at platinum and nickel electrodes*. **Journal of the Electrochemical Society**, 1988. **135**(5): p. 1154.
106. De Francesco, M. and P. Costamagna, *On the design of electrochemical reactors for the treatment of polluted water*. **Journal of Cleaner Production**, 2004. **12**(2): p. 159-163.

107. hhhjjh, *hgjfgkjgkffu*. **Electrochimica Acta**. **55**(19): p. 5287-5293.
108. Key, S.S. and F. Clearwater Beach, **Electrochemical Reduction of Nitrate**. 1998.
109. Inam-Ul-Haque and M. Tariq, *Electrochemical Reduction of Nitrate: Areview*. **Journal of the Chemical Society of Pakistan**,, 2010. **32**(3): p. 396-418.
110. Aouina, N., H. Cachet, C. Debiemme-Chouvy, and T.T.M. Tran, *Insight into the electroreduction of nitrate ions at a copper electrode, in neutral solution, after determination of their diffusion coefficient by electrochemical impedance spectroscopy*. **Electrochimica Acta**, **2010**. **55**(24): p. 7341-7345.
111. Lima, A.S., M.O. Salles, T.L. Ferreira, T.R. Paixão, and M. Bertotti, *Scanning electrochemical microscopy investigation of nitrate reduction at activated copper cathodes in acidic medium*. **Electrochimica Acta**, 2012. **78**: p. 446-451.
112. Huang, W., M. Li, B. Zhang, C. Feng, X. Lei, and B. Xu, *Influence of operating conditions on electrochemical reduction of nitrate in groundwater*. **Water environment research**, 2013. **85**(3): p. 224-231.
113. PÚrez, O.G. and J.M. Bisang, *Removal of nitrate using an activated rotating cylinder electrode*. **Electrochimica Acta**, 2016. **194**: p. 448-453.
114. Bouzek, K., M. Paidar, A. Sadilkova, and H. Bergmann, *Electrochemical reduction of nitrate in weakly alkaline solutions*. **Journal of Applied Electrochemistry**, 2001. **31**(11): p. 1185-1193.

115. Malinovic, B., M. Pavlovic, and N. Halilovic, *Electrochemical removal of nitrate from wastewater using copper cathode*. **J. Environ. Prot. Ecol.**, 2015. **16**(4): p. 1273-1281.
116. Pérez-Gallent, E., M.C. Figueiredo, I. Katsounaros, and M.T. Koper, *Electrocatalytic reduction of Nitrate on Copper single crystals in acidic and alkaline solutions*. **Electrochimica Acta**, 2017. **227**: p. 77-84.
117. Yang, S., L. Wang, X. Jiao, and P. Li, *Electrochemical reduction of nitrate on different Cu-Zn oxide composite cathodes*. **Int. J. Electrochem. Sci**, 2017. **12**: p. 4370-4383.
118. Mattarozzi, L., S. Cattarin, N. Comisso, R. Gerbasi, P. Guerriero, M. Musiani, and E. Verlato, *Electrodeposition of compact and porous Cu-Pd alloy layers and their application to nitrate reduction in alkali*. **Electrochimica Acta**, 2017. **230**: p. 365-372.
119. Zhang, Q., L. Ding, H. Cui, J. Zhai, Z. Wei, and Q. Li, *Electrodeposition of Cu-Pd alloys onto electrophoretic deposited carbon nanotubes for nitrate electroreduction*. **Applied surface science**, 2014. **308**: p. 113-120.
120. Mattarozzi, L., S. Cattarin, N. Comisso, A. Gambirasi, P. Guerriero, M. Musiani, L. Vázquez-Gómez, and E. Verlato, *Hydrogen evolution assisted electrodeposition of porous Cu-Ni alloy electrodes and their use for nitrate reduction in alkali*. **Electrochimica Acta**, 2014. **140**: p. 337-344.
121. Ehrenburg, M.R., A.I. Danilov, I.G. Botryakova, E.B. Molodkina, and A.V. Rudnev, *Electroreduction of nitrate anions on cubic and*

- polyoriented platinum nanoparticles modified by copper adatoms. Journal of Electroanalytical Chemistry*, 2017. **802**: p. 109-117.
122. Molodkina, E., M. Ehrenburg, Y.M. Polukarov, A. Danilov, J. Souza-Garcia, and J. Feliu, *Electroreduction of nitrate ions on Pt (1 1 1) electrodes modified by copper adatoms. Electrochimica acta*, 2010. **56**(1): p. 154-165.
123. Molodkina, E., I. Botryakova, A. Danilov, J. Souza-Garcia, and J.M. Feliu, *Kinetics and mechanism of nitrate and nitrite electroreduction on Pt (100) electrodes modified by copper adatoms. Russian Journal of Electrochemistry*, 2013. **49**(3): p. 285-293.
124. Amertharaj, S., M. Hasnat, and N. Mohamed, *Electroreduction of nitrate ions at a platinum-copper electrode in an alkaline medium: Influence of sodium inositol phytate. Electrochimica Acta*, 2014. **136**: p. 557-564.
125. Öznülüer, T., B. Özdurak, and H.Ö. Doğan, *Electrochemical reduction of nitrate on graphene modified copper electrodes in alkaline media. Journal of Electroanalytical Chemistry*, 2013. **699**: p. 1-5.
126. Hamam, A., D. Oukil, A. Dib, H. Hammache, L. Makhloufi, and B. Saidani, *Polypyrrole coated cellulosic substrate modified by copper oxide as electrode for nitrate electroreduction. Surface Review and Letters*, 2015. **22**(05): p. 1550065.
127. Çirimi, D., R. Aydın, and F. Köleli, *The electrochemical reduction of nitrate ion on polypyrrole coated copper electrode. Journal of Electroanalytical Chemistry*, 2015. **736**: p. 101-106.

128. Rajmohan, K. and R. Chetty, *Enhanced nitrate reduction with copper phthalocyanine-coated carbon nanotubes in a solid polymer electrolyte reactor*. **Journal of Applied Electrochemistry**, 2017. **47**(1): p. 63-74.
129. Couto, A., L. Santos, J. Matsushima, M. Baldan, and N. Ferreira, *Hydrogen and oxygen plasma enhancement in the Cu electrodeposition and consolidation processes on BDD electrode applied to nitrate reduction*. **Applied surface science**, 2011. **257**(23): p. 10141-10146.
130. Ribeiro, M.C.E., A.B. Couto, N.G. Ferreira, and M.R. Baldan, *Nitrate removal by electrolysis using Cu/BDD electrode cathode*. **ECS Transactions**, 2014. **58**(19): p. 21-26.
131. Zhang, Z., Y. Xu, W. Shi, W. Wang, R. Zhang, X. Bao, B. Zhang, L. Li, and F. Cui, *Electrochemical-catalytic reduction of nitrate over Pd-Cu/ γ -Al₂O₃ catalyst in cathode chamber: enhanced removal efficiency and N₂ selectivity*. **Chemical Engineering Journal**, 2016. **290**: p. 201-208.
132. Gootzen, J., L. Lefferts, and J. Van Veen, *Electrocatalytic nitrate reduction on palladium based catalysts activated with germanium*. **Applied catalysis A: general**, 1999. **188**(1-2): p. 127-136.
133. Brylev, O., M. Sarrazin, L. Roué, and D. Bélanger, *Nitrate and nitrite electrocatalytic reduction on Rh-modified pyrolytic graphite electrodes*. **Electrochimica Acta**, 2007. **52**(21): p. 6237-6247.
134. Leontiev, A.P., O.A. Brylev, and K.S. Napolskii, *Arrays of rhodium nanowires based on anodic alumina: Preparation and*

- electrocatalytic activity for nitrate reduction. Electrochimica Acta*, 2015. **155**: p. 466-473.
135. Mindler, A.B. and S.B. Tuwiner, *Electrolytic reduction of nitrate from solutions of alkali metal hydroxides*. 1970, Google Patents.
136. Cattarin, S., *Electrochemical reduction of nitrogen oxyanions in 1 M sodium hydroxide solutions at silver, copper and CuInSe₂ electrodes. Journal of applied electrochemistry*, 1992. **22**(11): p. 1077-1081.
137. Kato, M., M. Okui, S. Taguchi, and I. Yagi, *Electrocatalytic nitrate reduction on well-defined surfaces of tin-modified platinum, palladium and platinum-palladium single crystalline electrodes in acidic and neutral media. Journal of Electroanalytical Chemistry*, 2017. **800**: p. 46-53.
138. Li, H.-L., J. Chambers, and D. Hobbs, *Electroreduction of nitrate ions in concentrated sodium hydroxide solutions at lead, zinc, nickel and phthalocyanine-modified electrodes. Journal of applied electrochemistry*, 1988. **18**(3): p. 454-458.
139. Dima, G., A. De Vooy, and M. Koper, *Electrocatalytic reduction of nitrate at low concentration on coinage and transition-metal electrodes in acid solutions. Journal of Electroanalytical Chemistry*, 2003. **554**: p. 15-23.
140. Lau, K.T., M. Lu, and D. Hui, *Coiled carbon nanotubes: synthesis and their potential applications in advanced composite structures. Composites Part B: Engineering*, 2006. **37**(6): p. 437-448.

141. Ding, L., Q. Li, D. Zhou, H. Cui, H. An, and J. Zhai, *Modification of glassy carbon electrode with polyaniline/multi-walled carbon nanotubes composite: application to electro-reduction of bromate*. **Journal of Electroanalytical Chemistry**, 2012. **668**: p. 44-50.
142. Coleman, J.N., U. Khan, W.J. Blau, and Y.K. Gun'ko, *Small but strong: a review of the mechanical properties of carbon nanotube–polymer composites*. **Carbon**, 2006. **44**(9): p. 1624-1652.
143. Khare, R., *Carbon nanotube based composites-a review*. **Journal of minerals and Materials Characterization and Engineering**, 2005. **4**(01): p. 31.
144. Deck, C.P. and K. Vecchio, *Prediction of carbon nanotube growth success by the analysis of carbon–catalyst binary phase diagrams*. **Carbon**, 2006. **44**(2): p. 267-275.
145. Baughman, R.H., A.A. Zakhidov, and W.A. De Heer, *Carbon nanotubes--the route toward applications*. **science**, 2002. **297**(5582): p. 787-792.
146. Hu, R., L. Chu, J. Zhang, X.a. Li, and W. Huang, *Carbon materials for enhancing charge transport in the advancements of perovskite solar cells*. **Journal of Power Sources**, 2017. **361**: p. 259-275.
147. Chen, H. and S. Yang, *Carbon-based perovskite solar cells without hole transport materials: the front runner to the market*. **Advanced materials**, 2017. **29**(24): p. 1603994.

148. Ammara, S., S. Shamaila, A. Bokhari, and A. Sabah, *Nonenzymatic glucose sensor with high performance electrodeposited nickel/copper/carbon nanotubes nanocomposite electrode*. **Journal of Physics and Chemistry of Solids**, 2018. **120**: p. 12-19.
149. He, J., H. Feng, T. Wang, T. Wang, and H. Zeng, *Morphology-controlled Electrodeposition of Copper Nanospheres onto FTO for Enhanced Photocatalytic Hydrogen Production*. **Chinese Journal of Chemistry**, 2018. **36**(1): p. 31-36.
150. Chang, H., K.-C. Cho, T.-L. Chen, K.-H. Chu, and L.-J. Jiang, *Preparation and characterization of anthocyanin dye and counter electrode thin film with carbon nanotubes for dye-sensitized solar cells*. **Materials transactions**, 2011. **52**(10): p. 1977-1982.
151. Rahman, D.Y., F.D. Utami, A.R. Setiawan, E. Sustini, and M. Abdullah, *Very high efficiency of low cost graphite-based solar cell by improving the fill factor using optimal ion concentration in polymer electrolyte*. **arXiv preprint arXiv:1803.07701**, 2018.
152. Rahman, D.Y., M. Rokhmat, E. Yuliza, E. Sustini, and M. Abdullah, *New design of potentially low-cost solar cells using TiO₂/graphite composite as photon absorber*. **International Journal of Energy and Environmental Engineering**, 2016. **7**(3): p. 289-296.
153. Datsyuk, V., M. Kalyva, K. Papagelis, J. Parthenios, D. Tasis, A. Siokou, I. Kallitsis, and C. Galiotis, **Chemical oxidation of multiwalled carbon nanotubes**. **Carbon**, 2008. **46**(6): p. 833-840.

154. Saheblian, S., S. Zebarjad, J. Vahdati Khaki, and A. Lazzeri, *A study on the dependence of structure of multi-walled carbon nanotubes on acid treatment*. **Journal of Nanostructure in Chemistry**, 2015. **5**(3): p. 287-293.
155. Ramasamy, E., W.J. Lee, D.Y. Lee, and J.S. Song, *Spray coated multi-wall carbon nanotube counter electrode for tri-iodide (I_3^-) reduction in dye-sensitized solar cells*. **Electrochemistry Communications**, 2008. **10**(7): p. 1087-1089.
156. Widodo, S., G. Wiranto, and M.N. Hidayat, *Fabrication of dye sensitized solar cells with spray coated carbon nano tube (CNT) based counter electrodes*. **Energy Procedia**, 2015. **68**: p. 37-44.
157. Prasetio, A., A. Subagio, A. Purwanto, and H. Widiyandari. *Dye-sensitized solar cell based carbon nanotube as counter electrode*. in **AIP Conference Proceedings**. 2016. AIP Publishing LLC.
158. Mei, X., S.J. Cho, B. Fan, and J. Ouyang, *High-performance dye-sensitized solar cells with gel-coated binder-free carbon nanotube films as counter electrode*. **Nanotechnology**, 2010. **21**(39): p. 395202.
159. Pawar, M. and S. Chaure, *Synthesis of CdS nanoparticles using glucose as a capping agent*. **Chalcogenide Lett**, 2009. **6**(12): p. 689-693.
160. Manickathai, K., S.K. Viswanathan, and M. Alagar, *Synthesis and characterization of CdO and CdS nanoparticles*. **2008**.
161. Warren, B.E., *X-ray Diffraction*. **1990: Courier Corporation**.

162. Federation, W.E. and A.P.H. Association, *Standard methods for the examination of water and wastewater*. American Public Health Association (APHA): Washington, DC, USA, 2005.
163. Kirfel, A. and K. Eichhorn, *Accurate structure analysis with synchrotron radiation. The electron density in Al₂O₃ and Cu₂O*. Acta Crystallographica Section A: Foundations of Crystallography, 1990. 46(4): p. 271-284.
164. Niggli, P., *XII. Die Kristallstruktur einiger Oxyde I*. Zeitschrift für Kristallographie-Crystalline Materials, 1922. 57(1-6): p. 253-299.
165. Otte, H.M., *Lattice parameter determinations with an x-ray spectrogoniometer by the debye-scherrer method and the effect of specimen condition*. Journal of Applied Physics, 1961. 32(8): p. 1536-1546.
166. Swanson, H. and E. Tatge, *Standard X-ray diffraction powder patterns*. National Bureau of Standards (US). Circular, 1953. 359: p. 1.
167. Zhang, T., X. Zhang, L. Ding, and W. Zhang, *Study on resistance switching properties of Na 0.5 Bi 0.5 TiO 3 thin films using impedance spectroscopy*. Nanoscale research letters, 2009. 4(11): p. 1309-1314.
168. Wagner, C., A. Naumkin, A. Kraut-Vass, J. Allison, C. Powell, and J. Rumble Jr, *NIST X-ray Photoelectron Spectroscopy Database, NIST Standard Reference Database 20, Version 3.4 (Web Version)*. US Department of Commerce, 2003.

169. Bird, R. and P. Swift, *Energy calibration in electron spectroscopy and the re-determination of some reference electron binding energies*. **Journal of Electron Spectroscopy and Related Phenomena**, 1980. **21**(3): p. 227-240.
170. Biesinger, M.C., L.W. Lau, A.R. Gerson, and R.S.C. Smart, *Resolving surface chemical states in XPS analysis of first row transition metals, oxides and hydroxides: Sc, Ti, V, Cu and Zn*. **Applied surface science**, 2010. **257**(3): p. 887-898.
171. Karimzadeh, M., K. Niknam, N. Manouchehri, and D. Tarokh, *A green route for the cross-coupling of azide anions with aryl halides under both base and ligand-free conditions: exceptional performance of a Cu₂O, CuO, Cu–C nanocomposite*. **RSC advances**, 2018. **8**(45): p. 25785-25793.
172. Cheng, H., K. Scott, and P. Christensen, *Paired electrolysis in a solid polymer electrolyte reactor—Simultaneously reduction of nitrate and oxidation of ammonia*. **Chemical Engineering Journal**, 2005. **108**(3): p. 257-268.
173. Soares, O.S.G., J.J. Órfão, and M.F.R. Pereira, *Nitrate reduction in water catalysed by Pd–Cu on different supports*. **Desalination**, 2011. **279**(1-3): p. 367-374.
174. De, D., J.D. Englehardt, and E.E. Kalu, *Electroreduction of Nitrate and Nitrite Ion on a Platinum-Group-Metal Catalyst-Modified Carbon Fiber Electrode Chronoamperometry and Mechanism*

- Studies. Journal of the Electrochemical Society*, 2000. **147**(12): p. 4573.
175. Fayos, J., *Possible 3D carbon structures as progressive intermediates in graphite to diamond phase transition. Journal of Solid State Chemistry*, 1999. **148**(2): p. 278-285.
176. Blyth, R., H. Buqa, F. Netzer, M. Ramsey, J. Besenhard, P. Golob, and M. Winter, *XPS studies of graphite electrode materials for lithium ion batteries. Applied Surface Science*, 2000. **167**(1-2): p. 99-106.
177. Van Attekum, P.T.M. and G. Wertheim, *Excitonic effects in core-hole screening. Physical review letters*, 1979. **43**(25): p. 1896.
178. Wang, Y.-Q., F.-Q. Zhang, and P.M. Sherwood, *X-ray photoelectron spectroscopic study of carbon fiber surfaces. 23. Interfacial interactions between polyvinyl alcohol and carbon fibers electrochemically oxidized in nitric acid solution. Chemistry of materials*, 1999. **11**(9): p. 2573-2583.
179. Cheng, H., K. Scott, and P. Christensen, *Application of a solid polymer electrolyte reactor to remove nitrate ions from wastewater. Journal of applied electrochemistry*, 2005. **35**(6): p. 551-560.
180. Reddy, K.R., B.C. Sin, K.S. Ryu, J.-C. Kim, H. Chung, and Y. Lee, *Conducting polymer functionalized multi-walled carbon nanotubes with noble metal nanoparticles: synthesis, morphological characteristics and electrical properties. Synthetic Metals*, 2009. **159**(7-8): p. 595-603.

181. Xu, J., X. Lv, J. Li, Y. Li, L. Shen, H. Zhou, and X. Xu, *Simultaneous adsorption and dechlorination of 2, 4-dichlorophenol by Pd/Fe nanoparticles with multi-walled carbon nanotube support*. **Journal of hazardous materials**, 2012. **225**: p. 36-45.
182. Calos, N., J. Forrester, and G. Schaffer, *A crystallographic contribution to the mechanism of a mechanically induced solid state reaction*. **Journal of Solid State Chemistry**, 1996. **122**(2): p. 273-280.
183. Asbrink, S. and A. Waskowska, *CuO: X-ray single-crystal structure determination at 196 K and room temperature*. **Journal of Physics: Condensed Matter**, 1991. **3**(42): p. 8173.
184. Francisco, W., F.V. Ferreira, E.V. Ferreira, L.d.S. Cividanes, A.d.R. Coutinho, and G.P. Thim, *Functionalization of multi-walled carbon nanotube and mechanical property of epoxy-based nanocomposite*. **Journal of Aerospace Technology and Management**, 2015. **7**(3): p. 289-293.
185. Emtsev, K., F. Speck, T. Seyller, L. Ley, and J.D. Riley, *Interaction, growth, and ordering of epitaxial graphene on SiC (0001) surfaces: A comparative photoelectron spectroscopy study*. **Physical Review B**, 2008. **77**(15): p. 155303.
186. Casella, I. and M. Gatta, *Anodic electrodeposition of copper oxide/hydroxide films by alkaline solutions containing cuprous cyanide ions*. **Journal of Electroanalytical Chemistry**, 2000. **494**(1): p. 12-20.

187. Casella, I.G. and M. Contursi, *Electrochemical and spectroscopic characterization of a tungsten electrode as a sensitive amperometric sensor of small inorganic ions*. *Electrochimica acta*, 2005. **50**(20): p. 4146-4154.
188. Jin, S. and A. Atrens, *ESCA-Studies of the structure and composition of the passive film formed on stainless steels by various immersion temperatures in 0.1 M NaCl solution*. *Applied Physics A*, 1988. **45**(1): p. 83-91.
189. Li, K., Z. Zeng, L. Yan, M. Huo, Y. Guo, S. Luo, and X. Luo, *Fabrication of C/X-TiO₂@ C₃N₄ NTs (X= N, F, Cl) composites by using phenolic organic pollutants as raw materials and their visible-light photocatalytic performance in different photocatalytic systems*. *Applied Catalysis B: Environmental*, 2016. **187**: p. 269-280.
190. Organization, W.H., *Guidelines for drinking water quality, addendum to volume 2: Health criteria and other supporting information*. 1998: WHO Publications.
191. Enmili, A., A. Azzouz, V.-A. Arus, and F. Monette, *Aluminosilicate-catalyzed electroreduction of nitrate anion—An approach through alkalinity analysis*. *Electrochimica Acta*, 2016. **222**: p. 1064-1071.
192. Chakrabarti, M.H., M. Saleem, M.F. Irfan, S. Raza, D.u.B. Hasan, and W. Daud, *Application of waste derived activated carbon felt electrodes in minimizing NaCl use for electrochemical disinfection of water*. *Int. J. Electrochem. Sci*, 2011. **6**: p. 4470-4480.

193. Strebel, O., W. Duynisveld, and J. Böttcher, *Nitrate pollution of groundwater in western Europe. Agriculture, ecosystems & environment*, 1989. **26**(3-4): p. 189-214.
194. Lee, J., *Reaction Order Ambiguity in Integrated Rate Plots. Journal of chemical education*, 2008. **85**(1): p. 141.
195. Levenspiel, O., **Chemical reaction engineering**. 1999: John Wiley & Sons.
196. Makover, J., D. Hasson, Y. Huang, R. Semiat, and H. Shemer, *Electrochemical removal of nitrate from a Donnan dialysis waste stream. Water Science and Technology*, 2019. **80**(4): p. 727-736.
197. Ryan, M.A. and J. Ingle, *Fluorometric reaction rate method for the determination of thiamine. Analytical chemistry*, 1980. **52**(13): p. 2177-2184.
198. House, J.E., *Principles of chemical kinetics*. 2007: Academic press.
199. Justi, R., *Teaching and learning chemical kinetics, in Chemical education: Towards research-based practice*. 2002, Springer. p. 293-315.
200. De Vooy, A., R. Van Santen, and J. Van Veen, *Electrocatalytic reduction of NO₃⁻ on palladium/copper electrodes. Journal of Molecular Catalysis A: Chemical*, 2000. **154**(1-2): p. 203-215.
201. Ghodbane, O., M. Sarrazin, L. Roué, and D. Bélanger, *Electrochemical reduction of nitrate on pyrolytic graphite-supported*

- Cu and Pd–Cu electrocatalysts. Journal of the Electrochemical Society*, 2008. **155**(6): p. F117.
202. Kim, H.-K., J.-Y. Jeong, H.-N. Cho, and J.-Y. Park, *Kinetics of nitrate reduction with the packed bed iron bipolar electrode. Separation and Purification Technology*, 2015. **152**: p. 140-147.
203. Alam, M.S., M. Hasnat, M. Rashed, M.R. Miah, and I.S. Saiful, *Electrocatalytic formation of NO_2^- at a poly crystalline Ag surface in neutral medium. Electrochimica acta*, 2012. **76**: p. 102-105.
204. Amatore, C. and J. Savéant, *Do ECE mechanisms occur in conditions where they could be characterized by electrochemical kinetic techniques, Journal of Electroanalytical Chemistry and Interfacial Electrochemistry*, 1978. **86**(1): p. 227-232.
205. Katsounaros, I. and G. Kyriacou, *Influence of the concentration and the nature of the supporting electrolyte on the electrochemical reduction of nitrate on tin cathode. Electrochimica Acta*, 2007. **52**(23): p. 6412-6420.
206. Reyter, D., G. Chamoulaud, D. Bélanger, and L. Roué, *Electrocatalytic reduction of nitrate on copper electrodes prepared by high-energy ball milling. Journal of Electroanalytical Chemistry*, 2006. **596**(1): p. 13-24.
207. Vorlop, K. and T. Tacke, *Ist steps towards noble-metal catalyzed removal of nitrate and nitrite from drinking-water. Chemie Ingenieur Technik*, 1989. **61**(10): p. 836-837.

208. Shin, H., S. Jung, S. Bae, W. Lee, and H. Kim, *Nitrite reduction mechanism on a Pd surface*. **Environmental science & technology**, 2014. **48**(21): p. 12768-12774.
209. Vavilin, V. and S. Rytov, *Nitrate denitrification with nitrite or nitrous oxide as intermediate products: Stoichiometry, kinetics and dynamics of stable isotope signatures*. **Chemosphere**, 2015. **134**: p. 417-426.
210. Durivault, L., O. Brylev, D. Reyter, M. Sarrazin, D. Bélanger, and L. Roué, *Cu–Ni materials prepared by mechanical milling: their properties and electrocatalytic activity towards nitrate reduction in alkaline medium*. **Journal of alloys and compounds**, 2007. **432**(1-2): p. 323-332.
211. Ribeiro, M.C.E., A.B. Couto, N.G. Ferreira, and M.R. Baldan, *Nitrate Removal by Electrolysis Using Cu/BDD Electrode Cathode*. **ECS Transactions**, 2014. **58**(19): p. 21.

جامعة النجاح الوطنية

كلية الدراسات العليا

اختزال أيونات النترات من الماء باستخدام حفاز كهربي من النحاس النانوي

إعداد

هبة نصار عزت نصار

إشراف

أ. د. حكمت هلال

د. عاهد زيود

قدمت هذه الأطروحة استكمالاً لمتطلبات الحصول على درجة الدكتوراة في الكيمياء بكلية الدراسات
العليا في جامعة النجاح الوطنية، نابلس _ فلسطين.

2021م

ب

اختزال أيونات النترات من الماء باستخدام حفاز كهربائي من النحاس النانوي

إعداد

هبة نصّار عزت نصّار

إشراف

أ. د. حكمت هلال

د. عاهد زيود

الملخص

الزيادة المطردة في تركيز أيون النترات في المياه السطحية والجوفية، دفعت العديد من الباحثين إلى العمل على تطوير طرق آمنة لإزالة النترات من المحاليل المائية. هذا ويعتبر المسبب الأساسي لهذا التلوث، الاستخدام المفرط وغير المسؤول للأسمدة النيتروجينية في المجال الزراعي.

إنّ الهدف الرئيس لهذا البحث هو تطوير أقطاب كهربائية جديدة، آمنة بكلفة قليلة وكفاءة عالية من أجل الاختزال الكهروكيميائي للنترات من المحاليل المائية. في هذا البحث تمت عملية الاختزال الكهروكيميائي بتثبيت مقدار محدد من الجهد الكهربائي على القطب الكهربائي في المحاليل المائية. وأثناء التجارب تم قياس تركيز أيونات NO_3^- المتبقية، و الأيونات المتكونة من NO_2^- و NH_4^+ . في هذا البحث، تم الاختزال الكهروكيميائي للنترات من المحاليل المائية باستخدام خلية كهروكيميائية غير مجزأة تحتوي على ثلاثة أقطاب كهربائية. و كان القطب المرجعي في الخلية هو قطب (SCE)، واستخدمت صفيحة من البلاتين (Pt) كمصعد، وتم استخدام أحد الأقطاب المحضرة في هذا البحث كمهبط في كل تجربة.

تم تحضير ثلاث مجموعات مختلفة من الأقطاب الكهربائية في هذه الدراسة، حيث تم استخدام شرائح زجاجية مغطاة بطبقة رقيقة موصلة من أكسيد القصدير المطعم بالفلور (FTO/Glass) كركيزة لتحضير الأقطاب المختلفة. تم استخدام شرائح النحاس وشرائح FTO/Glass للمقارنة. تم تحليل الأقطاب و فحصها باستخدام المسح المجهر الإلكتروني (SEM) والتحليل الطيفي المشتت لطاقة العناصر (EDS)، وحيود الأشعة السينية (XRD)، و التحليل الطيفي الضوئي للأشعة السينية

(XPS). تم فحص السلوك الكهروكيميائي للأقطاب الكهربية التي تم تحضيرها عن طريق القياس الدوري لتغير فرق الجهد (CV).

شملت الفئة الأولى الأقطاب الكهربية FTO/Cu، التي تم تحضيرها بالترسيب الكهربي للنحاس على سطح FTO. تمت عملية الترسيب عند فرق جهد -0.80 فولت باستخدام محلول (CuSO_4 0.01 مول/لتر + 0.10 KCl مول/لتر)، و تمت عملية ترسيب أخرى للنحاس باستخدام محلول (CuSO_4 0.85 مول/لتر + H_2SO_4 0.55 مول/لتر). القطب الذي تم تحضيره عن طريق الترسيب الكهربي للنحاس على سطح FTO من المحلول الثاني تم تسميته FTO/Cu-b و استخدم في تجارب الاختزال الكهروكيميائي للنترات من المحاليل المائية، لأنه أظهر ثباتاً أكثر من القطب الكهربي الآخر.

النسبة المئوية لازالة النترات بواسطة القطب FTO/Cu-b كانت تكافيه 39.90%، و كانت نسبة الانتقائية لتحويل النترات إلى نيتروجين 35.13%. إن هذه النسبة أفضل من تلك التي تم الحصول عليها باستخدام قطب النحاس عند نفس الظروف، حيث كانت نسبة ازالة النترات 35.13% و انتقائية النيتروجين 1.10% و ذلك عند فرق جهد مقداره -1.80 فولت ولمدة ساعتين من التحليل الكهروكيميائي.

اشتملت المجموعة المحضرة الثانية على أقطاب FTO/Gr التي تم تحضيرها عن طريق تطبيق طبقة رقيقة من الغرافيت على سطح FTO. تم العمل على زيادة كفاءة هذا القطب عن طريق الترسيب الكهربي للنحاس على سطح FTO/Gr من محلول (CuSO_4 0.85 مول/لتر + H_2SO_4 0.55 مول/لتر)، و سمي هذا القطب FTO/Gr-Cu.

أدت معالجة القطب بالنحاس إلى زيادة طفيفة في نسبة ازالة النحاس من المحلول المائي، حيث كانت 24.00% و 25.69% للقطبين FTO/Gr و FTO/Gr-Cu على التوالي، بعد ساعتين من التحليل الكهروكيميائي على جهد -1.80 فولت. قد يكون هذا عائداً إلى الكمية المنخفضة من النحاس التي ترسب على سطح القطب FTO/Gr، حيث كانت النسبة الكتلية للنحاس على القطب FTO/Gr-Cu 12.92% وفقاً لتحليل EDS. من الجهة الأخرى أدى تحضير هذا القطب بهذه الآلية إلى المحافظة على ثباتية النحاس و حمايته من التأكسد، حيث أظهر فحص XRD وجود جسيمات النحاس النانوية على سطح القطب دون أكاسيده.

أما المجموعة الثالثة فقد شملت أقطاب FTO/MWCNT التي تم تحضيرها عن طريق الطلاء بالرش لمخلوط كربون متعدد الأنابيب على سطح FTO. تم تحضير القطب الجديد المحدث FTO/MWCNT-Cu عن طريق الطلاء بالرش أيضاً للمزيج النانوي MWCNT-Cu على سطح FTO. المزيج النانوي MWCNT-Cu تم تحضيره بطرق بسيطة غير مكلفة. و كان متوسط حجوم حبيبات النحاس النانوي في هذا القطب حسب تحليل XRD هو 35.28 نانومتر.

أفضل نسبة ازالة لأيونات النترات من المياه في هذه الدراسة ناتجة حين استخدم القطب FTO/MWCNT-Cu ، حيث وصلت هذه النسبة بعد ساعتين من التحليل الكهروكيميائي على فرق جهد مقداره -1.80 فولت، إلى 65.27%. لذلك فقد تم استخدام هذا القطب في استكمال هذا البحث. عند دراسة قانون السرعة لعملية الاختزال الكهروكيميائي لأيونات النترات، وجد أن مقدار رتبة التفاعل هو (0.76) و أن ثابت سرعة التفاعل $10 \times 4.50 \times 10^{-3}$ دقيقة⁻¹.

تم دراسة أثر العديد من العوامل على كفاءة الاختزال الكهروكيميائي لأيونات النترات بوساطة القطب FTO/MWCNT-Cu، مثل مقدار الجهد الكهربائي المطبق، نوع وتركيز المحلول الكهربي المستخدم، والمسافة بين الأقطاب، و تحريك مكونات محلول النترات، و درجة الحموضة، و درجة الحرارة، و تركيز أيون النترات، و وقت الاختزال الكهروكيميائي.

تشير النتائج إلى أن زيادة الجهد المطبق ودرجة الحرارة أثناء تحريك المحلول، عندما كانت المسافة بين الأقطاب 0.75 سم رفعت كفاءة اختزال النترات. عندما أجريت التجربة لسبع ساعات متواصلة، تم التخلص تقريباً من كامل أيونات النترات في المحلول، وبلغت انتقائية النيتروجين كنتاج آمن ومرغوب به عن هذه العملية 65.31%. هذا يوضح مدى كفاءة و أهمية القطب FTO/MWCNT-Cu في عملية اختزال النترات من المحاليل المائية. علاوة على ذلك، أظهرت نتائج XRD و EDS للقطب الكهربائي FTO/MWCNT-Cu المستخدم و غير المستخدم ثباتية هذا القطب. كما وجد أن كفاءة اختزال النترات بوساطة هذا القطب لم تتغير عندما أعيد استخدام نفس القطب لثلاث تجارب متتالية عند -1.80 فولت لمدة ساعتين لكل منها. كل هذا يثبت فعالية هذا القطب في ازالة أيونات النترات من المحاليل المائية بوساطة الاختزال الكهروكيميائي.